Proceedings

UNIVERSITY OF EASTERN FINLAND

Fifth International Workshop
Nanocarbon Photonics and Optoelectronics

1 - 6 August, 2016, Holiday Club Saimaa,
Lappeeranta, Finland

ISBN: 978-952-61-2172-7

Joensuu, 2016

University of Eastern Finland
Institute of Photonics

Proceedings

Fifth International Workshop
Nanocarbon Photonics and Optoelectronics

Holiday Club Saimaa, Lappeenranta, Finland

Editors:
Esko Kauppinen
Alexander Obraztsov
Yuri Svirko

Joensuu, Finland
2016

NPO2016 Schedule-at-a-Glance

	Monday August 1	Tuesday August 2	Wednesday August 3	Thursday August 4	Friday August 5	Saturday, August 6
		Graphene & 2D materials	Photonics & Optoelectronics	Photonics & Photovoltaics	Synthesis & Characterization	
9:00-9:45		**Annick Loiseau**	**Anna Swan**	**Shigeo Maruyma**	**Hiromichi Kataura**	**DEPARTURE**
9:45-10:30		**Pertti Hakonen** Tatiana Makarova	**Yutaka Ohno** Denis Bandurin	**Alex Barker** Dmitry Lyashenko	**Christophe Bichara** Wenyun Wu	
10:30-10:45		Coffee Break	Coffee Break	Coffee Break	Coffee Break	
10:45-12:15		**Cheol-Joo Kim** **Taishi Takenobu** **Naoki Ogawa**	**Zhipei Sun** **Amos Martinez** **Jun Wang**	**Polina Kuzhir** **Harri Lipsanen** **Lian-Mao Peng**	**Kaihui Liu** **Andrey Chuvilin** **Dmitry Golberg**	
12:15-14:00		Lunch	Lunch	Lunch	Lunch	
14:00-14:45	**ARRIVAL**	**Jörg Wrachtrup**	**Tobias Hertel**	**Laszlo Forro**	**Fedor Jelezko**	
14:45-15:30		**Sergey Tarasenko** Victor Kleshch	**Larry Luer**	Marina Avramenko Kerstin Müller Gennady Mikheev	Yuri Pershin Chi Chen Jonathan Houard	
15:30-15:45		Coffee Break	Coffee Break	Coffee Break	Coffee Break	
15:45-16:15		**Amir Boag**	**Elena Obraztsova**	**Jin Zhang**	**Yan Li**	
16:15-16:30			Tommi Kaplas	Mikhail Shuba	Lili Zhang	
16:30-16:45		Paul Fedotov	Yue Zhang	Georgy Fedorov	Yuri Shunin	
16:45-17:15	**Andrea Ferrari**	Alexander Osadchy Imge Namal	Qin Wang Zhi Yang	Diao Li Cai-bin Yu	Sophia Bokova-Sirosh **CLOSING**	
17:15-18:00						
18:00-19:30	Welcome Dinner	Dinner	Dinner	Dinner	NPO reception and Saimaa boat trip	
19:30-22:00			Poster Session I	Poster Session II		

Workshop Co-Chairs

Esko Kauppinen, Aalto University, Finland
Alexander Obraztsov, M.V. Lomonosov Moscow State University, Russia
Yuri Svirko, University of Eastern Finland, Finland

Program Committee

Hiromichi Kataura, AIST, Japan
Guglielmo Lanzani, Politecnico di Milano, Italy
Elena Obraztsova, A. M. Prokhorov General Physics Institute, Russia

Organizing Committee

Hannele Karppinen
Dmitry Lyashenko
Yuri Svirko

NPO2016 Sponsor Organisations

UNIVERSITY OF EASTERN FINLAND

JOENSUUN YLIOPISTO Tukisäätiö

Institute of Photonics

SUOMEN KULTTUURIRAHASTO

Welcome to NPO2016

We are pleased to welcome you to the 5th International Workshop on Nanocarbon Photonics and Optoelectronics (NPO2016) that continues a series of meetings organized by the University of Eastern Finland. UEF joins forces with the Aalto University to organize this year's event. Since 2008, NPO Workshops bring together research leaders from both academia and industry to discuss the latest achievements in this rapidly developing area of modern physics and nanotechnology, with strong focus on new carbon nanomaterials. The Workshops are also of strong educational importance allowing young researchers and students to attend lectures given by senior scientists and to be involved in intensive ideas exchange and networking. We hope that you will enjoy both scientific and social program of NPO2016.

The NPO2016 has attracted more than 100 researchers and students from around the globe. The Proceedings of the Workshops will be published in the special issue of Journal of Nanophotonics and will be available for downloading.

We are grateful to our sponsors for their financial backing, which has allowed us to provide travel support to our lecturers and to reduce the participation fee. The Workshop venue is Holiday Club Saimaa at Imatra in Eastern Finland, located on the shores of the lake Saimaa, whose broad waters and numerous islands offer magnificent scenery. We hope that the NPO2016 will expand on the success of previous Workshops and will provide its participants with the opportunity to enjoy the beauty of Finnish Lakeland.

Esko I. Kauppinen
Alexander Obraztsov
Yuri Svirko
NPO2016 Co-Chairs

Contents

Monday, August 1

©A. Obraztsov

The Roadmap for Applications of Graphene and Related Materials

Andrea Ferrari
Cambridge Graphene Centre, Engineering Department, University of Cambridge, 9, JJ Thomson Avenue, Cambridge, CB3 0F, UK

Disruptive technologies are usually characterised by universal, versatile applications, which change many aspects of our life simultaneously, penetrating every corner of our existence. In order to become disruptive, a new technology needs to offer not incremental, but dramatic, orders of magnitude improvements. Moreover, the more universal the technology, the better chances it has for broad base success. The Graphene Flagship has brought together universities, research centres and companies from most European Countries. At the end of the ramp-up phase significant progress has been made in taking graphene, related layered materials and hybrid systems from a state of raw potential to a point where they can revolutionize multiple industries. I will overview the progress done thus far and the future roadmap.

Tuesday, August 2

©J. Turunen

Towards 2D and 1D Heterostructures for Optoelectronics

E. Gaufres[1], A. Favron[2], F. Fossard[1], N.Tang[3], V. Gosselin[2], M. Côté[2], R. Martel[3] and A. Loiseau

[1]Laboratoire d'Etude des Microstructures, UMR 104 CNRS-Onera, Châtillon, France
[2]Regroupement Québécois sur les Matériaux de Pointe (RQMP) and Département de physique, Université de Montréal, Montréal QC H3C 3J7, Canada
[1]RQMP and Département de chimie, Université de Montréal, Montréal QC H3C 3J7, Canada
annick.loiseau@onera.fr

The field of two-dimensional materials has been gradually enriched by new structures such as hexagonal Boron Nitride (hBN) dichalcogenides (e.g MoS_2), Black Phosphorus… These nearly zero thickness crystals exhibit fundamental properties that, when strongly interacting in layered heterostructures, can offer new paradigms for photonics, electronics or magnetism.

In the first part of this talk, we focus on Black phosphorus and present some spectroscopic insights of exfoliated layers of this material (1) that highlight the potential of P(black) based Van der Waals heterostructures. First we discuss the quantum oxidation mechanism responsible for the high reactivity of P(black) on air based on combined Raman and TEM-EELS (Electron Energy Loss Spectroscopy) measurements and how this mechanism can be used for preparing suitable samples. Then we show that Electron Energy Loss Spectroscopy (EELS) in the 1eV-50eV range, coupled with *ab initio* calculations, provides a unique approach to the anisotropic dielectric response of P(Black) at the nanoscale. Indeed, thanks to its angular resolution, our EELS set-up implemented in a TEM –STEM machine is capable to probe excitonic effects, optical transitions and plasmons dispersions as a function of the q momentum, for selected crystallographic orientations in the Brillouin zone of different symmetries. Finally we apply this spectroscopy on other 2D materials involved in heterostructures such as hBN and MoS_2.

The quantum confinement phenomena and interlayer effects that are now scrutinized in 2D materials and their heterostructure also fully make sense for 1D hybrids based on SWCNT or BNNT. As an illustration of this consistency, we will show in the second part of the talk, that the control of the 1D aggregation of active molecules inside nanotube, observed by Raman and EELS hyperspectral imaging (2), enables the observation of original and specific optical properties (3). These confinement effects represent a great interest in various applicative fields such as multispectral bio-detection, multiplexing and super-dyes.

[1] Favron et al. Photooxidation and quantum confinement effects in exfoliated black phosphorus. Nature Materials 14, (2015)
[2] Gaufrès et al Isothermal encapsulation of sexithiophene in SWCNT (submitted)
[3] Gaufrès et al. Giant Raman scattering from J-aggregated dyes inside carbon nanotubes for multispectral imaging Nature Photonics, 8, (2014)

Electrical transport and electron-phonon coupling in suspended mono- and bilayer graphene

Antti Laitinen[1], Mika Oksanen[1], Aurélien Fay[1], Manohar Kumar[1], Daniel Cox[1], Matti Tomi[1], Pauli Virtanen[1], Bernard Plaçais[2,1], and Pertti Hakonen[1]

[1]*Low Temperature Laboratory, Dept. Appl. Phys., Aalto University, FI-00076 AALTO*
[2]*Laboratoire Pierre Aigrain, Ecole Normale Supérieure, 75231 Paris, France*
pertti.hakonen@aalto.fi

Electron-phonon coupling is the basic means to control energy transport in a variety of devices which provide extreme sensitivity in calorimetry, bolometry, and radiation detection (infra red/THz). Owing to thermal noise, such devices are typically operated at cryogenic temperatures, at which the coupling between electrons and phonons becomes weak in clean samples [1]. Under these conditions, graphene is expected to have an advantage owing to its small heat capacity that allows fast operation even though its electron-phonon coupling becomes exceedingly small near the Dirac point.

This talk summarizes our results on electron-phonon coupling obtained using electrical transport experiments on both mono- and bilayer suspended graphene [2,3]. In monolayer samples, our experiments indicate strong "supercollision cooling" due to the presence of ripples in suspended graphene. In the high temperature limit, our results yield the first demonstration of the T^5 dependence for the electron-phonon heat transfer. In the low-T limit, our results indicate quadratic dependence on the chemical potential, which is a characteristic signature of non-conventional cooling processes. This μ^2 behavior is in line with the cross-over, found at $T \sim \mu/k_B$, from the quintic high-T behavior to cubic in the low-T regime. On the contrary, we find that electron-optical phonon scattering dominates in bilayer graphene under similar measurement conditions (see Fig. 1). The strength of the scattering follows theoretical expectations with a specific thermal activation behavior, and indicates the presence of electron scattering by zone edge and zone center optical phonons. The connection of our results to results obtained on graphene on substrate [4,5] will also be discussed.

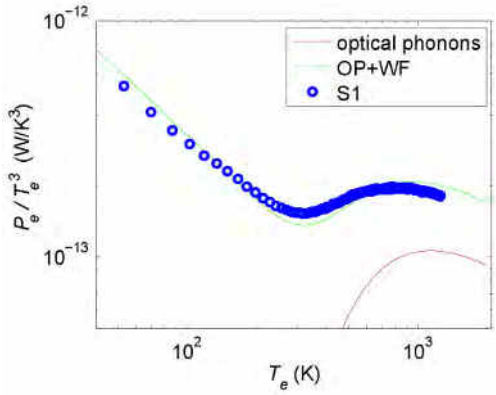

Fig. 1. Measured heat flow from electrons to phonons in a suspended bilayer graphene sample normalized by T_e^3 and displayed as a function of T_e. The green trace illustrates the theoretical curve: the red trace denotes the heat flow due to the optical phonon scattering alone, while the green curve contains additionally the electronic heat conduction. The existing theories are seen to match the data when long wave length longitudinal and transverse optical modes around zone center (Γ-point) are taken into account with additional contributions from zone edge modes (K-point).

Acknowledgement

We acknowledge fruitful discussions with J. Viljas, T. Heikkilä, M. Tomi, and F. Mauri. Our work was supported by the Academy of Finland (Contracts No. 135908 and No. 250280, LTQ CoE). The research leading to these results has received funding from the European Union Seventh Framework Programme under Grant Agreement No. 604391 Graphene Flagship, and the work benefited from the use of the Aalto University Low Temperature Laboratory infrastructure. M.O. is grateful to Väisälä Foundation of the Finnish Academy of Science and Letters for a scholarship.

References

[1] J. C. W. Song, M. Y. Reizer, and L. S. Levitov, Phys. Rev. Lett. **109**, 106602 (2012).
[2] A. Laitinen, *et al.*, Nano Lett. **14**, 3009 (2014).
[3] A. Laitinen, M. Kumar, M. Oksanen, B. Plaçais, P. Virtanen, and P. Hakonen, Phys. Rev. B **91**, 121414(R) (2015).
[4] A. Fay, *et al.*, Phys. Rev. B **84**, 245427 (2011).
[5] D. Cox, *et al.*, to be published.

Tabby Graphene

T. Makarova[1,2] A. Zyrianova[2], A. Okotrub[3], L. Bulusheva[3]

[1]*Lappeenranta University of Technology, FI-53851 Lappeenranta, Finland.*
[2]*Ioffe Physical Technical Institute, Polytechnicheskaya 26, 194021 St. Petersburg, Russia*
[3]*Nikolaev Institute of Inorganic Chemistry SB RA3, 630060, Novosibirsk, Russia*
Corresponding author e-mail: tatyana.makarova@lut.fi

”Zigzag” is the magic word in the graphite/graphene world: a zigzag edge changes the electronic structure of the whole sheet causing a plethora of intriguing phenomena: electronic, optical, thermodynamic, and unconventional magnetism. For graphene society, “Zigzag Edge Magnetism” is essentially the same phenomenon as Santa Claus: (i) Everyone believes in it; (ii) Everyone expects generous gifts; (iii) deep inside everyone suspects it does not exist. The reason is very simple: zigzag edge is very reactive and immediately becomes contaminated; zigzag edges are energetically unstable and undergo reconstruction via the Stone-Wales transformations. We synthesized a novel graphene derivative decorated by zigzag interfaces instead of edges and measured strong one-dimensional magnetism in this two-dimensional material [1]. We realized the peculiar Zigzag Edge States at interfaces by slow fluorination of graphite, which during the synthesis expands into graphenes. The fluorine chains are oriented chaotically with average length of 8 atoms. That’s why we call this material Tabby. Tabby is a pattern of kitty’s coat with tiger strips and leopard spots. Retention of π-electron system results in different electronic properties of Tabby graphene compared to fully functionalized graphene derivatives, which are insulators. Tabby graphene is luminescent, and the colour depends on the C/F ratio. Indeed, it contains confined islands of π-electron system, i.e. quantum dots. Do not try to attract Tabby graphene with a magnet. Graphene is a two-dimensional plane, whereas the stripes are one-dimensional lines. This magnetic configuration is called spin ladder. We entered an intriguing and surprising area for graphene: quantum antiferromagnetism which might further result in strongly correlated behaviours such as spin liquid, spin ice, spin Peierls states, etc.

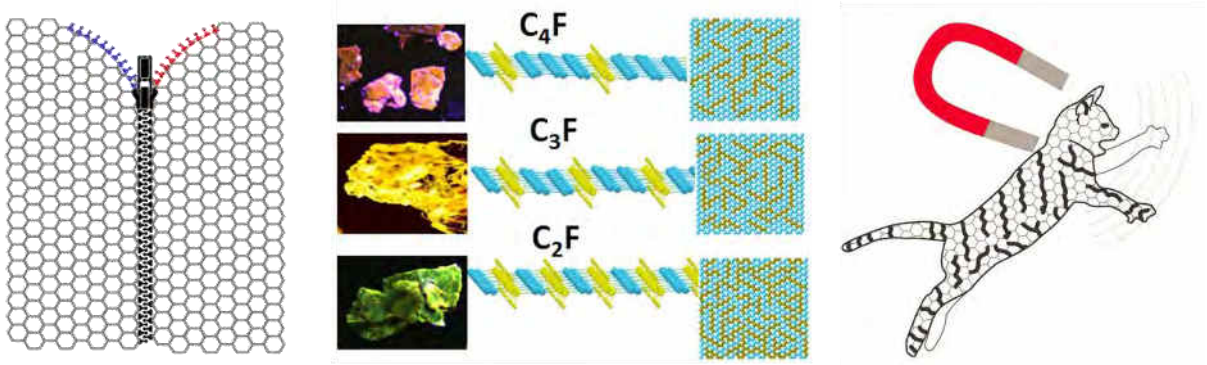

Fig. 1. Semiconducting and magnetic, transparent and luminescent: these properties make Tabby graphene unique

Acknowledgement.
Supported by FP7 MSCA project MagNonMag-295180"Magnetic order induced in nonmagnetic solids".

References

[1] T. Makarova, A. Shelankov, A. Zyrianova, A. Veinger, T. Tisnek, E. Lähderanta, A. Shames, A. Okotrub, L. Bulusheva, G. Chekhova, D. V. Pinakov, I. P. Asanov & Ž. Šljivančanin, Edge state magnetism in zigzag-interfaced graphene via spin susceptibility measurements, Scientific reports. 5 (2015) 13382.

Chiral Atomically Thin Films

Cheol-Joo Kim[1*], A. Sánchez-Castillo[2], Zack Ziegler[1], Yui Ogawa[1,3], Cecilia Noguez[4] and Jiwoong Park[1,5*]

[1]*Department of Chemistry and Chemical Biology, Cornell University, Ithaca, New York 14853, USA.*
[2]*Escuela Superior de Apan, Universidad Autónoma del Estado de Hidalgo, Chimalpa Tlalayote, Municipio de Apan, Hidalgo 43920, México.*
[3]*Institute for Materials Chemistry and Engineering, Kyushu University,Kasuga, Fukuoka 816-8580, Japan.*
[4]*Instituto de Física, Universidad Nacional Autónoma de México, Apartado Postal 20-364, México D.F. 01000, México.*
[5]*Kavli Institute at Cornell for Nanoscale Science, Cornell University, Ithaca, New York 14853, USA.*
Corresponding author e-mail: ck389@cornell.edu, jpark@cornell.edu

Chiral materials possess left- and right-handed counterparts linked by mirror symmetry. These materials are useful for advanced applications in polarization optics[1,2], stereochemistry[3,4] and spintronics[5]. In particular, the realization of spatially uniform chiral films with atomic-scale control of their handedness could provide a powerful means for developing nanodevices with novel chiral properties. However, previous approaches based on natural or grown films[1,2], or arrays of fabricated building blocks[6–8], could not offer a direct means to program intrinsic chiral properties of the film on the atomic scale. Here, we report a chiral stacking approach, where two-dimensional materials are positioned layer-by-layer with precise control of the interlayer rotation (θ) and polarity, resulting in tunable chiral properties of the final stack.[9] Using this method, we produce left- and right-handed bilayer graphene, that is, a two-atom-thick chiral film. The film displays one of the highest intrinsic ellipticity values (6.5 deg μm^{-1}) ever reported, and a remarkably strong circular dichroism (CD) with the peak energy and sign tuned by θ and polarity. We show that these chiral properties originate from the large in-plane magnetic moment associated with the interlayer optical transition.[10] Furthermore, we show that we can program the chiral properties of atomically thin films layer-by-layer by producing three-layer graphene films with structurally controlled CD spectra. Our approach, which is generally applicable to other layered materials, can provide a powerful platform for generating and integrating ultrathin devices based on chiral metamaterials with programmed interactions with other chiral objects, including photons, molecules, and spin polarized electrons.

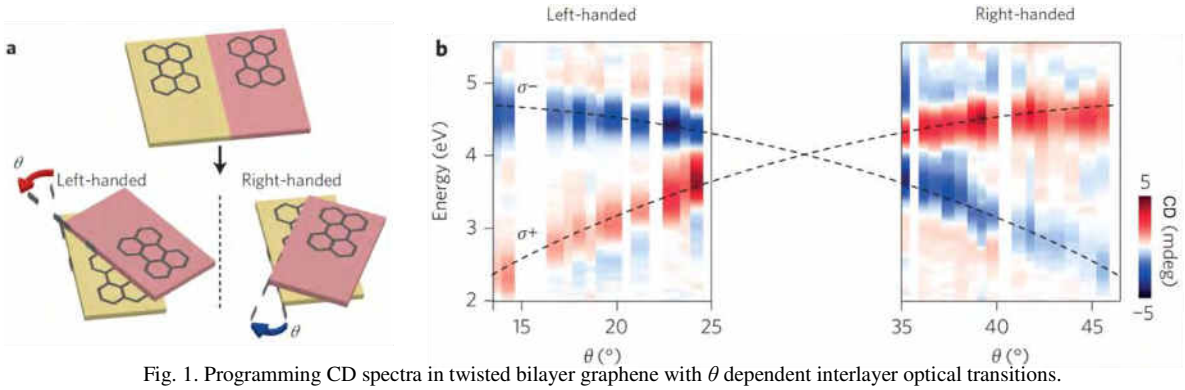

Fig. 1. Programming CD spectra in twisted bilayer graphene with θ dependent interlayer optical transitions.

Acknowledgement

This work was supported by the National Science Foundation (NSF) through the Cornell Center for Materials Research (NSF DMR-1120296), the AFOSR (FA2386-13-1-4118), and the Nano Material Technology Development Program through the National Research Foundation of Korea (NRF) funded by the Ministry of Science, ICT, and Future Planning (2012M3A7B4049887). Y. Ogawa was partially supported by Grant-in-Aid for JAPS Fellows. A. Sánchez-Castillo and C. Noguez were supported by DGAPA-UNAM(PAPIIT IN107615) and CONACyT (179454). Sample fabrication was performed at the Cornell Nanoscale Science & Technology Facility, a member of the National Nanotechnology Infrastructure Network, which is supported by the National Science Foundation (ECS-0335765).

4. References

1. Y. Tang and A. E. Cohen, Phys. Rev. Lett. **104**, 163901 (2010).
2. L. D. Barron, *Molecular Light Scattering and Optical Activity* (Cambridge Univ.Press, 2009).
3. M. B. Smith and J. March, *March's Advanced Organic Chemistry: Reactions, Mechanisms and Structure* (Wiley, 2007).
4. Y. Inoue and V. Ramamurthy, *Chiral Photochemistry* (Marcel Dekker, 2004).
5. B. Göhler *et al*, Science **331**, 894–897 (2011).
6. M. Kuwata-Gonokami *et al*, Phys. Rev. Lett. **95**, 227401 (2005).
7. J. G. Gibbs, A. G. Mark, S. Eslami and P. Fischer, Appl. Phys. Lett. **103**, 213101 (2013).
8. K. E. Shopsowitz, H. Qi, W. Y. Hamad and M. J. Maclachlan, Nature **468**, 422–425 (2010).
9. L. Brown *et al*, Nano Lett. **14**, 5706–5711 (2014).
10. R. W. Havener, Y. Liang, L. Brown, L. Yang and J. Park, Nano Lett. **14**, 3353–3357 (2014).

Ion-gating control of optical properties in 2D semiconductors

Taishi Takenobu
Department of Applied Physics, Nagoya University, Nagoya 464-8603, Japan
takenobu@nuap.nagoya-u.ac.jp

Recently, transition metal dichalcogenide (TMDC) monolayers, such as molybdenum disulfide (MoS_2) and tungsten diselenide (WSe_2), have attracted strong attention as novel two-dimensional (2D) semiconducting materials due to their large bandgap (1−2 eV) and excellent transport properties. Moreover, the thickness of monolayer TMDCs is less than 1 nm, which is one of the thinnest materials, and it leads to strong confinement effects, resulting in large binding energy of exciton (> 100 meV) and formation of charged excitons. Particularly, due to their layered structure, there are no dangling-bond states on the surface of TMDC monolayers and it could be an ideal quantum well. Here, we will report the optical functionalities of TMDC monolayers.

In this study, we fabricated ion-gel-gated electric double layer transistors (EDLTs) using large-area TMDC monolayers, MoS_2, WS_2 and WSe_2, grown by chemical vapor deposition [1-8]. The Fermi level of TMDCs can be continuously shifted by applying gate voltage, and we can induce both hole and electron transport in these devices. The hole mobility of WSe_2 can be enhanced up to 90 cm^2/Vs at high carrier density of 10^{14} cm^{-2}, whereas the MoS_2 showed electron mobility of 60 cm^2/Vs. By the combination of MoS_2 and WSe_2, we have demonstrated CMOS inverters [9].

Using EDLT technique, we investigated the optical functionalities of TMDC monolayers. As the first step, the electric field modulation spectroscopy of TMDC monolayers was performed by electric double layer capacitors (EDLCs). Interestingly, The PL spectra of TMDC EDLCs revealed clear peak shifts (~10 meV) and it is the direct signature of quantum confined Stark effect. Based on these successes, we fabricated both electric double layer photodetectors (EDLPD) and light-emitting diodes (EDLED), and the both opto-electric and electro-optic conversion were successfully demonstrated. Finally, we investigated the strength of the Stark effect in WSe_2 EDLED and the giant Stark effect (~40 meV) was realized, suggesting the extremely strong electric field due to electric double layers.

References

[1] J. Pu, L.-J. Li, T. Takenobu, et al., Nano Lett. **12**, 4013 (2012).
[2] J.-K. Huang, T. Takenobu, L.-J. Li, et al., ACS Nano. **8**, 923 (2014).
[3] J. Pu, L.-J. Li, T. Takenobu, et al., Appl. Phys. Lett., **103**, 23505 (2013).
[4] J. Pu, L.-J. Li and T. Takenobu, Phys. Chem. Chem. Phys., 10.1039/C3CP55270E (2014).
[5] Y.-H. Chang, T. Takenobu, L.-J. Li, et al., ACS Nano. **8**, 8582 (2014).
[6] C.-H. Chen, T. Takenobu, L.-J. Li, et al., 2D Materials, **1**, 034001 (2014).
[7] L. Chu, T. Takenobu, G. Eda, et al., Scientific Reports, **4**, 7293 (2014)
[8] K. Funahashi, L.-J. Li, T. Takenobu, et al., Jpn. J. Appl. Phys. **54**, 06FF06 (2015).
[9] J. Pu, L.-J. Li, T. Takenobu, et al., Adv. Mater., accepted.

Photoresponse in magnetic topological insulators

Naoki Ogawa
RIKEN Center for Emergent Matter Science (CEMS), Wako, Saitama 351-0198, Japan
naoki.ogawa@riken.jp

Doping topological insulators (TIs) with magnetic elements brings about essential modifications in their originally mass-less surface states, providing a new path towards exotic physics and future applications. Examples are the quantized magnetoelectric effects [1] and quantum anomalous Hall (QAH) effects [2,3], which would materialize dissipation-less electronics. The nonequilibrium electron/spin dynamics at the modified Dirac states induced by doped magnetic moments are still elusive, possibly unveiling additional functions of TIs, such as highly-efficient photon to spin-current conversion. Furthermore, with the progress of film fabrication techniques including superlattices and modulation dopings [4], variety of cooperative phenomena between two surface states (top and bottom of a film) would be explored.

In this paper, we discuss several optical phenomena observed recently in thin films of (magnetic) topological insulators; (i) generation of large zero-bias photocurrent resulting from magnetic modifications of the Dirac states, (ii) enhancement of photogalvanic current by chemically tuning the Fermi energy, and (iii) topological magnetoelectric effects (giant Faraday and Kerr rotations).

When a TI is doped with magnetic elements, such as Cr, its easy-axis anisotropy induces an energy gap at the Dirac point [5] [Fig. 1(a)]. The surface-state dispersion recovers to be mass-less by the application of in-plane magnetic field (e.g., B_y), due to the in-plane helical nature of its spin state, and further shifts/deforms through the Zeeman effect [Fig. 1(b)]. In this situation, the photoexcitation at $+k_x$ and $-k_x$ becomes non-equivalent, even for non-polarized photons, leading to a finite spin-polarized photocurrent j_x [6]. We realized that this zero-bias photocurrent dramatically increases for the mid-infrared photoexcitation [Fig. 1(c)][7], pointing to the relevance of surface-state dispersion and strong influence of bulk-surface scatterings. It is also demonstrated that it is critical to precisely control the Fermi energy to observe intrinsic nature of TIs. For example, the photogalvanic current [8,9] shows a pronounced peak when we tune the Fermi energy across the Dirac cone [10], and topological magnetoelectric effects appear in the QAH regime [11].

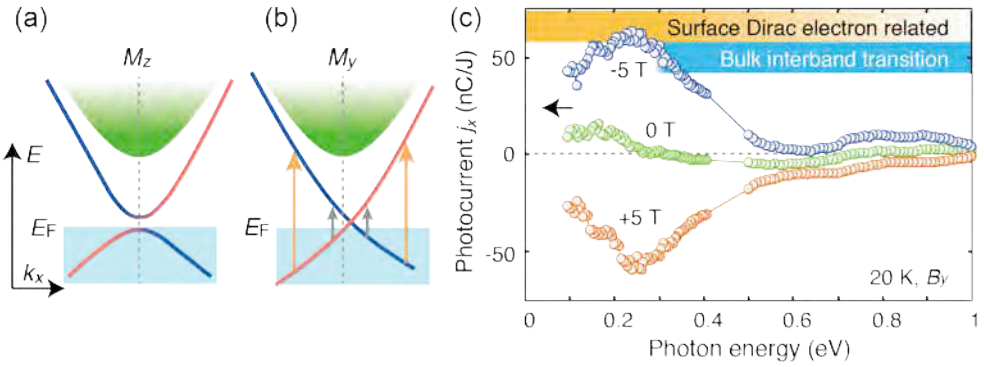

Fig. 1. (a) Dirac mass gap induced by the easy-axis anisotropy of magnetic dopants. (b) Closing of the mass gap and shift/deformation of surface-state dispersions. (c) Photocurrent observed under the in-plane magnetic field. A peak structure around 0.25 eV reflects the *k*-space asymmetry of optical transitions as shown in (b).

This research is supported by the JSPS KAKENHI No. 24224009 and 16K13705.

[1] A. M. Essin, J. E. Moore, and D. Vanderbilt, Phys. Rev. Lett. **102**, 146805 (2009).
[2] C. Z. Chang *et al.,* Science **340**, 167 (2013).
[3] J. G. Chekelsky, R. Yoshimi, A. Tsukazaki, K. S. Takahashi, Y. Kozuka, J. Falson, M. Kawasaki, and Y. Tokura, Nature Phys. **10**, 731 (2014).
[4] M. Mogi, R. Yoshimi, A, Tsukazaki, K, Yasuda, Y. Kozuka, K. S. Takahashi, M. Kawasaki, and Y. Tokura, Appl. Phys. Lett. **107**, 182401 (2015).
[5] I. Lee *et al.,* Proc. Natl. Acad. Sci, **112**, 1316 (2015).
[6] Y. G. Semenov, X. Li, and K. W. Kim, Phys. Rev. B **86**, 201401(R) (2012).
[7] N. Ogawa, R. Yoshimi, K. Yasuda, A. Tsukazaki, M. Kawasaki, and Y. Tokura, Nature Commun. (2016).
[8] J. W. McIver, D. Hsieh, H. Steinberg, P. Jarillo-Herrero, and N. Gedik, Nature Nanotech. **7**, 96 (2012).
[9] N. Ogawa, M. S. Bahramy, Y. Kaneko, and Y. Tokura, Phys. Rev. B **90**, 125122 (2014).
[10] K. N. Okada, N. Ogawa, R. Yoshimi, A. Tsukazaki, K. S. Takahashi, M. Kawasaki, and Y. Tokura, Phys. Rev. B **93**, 081403(R) (2016).
[11] K. N. Okada, Y. Takahashi, M. Mogi, R. Yoshimi, A. Tsukazaki, K. S. Takahashi, N. Ogawa, M. Kawasaki, and Y. Tokura, Nature Commun. (2016), arXiv:1603.02113.

Spin quantum registers and their use in sensing and quantum communication

Jörg Wrachtrup
3rd Institute of Physics and Institute for Quantum Science and Technology IQST, University of Stuttgart, Germany
wrachtrup@physik.uni-stuttgart.de

Small spin quantum registers have a central role in various quantum techniques. Scalable communication and quantum repeater schemes for example require few qubit memories to store single photon states, which need to be robust against multiple readout. They also need to have local processing capabilities for e.g. error correction of entanglement purification. Less prominent is the use in sensing application. Here, robust memories are central for e.g. high resolution NMR. Entanglement enables high precision measurement, both with respect to sensitivity and spectral resolution. The talk shall discuss the physics of nuclear spin quantum registers in diamond and SiC as processing and memory qubits under relevant operation conditions and demonstrate applications.

Fine structure of Si-vacancy spin qudits in silicon carbide

S. A. Tarasenko
Ioffe Institute, 194021 St. Petersburg, Russia
tarasenko@coherent.ioffe.ru

The vacancy-related spin centers in silicon carbide (SiC), a material compatible with Si-MOS technology, are promising for the realization of sensors and quantum information devices. The silicon vacancy (V_{Si}) in SiC possesses the half-integer spin 3/2; its spin states can be selectively initialized and read-out by optical means and efficiently manipulated by a radiofrequency (RF) field [1-4]. The high half-integer spin of the Si vacancy provides additional degree of freedom and functionality.

Here, we discuss the fine structure of V_{Si} centers in zero and external magnetic fields, which is a key to understanding the spin dynamics and relaxation processes. We show that the C_{3v} point group of the V_{Si} center imposed by the real atomic arrangement of the vacancy gives rise to additional terms in the spin Hamiltonian, which are absent in axial models. Particularly, the trigonal pyramidal symmetry of the V_{Si} center enables the ``forbidden'' RF field-driven spin transitions with a change in the spin projection $\Delta m = \pm 2$ ($\nu_3$ and $\nu_4$ lines in Fig. 1). As compared to the commonly studied ``allowed'' spin transitions with $\Delta m = \pm 1$ (ν_1 and ν_2 lines in Fig. 1), they are induced by counter circularly polarized radiation and their energies shift with the double slope in the magnetic field. Comparison with the experimental data on optically detected magnetic resonance (ODMR) allows us to determine the parameters of the spin Hamiltonian [5].

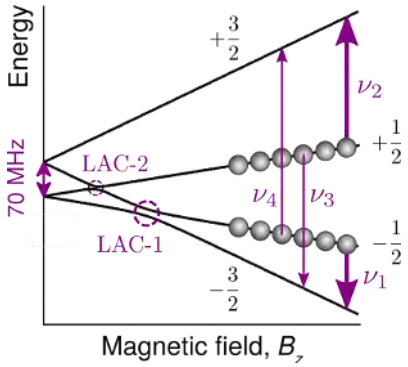

Fig. 1. Spin structure of the V_{Si} center in magnetic field. Vertical arrows denote ``allowed'' ($\nu_1$ and $\nu_2$) and ``forbidden'' (ν_1 and ν_2) transitions.

In an external magnetic field, the otherwise degenerate sublevels $m = \pm 1/2$ as well as $m = \pm 3/2$ split and, at certain fields, one observes the level anticrossings (LACs in Fig. 1): LAC-1 between the states with $\Delta m = 1$ and LAC-2 between the states with $\Delta m = 2$. The intensity of photoluminescence demonstrates resonance-like behavior in the vicinity of the LACs. The sharpest resonance is detected for the level anticrossing with $\Delta m = 2$, determined by the parameters related to the trigonal pyramidal symmetry of the V_{Si} center. This phenomenon can be used for a purely optical sensing of dc magnetic fields, without a need for the application of a RF field, with nanotesla resolution [5]. The effect is robust up to at least 500 K, suggesting a simple, contactless method to monitor weak magnetic fields in a broad temperature range. The proposed method can potentially be extended to RF-free sensing of other physical quantities, particularly, temperature and axial stress.

References

[1] H. Kraus, V.A. Soltamov, D. Riedel, S. Väth, F. Fuchs, A. Sperlich, P.G. Baranov, V. Dyakonov, and G.V. Astakhov, Nat. Physics **10**, 157 (2014).
[2] D.J. Christle, A.L. Falk, P. Andrich, P.V. Klimov, J. Hassan, N.T. Son, E. Janzén, T. Ohshima, and D.D. Awschalom, Nat. Materials **14**, 160 (2015).
[3] M. Widmann, S.-Y. Lee, T. Rendler, N.T. Son, H. Fedder, S. Paik, L.-P. Yang, N. Zhao, S. Yang, I. Booker, A. Denisenko, M. Jamali, S.A. Momenzadeh, I. Gerhardt, T. Ohshima, A. Gali, E. Janzén, and J. Wrachtrup, Nat. Materials **14**, 164 (2015).
[4] D. Simin, H. Kraus, A. Sperlich, T. Ohshima, G. V. Astakhov, and V. Dyakonov, arXiv:1602.05775 (2016).
[5] D. Simin, V.A. Soltamov, A.V. Poshakinskiy, A.N. Anisimov, R.A. Babunts, D.O. Tolmachev, E.N. Mokhov, M. Trupke, S.A. Tarasenko, A. Sperlich, P.G. Baranov, V. Dyakonov, and G.V. Astakhov, arXiv:1511.04663 (2015).

Coulomb Blockade of Field Emission from Diamond Needle

V.I. Kleshch[1,*], S. Mingels[2], D. Lützenkirchen-Hecht[2], G. Müller[2], and A.N. Obraztsov[1,3]
[1]*Department of Physics, M.V. Lomonosov Moscow State University, Moscow, Russia*
[2]*School of Mathematics and Natural Sciences, Physics department, University of Wuppertal, Wuppertal, Germany*
[3]*Department of Physics and Mathematics, University of Eastern Finland, Joensuu, Finland*

[*]*Corresponding author e-mail: klesch@polly.phys.msu.ru*

An observation of a Coulomb staircase in the current-voltage characteristic of field emission (FE) from a single crystal diamond needle at room temperature is reported. The diamond needles were produced by selective oxidation of polycrystalline CVD diamond films [1]. The needles had shape close to a square-based pyramid with a height of ~50 μm, a thickness at the base of ~1 μm and a tip apex radius of ~50 nm. FE was observed from the apex of a needle using an UHV system equipped with an electron spectrometer.

At FE currents below 100 nA the needles demonstrated a strong saturation in the Fowler-Nordheim (FN) plots usually observed for highly resistive emitters. At higher current the needles underwent abrupt decrease of the resistance and consequently their FN plots became much less saturated. After this transformation the FE current increased in a step-like fashion during the voltage ramp. Such staircase behavior was previously predicted theoretically for nanoscale field emitters and explained by the Coulomb blockade effect [2].

Transmission electron microscopy (TEM), Raman spectroscopy and electron energy loss spectroscopy (EELS) were used to characterize structural changes after the FE experiment. It was found that the diamond needle is covered by a layer of amorphous carbon which is responsible for the resistance decrease. Furthermore, the TEM revealed a nanoscale protrusion on the apex of the needle which can explain Coulomb blockade behavior. The analysis of the obtained data and discussion of the results will be presented.

This work was supported by Russian Science Foundation (Grant No. 14-12-00511).

The work at the University of Wuppertal is funded by the German Federal Ministry of Education and Research BMBF under the Contract No. 05K13PX2.

[1] A. N. Obraztsov, P. G. Kopylov, A. L. Chuvilin, N. V. Savenko, Diamond and Related Materials, **18**, 1289 (2009).
[2] O. E. Raichev, Physical Review B, **73**, 195328 (2006).

Ultra-Wideband Nano-Antenna Arrays

Nadav Neuberger, Zeev Iluz, and Amir Boag
School of Electrical Engineering, Tel Aviv University, Tel Aviv 69978, Israel
boag@eng.tau.ac.il

1. Introduction

Efficient ultra-wideband nano-antennas are becoming key components for novel photonic applications, such as energy harvesting and optical sensing of particles, fluid refractive index, chemical and biological agents, etc. Downscaling the well-known configurations of metallic antennas from radio to the optical and infra-red (IR) frequencies offers unique advantages for many of these applications. Furthermore, metallic nano-antennas can be loaded with carbon nano-devices to provide specific functionality. Two types of ultra-wideband highly efficient nano-antenna arrays developed by our group are briefly described below. Also, a novel technique for antenna and load impedance measurements using scattering data will be presented. Various applications of nano-antennas will be discussed.

2. Linear-polarized Nano-Antenna Arrays

Dual-Vivaldi nano-antenna (see Fig. 1a) has been proposed to achieve linear-polarized wideband operation at IR and visible frequencies [1]. In this design, two Vivaldi antennas placed on a substrate are operating as a pair (instead of a conventional single element). Such pair of Vivaldi antennas oriented in opposite directions produces the main lobe in the broadside direction (normal to the axes of the antennas), rather than the usual peak gain along the axis (end-fire) of a single Vivaldi antenna. The Dual-Vivaldi nano-antenna arrays were designed, fabricated, and optically characterized in the IR and visible regimes [1]. The radiation efficiency and the spectral response of the antennas were found to be in good agreement with numerical simulations. This nano-antenna has both high radiation efficiency and good impedance matching properties over a wide frequency band. The strong impact of load at the antenna terminals on its scattering response [2] renders the Dual-Vivaldi nano-antennas excellent candidates for optical sensing applications and energy harvesting.

3. Dual-Polarized Nano-Antenna Arrays

A novel nano-antenna array depicted in Fig. 1b is proposed for harvesting and sensing of solar, thermal, and other types of electromagnetic wave energy. This is a dual-polarized receiving array resembling a checkerboard self-complementary geometry [3]. Bimetallic design facilitates implementation of metal-insulator-metal (MIM) rectifiers. Thus, it may be used for wideband energy harvesting and polarimetric sensing at terahertz, IR, and optical frequencies. In polarimetric applications, high isolation between polarizations can be achieved. Moreover, this nano-antenna array design shows high efficiency over a wide range of angles of incidence, high bandwidth, and polarization independence.

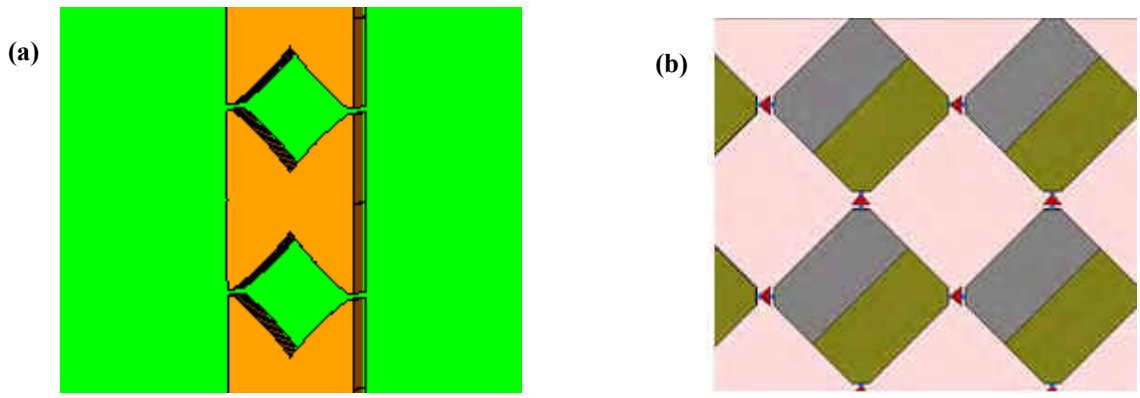

Fig. 1. Nano-antenna arrays: (a) Dual-Vivaldi; and (b) Bimetallic Checkerboard.

4. References

[1] Z. Iluz and A. Boag, "Dual-Vivaldi wide band nano-antenna with high radiation efficiency over the infrared frequency band," *Optics Letters*, **36**(15), 2773-2775 (2011).
[2] Y. Yifat, Z. Iluz, D. Bar-Lev, M. Eitan, Y. Hanein, A. Boag, and J. Scheuer, "High load-sensitivity in wideband infrared dual-Vivaldi nanoantennas," *Optics Letters*, **38**(2), 205–207 (2013).
[3] M. Gustafsson, "Broadband array antennas using a self-complementary antenna array and dielectric slabs," *Ultra-Wideband Short-Pulse Electromagnetics*, **8**, (2007).

Hybrid material based on conductivity type sorted single-wall carbon nanotubes filled with CuCl

Pavel V. Fedotov[*,1], Valentina A. Eremina[1,2], Alexander A. Tonkikh[1,3], Elena D. Obraztsova[1,4]

1 A.M. Prokhorov General Physics Institute, RAS, 38 Vavilov Street, 119991, Moscow, Russia
2 Physics Department of M.V. Lomonosov Moscow State University, 1 Leninskie gory Street, 119234, Moscow, Russia
3 Southern Federal University, Faculty of Physics, Zorge Street 5, Rostov-on-Don, Russia, 344090
4 National Research Nuclear University MEPhI (Moscow Engineering Physics Institute), 31 Kashirskoe hwy., 115409, Moscow, Russia

fedotov@physics.msu.ru

Single-wall carbon nanotubes (SWCNTs) represent a very attractive material which appears to be promising in various fields of application. One of possible applications is to utilize nanotubes as a transparent conductive material for the future photovoltaic. SWCNT properties can be significantly improved by various functionalization methods. For instance, one can modify SWCNTs properties by filling them with other material and utilize them as nanoscale reactors. To increase their electric conductivity and to decrease optical absorption, it is crucial to fill nanotubes with such material that has strong acceptor/donor behaviour. In this case functionalized SWCNTs become highly doped, which leads to increase of both transparency and electro conductivity.

In this work, we functionalize SWCNTs by filling them with strong acceptor material (CuCl) via a gas phase method [1]. The electrical and optical properties of nanotubes strongly depend on a metallic/semiconducting (m/s) type of SWCNTs. To form m/s SWCNT fractions the arc discharge nanotubes (with an average diameter 1.4 nm) were sorted via ATPE method [2]. To verify the effect of nanotube conductivity type on the properties of the hybrid material CuCl@SWCNT the films containing predominantly metallic or semiconducting SWCNTs were filled with CuCl. The specific optical features of produced CuCl@m-SWCNT and CuCl@s-SWCNT were obtained (Fig. 1).

We demonstrate that the functionalization of both metallic and semiconducting SWCNT films by filling nanotubes with CuCl leads to a significant increase of optical transmittance (above 88% in NIR). We discovered that the best absolute optical transmittance is observed in CuCl@m-SWCNT films. The efficiency of filling and doping with CuCl for metallic-enriched SWCNT fraction has been evaluated to be higher comparing with semiconducting SWCNTs. According to the optical absorption spectroscopy and Raman studies the metallic nanotubes filled with CuCl can serve as electron acceptors for neighbouring semiconducting nanotubes in m/s mixed SWCNTs films.

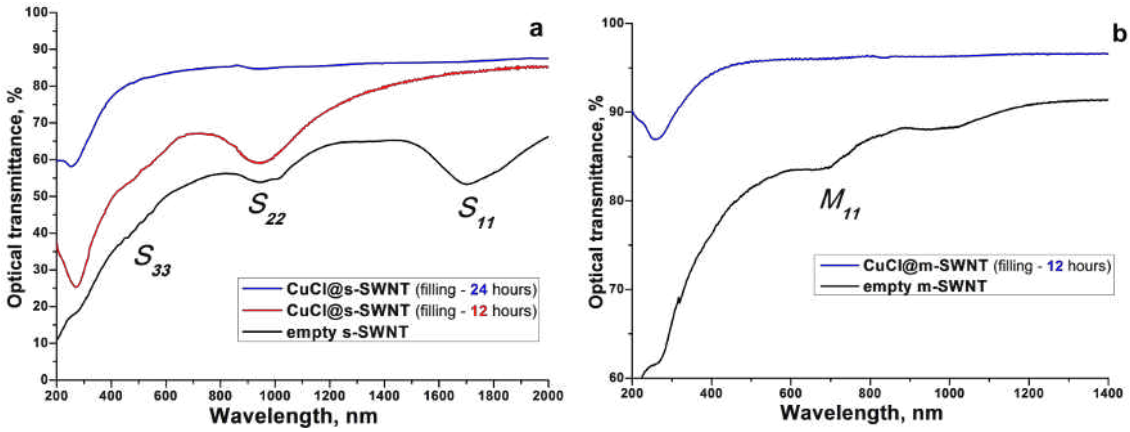

Fig. 1. UV-vis-NIR optical transmittance spectra of s-SWCNT (a) and m-SWCNT (b) films depending on the time exposed to a gas-phase CuCl

The work was supported in frames of project 15-12-30041 of Russian Science Foundation. P.V. Fedotov thanks grant SP-170.2015.3 of Ministry of Education and Science of Russian Federation.

[1] P. V. Fedotov, A. A. Tonkikh, E. A. Obraztsova et al, PSS (b) 251, 2466–2470 (2014).
[2] C. Y. Khripin, J. A. Fagan and M. J. Zheng, Am. Chem. Soc., 135, 6822−6825 (2013).

Computer modeling of edge-terminated carbon nanoribbons

Alexander V. Osadchy [a,b], Elena D. Obraztsova [a,b], Valery V. Savin [c]

[a] *A. M. Prokhorov General Physics Institute, Russian Academy of Sciences, 38 Vavilov Street, Moscow, Russia, 119991*

[b] *National Research Nuclear University MEPhI (Moscow Engineering Physics Institute), 31 Kashirskoye Shosse, Moscow, Russia, 115409*

[c] *Immanuel Kant Baltic Federal University, Nevskogo str., 14, Kaliningrad, Russia, 236041*

aosadchy@kapella.gpi.ru

In this work we present the results of ab-initio investigations of edge-terminated carbon nanoribbons (GNR). The calculations have been performed using the density functional theory (DFT) with decomposition of electronic wave functions into plane waves as implemented in Quantum Espresso software package [1,2]. We performed studies of the effect of different kinds of edge termination on the band structure of graphene nanoribbons. The results showed that the termination by hydrogen and fluorine has very little influence on the structure (fig. 1). Termination by chlorine, bromine and sulfur results in a change of conductivity type from semiconducting to metallic (fig. 2). The reason of the changes is appearing in the band structure new electron dispersion curve crosses diagonally the source band gap of the nanoribbon. At the same time, the band structure of nanoribbons terminated at the edges by alternating atoms of chlorine and hydrogen do not show this change and the diagonal curve is not observed. The obtained information agrees well with the results of recently published experimental studies [3, 4]. This work investigates the patterns of change in the band structure of edge-terminated graphene nanoribbons and analyzed the causes of the observed effects.

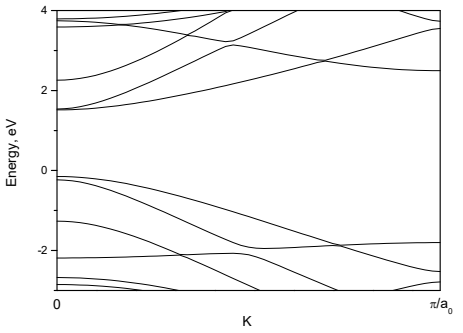

Fig. 1. Electron dispersion curves of H-terminated 7-AGNR

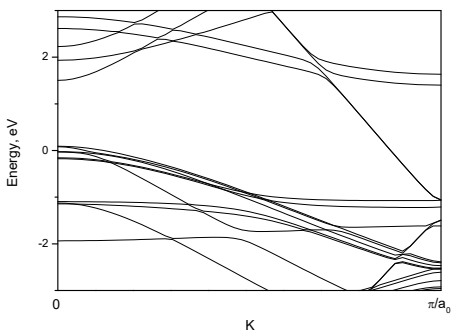

Fig. 2. Electron dispersion curves of Cl-terminated 7-AGNR

This work was supported by RFBR 15-02-09073 A and RAS research programs.

[1] P. Giannozzi et al., *J. Phys. Condens Matter 21, 395502 (2009).*

[2] Arno Schindlmayr, P. Garcia-Gonzalez, et al., *Phys. Rev. B 64, 235106 (2001)*

[3] Alexander I. Chernov, Pavel V. Fedotov, et. al., *ACS Nano, Vol. 7, No. 7, 6346–6353 (2013)*

[4] Rui Li, Ting Hu, Jinming Dong, *Physica E*, *Vol. 49, 76–82 (2013)*

Optical and electronic transport properties of 18 nm to 750 nm thick (6,5) SWNT film networks

Imge Namal[1], Francesca Bottachi[2], Friedrich Schöppler[1], Thomas Anthopoulos[2], Tobias Hertel[1]

[1]*Institute of Physical and Theoretical Chemistry, Faculty of Chemistry and Pharmacy,Julius-Maximilian University Würzburg, Am Hubland, 97074 Würzburg, Germany*

[2] *Department of Physics and Centre for Plastic Electronics, Blackett Laboratory, Imperial College London, London SW7 2BW, United Kingdom*

Thanks to their remarkable light absorption and energy transport characteristics, single wall carbon nanotubes are promising candidates for applications in organic photovoltaics and thin film transistors. Such applications should benefit from scalable production of chirality enriched semiconducting SWNT thin films with low metallic or other type of impurity concentrations.

Here we report on the fabrication and optical as well as electronic characterisation of thin SWNT films using an adaptation of the filtration wet thin film transfer method pioneered by Wu et al[1]. Here, this process has been optimized for use in combination with polymer wrapping for enrichment of (6,5) SWNTs in organic solvents. Thin films with thicknesses ranging from 18 to 750 nm were here deposited on glass, sapphire and silica substrates. Films were characterized optically by absorption and photoluminescence spectroscopy. We find no significant changes in the NIR or VIS range of absorption or emission spectra with film thickness. Likewise the PLQY does not appear to be affected by increasing the film thickness suggesting that electronic devices based on such films should show excellent vertical scaling behaviour.

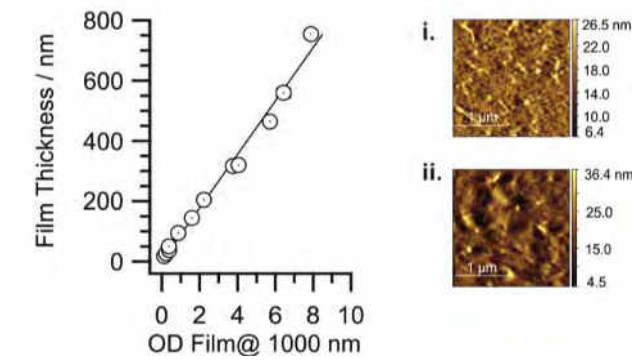

Fig. 1. Dependence of the film thickness on the optical density of the films measured by absorption spectroscopy (i) AFM image of the thinnest film(18 nm) on glass. (ii) AFM image of the thickest film (750 nm) on glass.

Electronic transport properties of thin films were studied by preparing thin film transistors on silica, with varying active layer thicknesses and channel lengths. Carrier mobilities were found to increase linearly with film thickness up to at least 60 nm.

[1]Wu, Z.. *Science* 305, Nr. 5688 (2004): 1273–76.

Wednesday, August 3

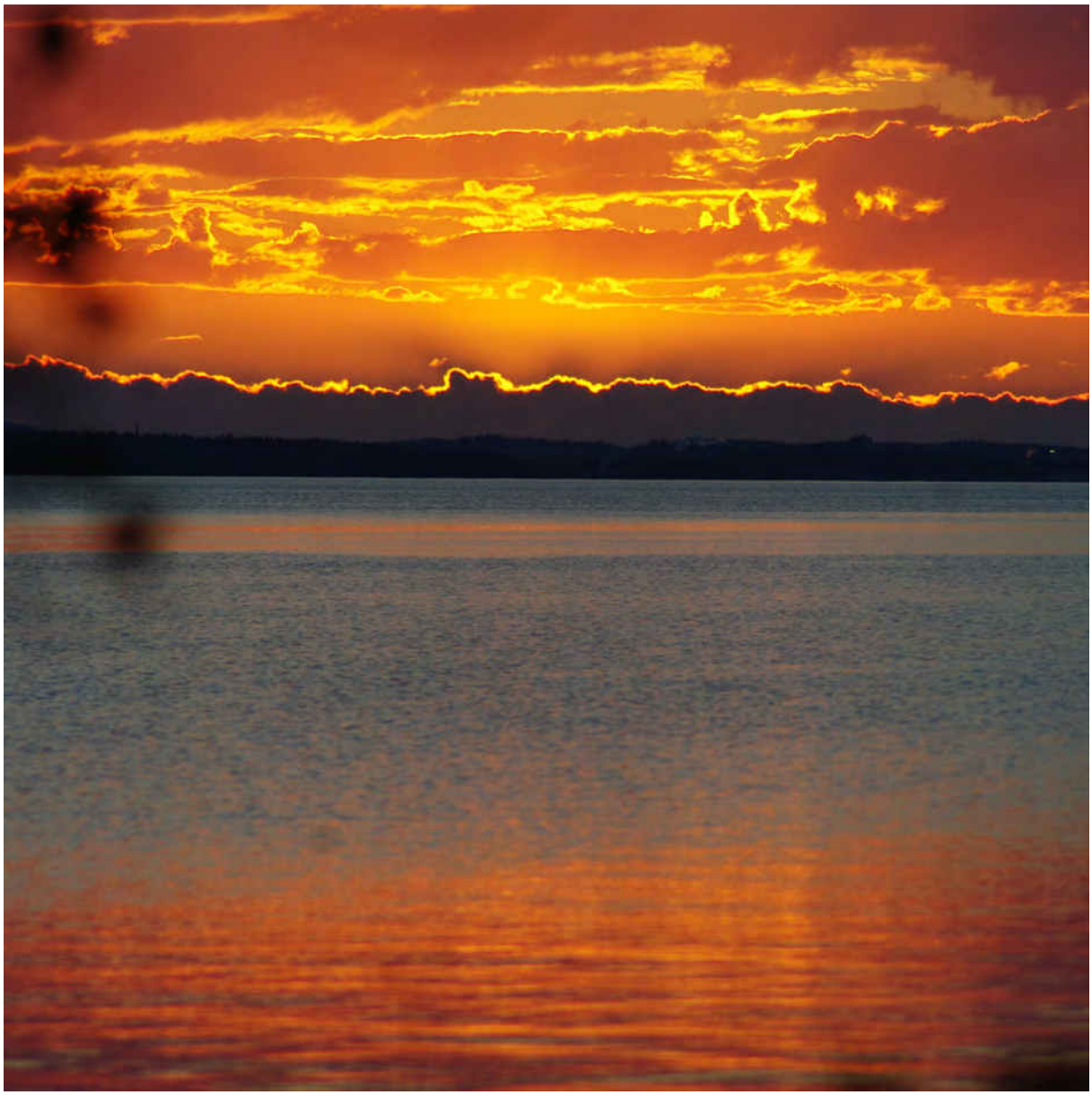

©S. Tutunen

Long tailed trions in MoS_2, and charge and screening signatures in graphene/hBN sandwiches

Jason Christopher[1], Xuanye Wang[2], Bennett Goldberg[1,2,3] and Anna Swan[2,1,3]

[1]Physics Department Boston University 590 Commonwealth Avenue, Boston, MA, 02215, USA
[2]Electrical and computer Engineering Department, Boston University 8 St Mary's street, Boston, MA, 02215, USA
[3]Photonics Center, Boston University, 8 St Mary's street, Boston, MA, 02215, USA
swan@bu.edu

Monolayer MoS2 has emerged as an excellent 2D semiconducting model system because of its two inequivalent, direct-gap valleys that lead to exotic bound and excited states. Here we focus on one such bound state, the negatively charged trion. Since trions are charged particles and are produced in abundance upon photoexcitation makes them interesting candidates for both scientific and technological pursuits because it is possible to control trion transport and density. Unlike excitons, trions can radiatively decay with non-zero momentum by kicking out an electron, resulting in an asymmetric trion photoluminescence (PL) peak with a long low-energy tail [1]. As a consequence, the PL peak position does not correspond to the zero momentum trion energy. Hence, the zero momentum trion energy, E_{0tr}, will be erroneously determined when using a symmetric, Lorentzian peak, which will result in over-estimating the trion binding energy.

Here we show that including the trion's long tail in our analysis we are able to accurately separate the exciton from the trion contributions to the PL spectra. According to theory, the asymmetric energy tail has both a size-dependent and a temperature-dependent contribution. Analysis of the temperature-dependent data reveals the effective trion size, consistent with literature, and the temperature dependence of the band gap and spin-orbit splitting of the valence band. Our model can be used to analyze trions in other systems such as MoSe2 and WSe2 and applied to heterostructures of TMDCs where only the interlayer excitons have been investigated. For interlayer trions, measuring the hole to electron mass ratio via the tail length as presented here would provide significant insight into which material donates the hole and which donates the electrons.

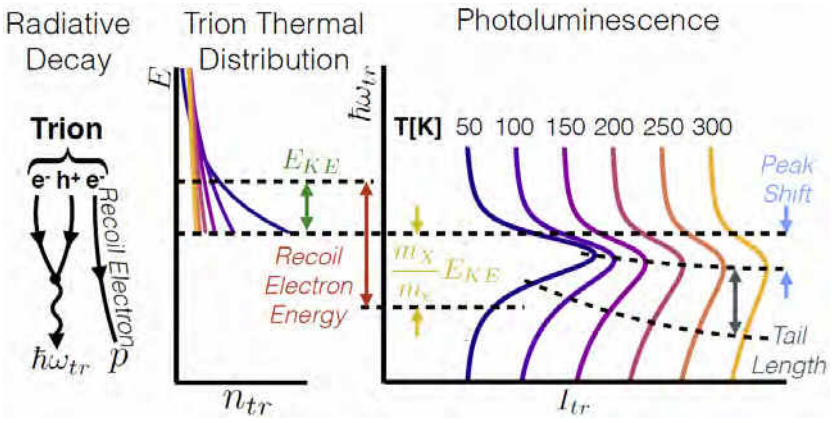

Figure 1. a) The radiative decay of trions allow for optical decay of particles with non-zero momentum. b) The momentum distribution of the trion depends on *T*. c) The recoil electron produces a temperature dependent asymmetric peak shape with a low energy tail.

Raman characterization of graphene has a long and illustrious history. The relative ease, speed, local information and non-destructive measurements makes Raman a valuable characterization tool to determine *e.g.,* strain, charge, layer thickness, defect concentration *etc*. Recent work by Lee *et al*. [2], showed that using statistically significant number of measurements, one can determine a samples local charge and strain state under certain conditions by using the relation between the 2D and G band positions. Here we focus on pristine graphene sandwiched in hBN and show that the Raman 2D peak split can be used as a good measure of very low charge density [3]. We revisit the origin of the asymmetry in the 2D peak that is observed at low doping [4,5] and screening effects on Fermi velocity and the TO phonon dispersion.

[1] Jason Christopher, Bennett Goldberg and Anna Swan, *arXiv*:1605.09741, 2016 - arxiv.org, (2016)
[2] JE Lee, G Ahn, J Shim, YS Lee, S Ryu - *Nature communications*, **3**, 1024 (2012)
[3] Xuanye Wang, Anna K Swan, In preparation. (2016).
[4] S Berciaud, X Li, H Htoon, LE. Brus, SK. Doorn, and TF. Heinz- *Nano Lett.,* **13** 3517–3523, (2013)
[5] Rohit Narula and Stephanie Reich, *Phys. Rev. B*, **90**, 085407, (2014)

Bio-electronics Applications of Carbon Nanotube Thin Films

Yutaka Ohno
Institute of Materials and Systems for Sustainability, Nagoya University, Furo-cho, Chikusa-ku, Nagoya 464-8603, Japan
yohno@nagoya-u.jp

1. Introduction

Flexible, body-worn healthcare/medical devices have the potential to revolutionize preventive medical care and health promotion. Carbon nanotube (CNT) thin films are promising bio-electronic materials for transistors, biosensors, and other passive components to build such wearable devices because of the excellent electronic and mechanical properties and biocompatibility.

In our recent works, we have studied CNT thin film technologies from the growth of CNTs and the thin film formation to device fabrication and characterization on flexible and stretchable films. High-mobility flexible thin-film transistors (TFTs) and their integrated circuits have been realized on a transparent plastic film. We have also demonstrated extreme stretching ability of CNT TFTs on dimethylpolysiloxane (PDMS) thin film. Highly-sensitive, flexible biosensors with excellent uniformity in the sensing property have also been realized.

2. Flexible/stretchable CNT TFTs and ICs

First, we have developed a method to realize high-mobility CNT thin films, based on a gas-phase filtration and transfer process. CNTs were grown by a floating-catalyst CVD technique. The CNT network was collected by filtering through membrane filters at room temperature. The CNT network was transferred from a membrane filter to the substrate with electrodes of TFTs. This technique enables to form CNT films with high mobility and controllable threshold voltage on a plastic film. A TFT fabricated on a Si substrate with the transfer technique exhibited a high mobility of 634 cm^2/Vs with on/off ratio of $6x10^6$.

CNT films can also be used as electrodes and interconnections, which are flexible, transparent, stable, and free of rare metals. By using CNT transparent conductive films, we realized all-carbon TFTs and ICs, in which the electrodes and interconnections consist of CNT film and the insulators consist of PMMA. The all-carbon device was able to be formed into three-dimensional dome-shape devices by the thermo-pressure forming technique. We also demonstrate extreme stretching ability of all-carbon devices fabricated on PDMS thin film.

3. CNT biosensors

One of critical issues of CNT biosensors is reproducibility in terms of device fabrication and characteristics. In this work, uniform and ultra-clean CNT thin film was formed on a plastic film by the dry transfer process based on the floating-catalyst CVD technique. Both amperometric (electrochemical) and potentiometric (field-effect transistor) sensors were fabricated using the CNT thin film. To prevent the contamination, the CNT thin film was covered with an oxide layer during the fabrication process.

The electrochemical property of the CNT-thin film electrode was investigated by measuring cyclic voltammetry with $K_3[Fe(CN)_6]$. The fabricated CNT-thin film electrodes exhibited almost ideal characteristics. The quartile potential was 60.4 mV, which was close to an ideal value of 56.4 mV. The steady-state current (I_{SS}) of the micro-electrodes well-agreed with the theoretical diffusion-controlled I_{SS}. The device-to-device variation in steady state current was less than 6%, showing excellent reproducibility of CNT amperometric sensors.

We also fabricated CNT TFT-based potentiometric sensors on a plastic film (Figure). The device-to-device variation in the drain current was as small as 7%. To detect dopamine, the CNTs were decorated with pyrene-1-boronic acid. The boronic acid chemically react with dopamine, so that, boron is negatively charged. An increase in hole current was observed when dopamine solution was applied. High-sensitivity and wide-range detection of dopamine was confirmed. The limit of sensitivity was 10 pM and the dynamic range was 10^6.

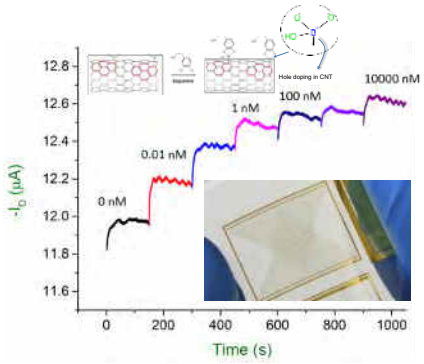

Figure. High-sensitivity detection of dopamine by biosensor based on pyrene-1-boronic-acid-decorated CNT TFT

Experimental Evidence to the Hydrodynamic Electron Flow in Graphene

D. A. Bandurin[1], R. Krishna Kumar[1,4], I. Torre[2,3], M. Ben Shalom[1,5], L. A. Ponomarenko[1,4], I. V. Grigorieva[1], M. Polini[3,6], A. K. Geim[1]

[1]*School of Physics & Astronomy, University of Manchester, Oxford Road, Manchester M13 9PL, UK*
[2]*National Enterprise for nanoScience and nanoTechnology, Scuola Normale Superiore, I-56126 Pisa, Italy*
[3]*Istituto Italiano di Tecnologia, Graphene labs, Via Morego 30 I-16163 Genova (Italy)*
[4]*Physics Department, Lancaster University, Lancaster LA14YB, United Kingdom*
[5]*National Graphene Institute, University of Manchester, Manchester M13 9PL, United Kingdom*
[6]*National Enterprise for nanoScience and nanoTechnology, Istituto Nanoscienze-Consiglio Nazionale delle Ricerche and Scuola Normale Superiore, I-56126 Pisa, Italy*
denis.bandurin@manchester.ac.uk

Theoretical and experimental studies of systems in which particles undergo frequent mutual collisions date back to more than two centuries ago. Transport in such systems is described by hydrodynamic theory that was found very successful in explaining the response of classical liquids and gases to external fields [1]. It has been argued for a long time that collective behaviour of charge carriers in solids can be also treated by hydrodynamic approach. However, there has been almost no direct evidence to hydrodynamic electron transport so far [2]. This is because the conditions at which the hydrodynamic effects become observable are very strict: the electron-electron scattering length should provide the shortest spatial scale in the problem. First of all, this requires ultra clean systems where the scattering at impurities is diminished. Second, the electron-phonon scattering rate should be smaller than that of electron-electron scattering.

Due to weak electron-phonon coupling high mobility graphene devices offer an ideal system to study electron hydrodynamics. To amplify the hydrodynamic effects we employed a special measurement geometry shown in Fig. 1C [3]. The idea is that in case of hydrodynamic electron flow, vortices emerge in the spatial electric current distribution near the current injection contact (Fig.1 B). That results in a development of a negative voltage drop at the nearby contacts (Fig. 1E). We were able to detect such negative signal over the range of temperatures when the electronic system is in a hydrodynamic regime. Finally, we performed a rheological study of electron liquid in graphene. The electron viscosity was found to be an order of magnitude larger than that of honey which is in good agreement with many-body calculation.

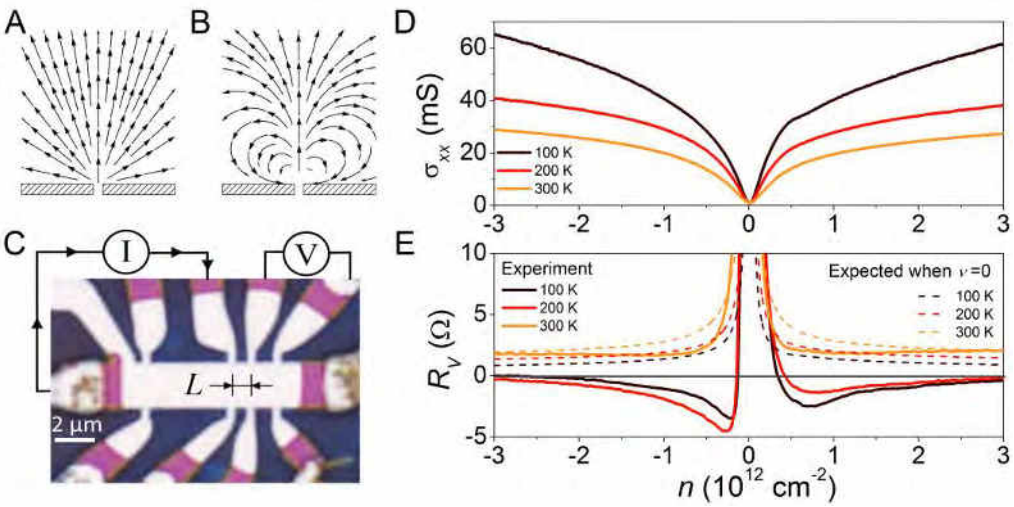

Fig. 1. (A,B) Steady-state distribution of current injected through a narrow slit for a classical conducting medium with zero viscosity (A) and a viscous Fermi liquid (B). (C) Optical micrograph of one of our SLG devices. The schematic explains the measurement geometry for vicinity resistance. (D,E) Longitudinal conductivity and vicinity resistance for this device as a function of the carrier density induced by applying voltage to top and back gates. Dotted lines correspond to the expected values in case of zero viscosity.

[1]L. D. Landau & E. M. Lifshitz. *Fluid Mechanic,* (Pergamon, New York, 1987).
[2] M. J. M. de Jong, L. W. Molenkamp. Hydrodynamic electron flow in high-mobility wires. Phys. Rev. B **51**, 13389 (1995).
[3]D. Bandurin et al., Science, **351**, 2016.

Optical modulators with two-dimensional layered materials

Zhipei Sun
Department of Micro- and Nanosciences, Aalto University, FI-00076, Finland
Zhipei.Sun@aalto.fi

Light modulation is an essential operation in photonics and optoelectronics. The recent demonstration that two-dimensional layered materials could modulate various light properties (e.g., wavelength, amplitude, phase, and polarization) with superior performance has stimulated intense research and significant advances [1-7], paving the way for realistic photonic and optoelectronic applications [1-12]. I will discuss the state-of-the-art of optical modulators based on two-dimensional layered materials including graphene [4-5,10], transition metal dichalcogenides [8] and black phosphorus (Fig.1a) [9]. I will present recent advances employing hybrid structures, such as two-dimensional heterostructures [1], plasmonic structures (Fig.1b) [12], and silicon/fibre integrated structures [5,8-12]. I will also take a look at future perspectives of optical modulation technologies with two-dimensional layered materials.

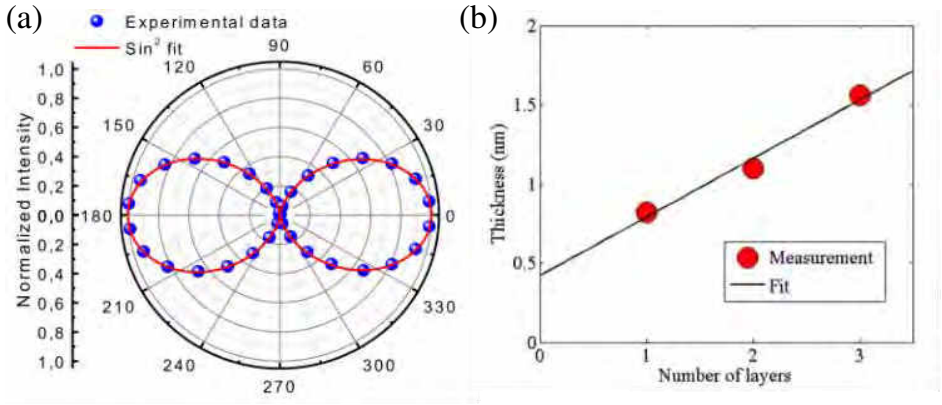

Figure 1. a. Linear polarization output of a black phosphorus modulated all-fiber laser [9]; b. Thickness measurement of graphene with surface plasmon resonance [12].

References

[1] Z. Sun *et al.*, Nat. Photonics, **15**, 227 (2016).
[2] F. Bonaccorso *et al.*, Nat. Photonics, **4**, 611 (2010).
[3] A. Ferrari, *et al.*, Nanoscale, **7**, 4598-4810 (2015).
[4] Z. Sun, *et al.*, ACS Nano **4**, 803 (2010).
[5] T. Hasan, *et al.*, Adv. Mater. **21**, 3874 (2009).
[6] Z. Luo, et.al. Nanoscale **8**, 1066 (2016).
[7] X. Yang et.al., Adv. Mater. DOI:10.1002/adma.201505765 (2016).
[8] F. Bonaccorso, Z. Sun, Opt. Mater. Exp. **4**, 63 (2014).
[9] D. Li, *et al.,* Sci. Rep. **5**, 15899 (2015).
[10] A. Martinez, Z. Sun, Nat. Photonics **7**, 842 (2013).
[11] Z. Sun et al., Physica E, **44**, 1082 (2012).
[12] H. Jussia *et al.*, Optica **3**, 151 (2016).

The role of nano-carbon materials in advancing fiber laser technologies

Amos Martinez
Aston Institute of Photonic Technologies, Aston University, Aston Triangle, Birmingham B4 7ET, UK
a.martinez3@aston.ac.uk

Abstract

The rising presence of ultrafast fibre lasers in industry and scientific applications can be credited to the impressive pace at which the understanding and harnessing of pulse propagation and the interplay between pulses in optical fibres is developing. Multiple factors have contributed to this advancement in fibre laser technologies, starting from an improved understanding and control over the nonlinearities that govern the propagation dynamics of ultrashort pulses [1], the development of novel purpose-made optical fibres and the development of new interrogation approaches to understand, characterize and design laser pulses. Another aspect that has contributed to the advance of ultrafast fibre laser technologies, both from the industrial and scientific point of view is the advent of a new class of saturable absorbers consisting on nanomaterials such as carbon nanotubes and graphene [2] and the more recent introduction of other 2D layered materials [3]. In this talk, I will discuss the role of these saturable absorbers in advancing the field of ultrasfast fibre lasers. First, I will discuss the role that we envisage these materials may have in facilitating ultrashort pulse generation at wavelength ranges that have traditionally been challenging for fibre laser configurations such as the mid-infrared [4] and the visible [5]. Second, we will discuss the contribution of these saturable absorbers in observing, understanding and controlling nonlinear dynamics in fibre laser configurations [6].

Acknowledgement

A.M. acknowledges support from the H2020 Marie-Sklodowska-Curie Individual Fellowship scheme.

References

[1] S.K. Turitsyn et al. "Dispersion-managed solitons in fibre systems and lasers." Physics reports **521**, 135-203 (2012).
[2] A. Martinez and Z. Sun "Nanotube and graphene saturable absorbers for fibre lasers." Nature Photonics **7**, 842-845 (2013).
[3] Z. Sun et al. "Optical modulators with 2D layered materials." Nature Photonics **10**, 227-238 (2016)
[4] G. Zhu et al. "Fe 2+: ZnSe and graphene Q-switched singly Ho 3+-doped ZBLAN fiber lasers at 3 μm." Optical Materials Express **3**, 1365-1377 (2013).
[5] Z. Luo et al. "Two-dimensional material-based saturable absorbers: towards compact visible-wavelength all-fiber pulsed lasers." Nanoscale **8**, 1066-1072 (2016).
[6] S.V. Sergeyev et al. "Spiral attractor created by vector solitons." Light: Science & Applications **3**, e131 (2014).

Ultrafast Nonlinear Optical Effects in 2D Semiconductors

Jun Wang
Key Laboratory of Materials for High-Power Laser, Shanghai Institute of Optics and Fine Mechanics, Chinese Academy of Sciences, Shanghai 201800, China
jwang@siom.ac.cn

As a class of semiconductors, transition metal dichalcogenides (TMDs) have the formula MX_2, where M stands for a transition metal (i.e., Mo, W, Ti, Nb, etc.) and X stands for a chalcogen (i.e., S, Se or Te). TMDs show graphene-like layered structure. Strong covalent bonds in layers and weak van der Waals interaction between layers allow TMDs to form a robust 2D nanostructure. In a TMD monolayer, the single transition metal layer is sandwiched between the two chalcogen layers. Owing to the specific 2D confinement of electron motion and the absence of interlayer coupling perturbation, 2D layered TMDs show unique photonics-related physical properties, e.g.,

1) Sizable and layer-dependent bandgap, typically in the 1-2 eV range;
2) Indirect-to-direct bandgap transition as the decreasing of the number of monolayer;
3) Fairly good photoluminescence and electroluminescence properties;
4) Remarkable excitonic effects, i.e., high binding energy, large oscillator strength and long lifetime.

In combination of the ultrafast carrier dynamics and molecular-scale thickness, the prominent properties manifest the 2D TMDs a huge potential in the development of photonic devices and components with high performance and unique functions.

We have extensively studied the ultrafast nonlinear absorption and nonlinear refraction of layered MX_2 (X=S, Se, Te) over broad wavelength (Vis-NIR) and time (fs-ps-ns) ranges [1-9]. Large area MoS_2 neat films with controllable thicknesses were fabricated from liquid-exfoliated MoS_2 dispersions by vacuum filtration. The MoS_2 films show superior broadband ultrafast saturable absorption (SA) performance, in comparison with the graphene films and the MoS_2 dispersions [4]. Very recently, we observed giant two-photon absorption (TPA) coefficient in a WS_2 monolayer [5]. The order of magnitude of TPA coefficient in WS_2 monolayer (~100 cm/MW) exceeds that of the conventional semiconductors (e.g., CdTe, GaAs, ZnS, ZnO, etc.) by a factor of 3-4. This is also the first Z-scan performance on an optical medium with a thickness as tiny as 0.75 nm. Moreover, a comprehensive study on the layer-dependent nonlinear photonic effect was carried out in MoS_2 mono- and few-layers by CVD growth [6]. SA to TPA transition was confirmed when the thickness changes from few-layer to monolayer. In addition, a spatial self-phase modulation method has been applied to tune the nonlinear refractive index of TMD dispersions [7].

The above-mentioned works have opened up a door towards 2D semiconductor based nonlinear photonics, spectroscopy and relevant photonic devices [8,9].

Acknowledgement.

These works were supported in part by NSFC (No. 61522510) and the External Cooperation Program of BIC, CAS (no. 181231KYSB20130007). J.W. thanks the National 10000-Talent Program for financial support.

References

[1] K. Wang, J. Wang, J. Fan, M. Lotya, A. O'Neill, D. Fox, Y. Feng, X. Zhang, B. Jiang, Q. Zhao, H. Zhang, J.N. Coleman, L. Zhang, W. J. Blau, ACS Nano **7**, 9260(2013).
[2] K. Wang, Y. Feng, C. Chang, J. Zhan, C. Wang, Q. Zhao, J.N. Coleman, L. Zhang, W.J. Blau, J. Wang, Nanoscale **6**, 10530(2014).
[3] N. Dong, Y. Li, Y. Feng, S. Zhang, X. Zhang, C. Chang, J. Fan, L. Zhang, J. Wang, Scientific Reports **5**, 14646 (2015).
[4] X. Zhang, S. Zhang, C. Chang, Y. Feng, Y. Li, N. Dong, K. Wang, L. Zhang, W.J. Blau, J. Wang, Nanoscale, **7**, 2978-2986 (2015).
[5] S. Zhang, N. Dong, N. McEvoy, M. O'Brien, S. Winters, N.C. Berner, C. Yim, X. Zhang, Z. Chen, L. Zhang, G.S. Duesberg, J. Wang, ACS Nano **9**, 7142-7150 (2015).
[6] Y. Li, N. Dong, S. Zhang, X. Zhang, Y. Feng, K. Wang, L. Zhang, J. Wang, Laser & Photonics Reviews **9**, 427-434 (2015).
[7] G. Wang, S. Zhang, X. Zhang, L. Zhang, Y. Cheng, D. Fox, H. Zhang, J.N. Coleman, W.J. Blau, J. Wang, Photonics Research, **3**, A51-A55 (2015).
[8] Y. Li, N. Dong, S. Zhang, K. Wang, L. Zhang, J. Wang, Nanoscale **8**, 1210 (2016).
[9] X. Zhang, Y. Chen, B. Chen, H. Wang, K. Wu, S. Zhang, J. Fan, S. Qi, X. Cui, L. Zhang, J. Wang, Nanoscale **8**, 431 (2016).

Evidence for Strong Electronic Correlations and Band-Gap Renormalization in Doped Single-Wall Carbon Nanotubes

T. Hertel, H. Hartleb, F. Spaeth, K. Eckstein, M. Achsnich, and F. Schoeppler
Institute of Physical and Theoretical Chemistry, Julius-Maximilians University Würzburg, Germany
tobias.hertel@uni-wuerzburg.de

We have investigated the photophysical properties of chemically and of gate-doped semiconducting single-wall carbon nanotubes (s-SWNTs) using stationary [1] and femtosecond time-resolved spectroscopy [2]. The continuous wave (CW) measurements have focussed on doping induced changes of exciton oscillator strengths and their spectroscopic quantification as well as on the appearance of trion-like absorption and emission features below the first subband exciton transition. Time-resolved spectroscopy has aimed at elucidating the coupling between trion- and exciton-states in moderately charged SWNTs.

Stationary measurements revealed that the first subband exciton oscillator strength - as obtained from absorption spectra - can be used for assessment of carrier densities and that they provide evidence for band-gap renormalisation (BGR) in (6,5) SWNTs. We predict that BGR of one-dimensional gate doped semiconductors is accompanied by a stepwise increase of the carrier density by $\Delta n = 32 m_{eff}\, b/(\pi\hbar)^2$ once the electrochemical potential reaches the valence or conduction band offset with b = (0.15 ± 0.05) eV nm (m_{eff} - effective carrier mass). Moreover, we show that the width of the spectroelectrochemical window of the first subband exciton of (1.55±0.05) eV corresponds to the fundamental band gap of the undoped (6,5) SWNTs in our samples and not to the renormalized band gap of the doped system. We also compare spectral changes in gate doped SWNTs with those of chemically doped SWNTs.

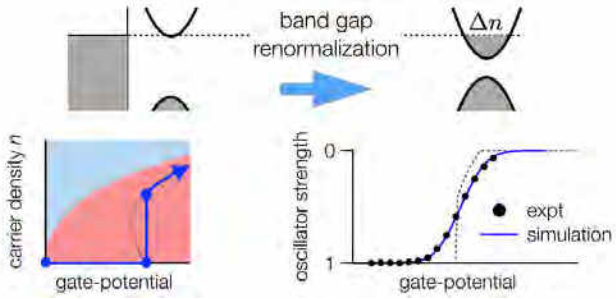

Figure 1. Schematic illustration of gate doping and band gap renormalization in a 1D semiconductor.

Femtosecond time-resolved pump-probe spectroscopy of chemically doped SWNTs provides evidence of strong exciton-trion coupling. These observations as well as a previously unidentified absorption band emerging at high doping levels in the Pauli-blocked region of the single-particle Hartree band structure, provide clear evidence for strong electronic correlations in the optical spectra of SWNTs.

[1] H. Hartleb, F. Späth and T. Hertel *Evidence for Strong Electronic Correlations in the Spectra of Gate-Doped Single-Wall Carbon Nanotubes*, ACS Nano, **9**, 10461 (2015).
[2] K. Eckstein and T. Hertel (in preparation).

Dynamics of Long – Lived Photoexcitations in SWNT – Polymer Blends

Larry Lüer,[a] Abasi Abudulimu,[a] Florian Spaeth,[b] Imge Namal,[b] Tobias Hertel[b]
[a] *IMDEA Nanociencia, C/ Faraday, 9, 28049 Cantoblanco, Spain, larry.luer@imdea.org*
[b] *Institute of Physical and Theoretical Chemistry, Julius-Maximilians University Würzburg, Germany*

Single-walled carbon nanotubes (SWNT) present favorable properties that encourage their use in organic photovoltaic (OPV) devices, namely, high charge carrier mobilities, near infrared optical absorption and thermal and chemical stability. Nonetheless, the maximum power conversion efficiencies (PCE) of systems comprising SWNT do not yet approach those of the SWNT - free OPV materials. This has been ascribed to the lack of knowledge and control of electronic processes happening on the nanoscale [1]. Elementary processes in organic photovoltaics occur on very different time scales, from femtoseconds to microseconds and must be studied specifically and in relation to sample morphology in order to quantify and overcome the respective loss processes [2]. We have shown that in SWNT, inter-tube singlet exciton transfer can occur in a few femtoseconds [3], and that charge trapping is a subpicosecond process [4]. Recently, photoinduced triplet exciton generation has been demonstrated on SWNT-polymer blends, with yields up to 32% and lifetimes in the microsecond range [5]. Triplet excitons are therefore expected to interfere with charge extraction in SWNT - based OPV devices, making it important to investigate the generation and relaxation pathways of triplet states.

Here, we present recent results on chirality specific triplet exciton dynamics in SWNT-PFO-Bpy blends of different composition. Comparing data from femtosecond transient absorption spectroscopy with recently published spectroelectrochemical data [6], we quantify the amount of transient photobleach associated with charged states and singlet and triplet excitons (Fig. 1a). We show that in samples rich in (6,5) tubes, triplet exciton transfer between (6,5) and (7,5) tubes occurs with first order kinetics with a transfer constant of about 70 ps (Fig. 1b). In contrast, in (7,5) rich samples, we do not observe the analogous transfer of triplet excitons from (7,5) → (8,4) tubes. We find a reduction of the overall triplet yields with pump intensity, an indication that singlet exciton annihilation is competing with triplet formation. We discuss possible mechanisms for triplet generation and inter-tube transfer of triplet excitons.

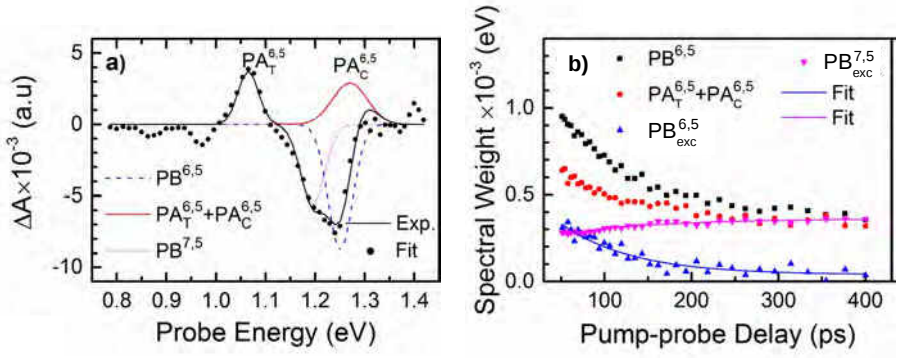

Fig.1 (a). Transient absorption (TA) spectrum of (6,5) rich SWNT-PFO-Bpy blend at t = 167 ps after pumping with 150 fs pulses at λ = 387 nm (symbols). Lines are global spectral fits, using data from [6] as spectral model for charged states considering trion absorption and charge induced absorption in (6,5) tubes ($PA_T^{6,5}$ and $PA_C^{6,5}$, respectively) and transient photobleach PB of (6,5) and (7,5) tubes . b) Spectral weights of the PA and PB bands in panel (a) as function of pump-probe delay. For t > 50 ps, the excess photobleach PB_{exc} is proportional to the number of triplet excitons on the respective chirality. Solid lines are monoexponential fits.

We acknowledge financial support from Autonomous Community of Madrid (Project "FotoCarbon", s2013/Mtr-2841), Ministry of economy and competitiveness (Plan Nacional, Project "MultiCrom"), and the European Commission (ITN "POCAONTAS", Project No: 316633)

[1] M. Gong et al., ACS applied materials & interfaces **7**, 7428 (2015)
[2] S. Karuthedath, T. Sauermann, H. – J. Egelhaaf, R. Wannemacher, C.J. Brabec, L. Lüer, J. Mater. Chem. A, **3**, 3399-3408 (2015)
[3] L. Lüer, J. Crochet, T. Hertel, G. Cerullo, and G. Lanzani, ACS Nano **4(7)**, 4265-4273 (2010)
[4] (a) J. J. Crochet, S. Hoseinkhani, L. Lüer, T. Hertel, S. K. Doorn, and G. Lanzani, Phys Rev Lett **107**, 257402 (2011); (b) B. Yuma et al., Physical Review B **87**, 205412 (2013)
[5] (a) D. Stich, F. Spaeth, H. Kraus, A. Sperlich, V. Dyakonov, and T. Hertel, Nature Photonics **8**, 139 (2014).; (b)F. L. Späth, Doctoral Thesis, Universität Würzburg, Fakultät für Chemie und Pharmazie (2015)
[6] H. Hartleb, F. Späth, and T. Hertel, ACS Nano **9**, 10461 (2015)

Electrical resistance of films composed from filled single-wall carbon nanotubes or doped graphene

E.D. Obraztsova[1*], A.A.Tonkikh[1], V.I. Tsebro[2], D.V. Rybkovskiy[1], M.G. Rybin[1], E.A. Obraztsova[1,3], E.I. Kauppinen[4], A.S. Orekhov[1], A.L. Chuvilin[5]

[1] A. M. Prokhorov General Physics Institute, RAS, 38 Vavilov street, 119991 Moscow, Russia
[2] P.N. Lebedev Physical Institute, RAS, Leninskiy prosp., 53, 119991 Moscow, Russia
[3] M.M. Shemyakin and Yu.A. Ovchinnikov Institute of Bioorganic Chemistry, RAS, Moscow, Russia
[4] Department of Applied Physics, Aalto University, FI-00076 Espoo, Finland
[5] CIC NanoGUNE Consolider, San Sebastian 20018, Spain

Gas phase filling of inner space of single-wall carbon nanotubes integrated into thin films by donor or acceptor molecules or covering graphene by a thin film of such molecules allow to form a new prospective material for transparent conductive electrodes with characteristics comparable with those of indium-tin oxide (ITO). The HRTEM images of such nanotubes reveal formation of one-dimensional crystals inside (Fig.1). The optical spectroscopy confirms a Fermi level shift into a valence band and a complete metallization of the nanotubes [1]. To confirm metallization we have measured the electrical resistance of filled SWNT films of different transparency and registered a big drop of electrical resistance (of one order of magnitude) after filling. The best values were about 50 Ohm/square at 90% transparency. The temperature dependence of resistance (R(T)) demonstrated two contributions – from the inter-tube interactions and from the filled nanotubes by themselves (Fig.2). For the stronger acceptor (CuCl instead of iodine) the minimum value of R(T) shifted toward low temperatures. The mechanisms of electron-phonon interactions in doped materials are discussed.

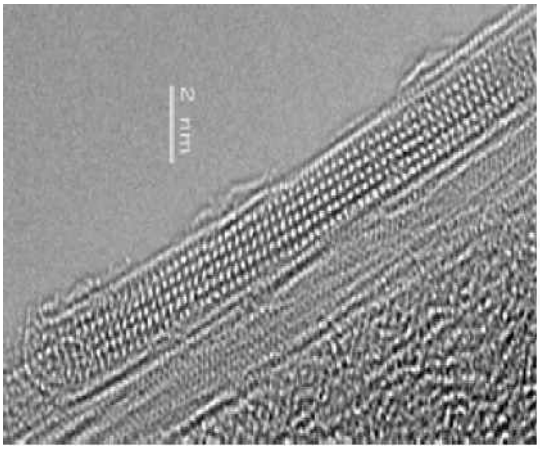

Fig.1. One-dimensional crystals formed inside SWNTs from donor or acceptor molecules.

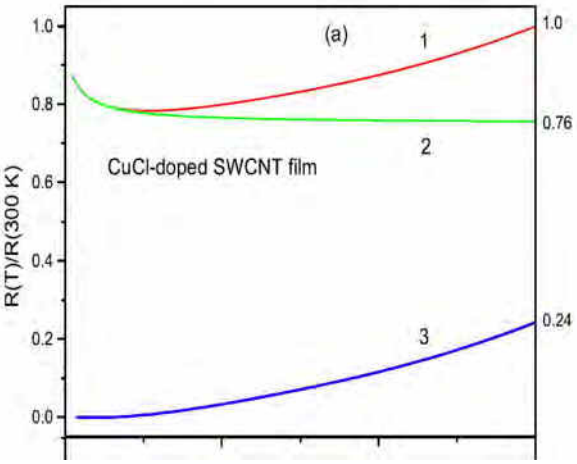

Fig.2. The electrical resistance of CuCl@SWNT film. (1) experimental data, (2) tunneling between nanotubes, (3) nanotube contribution.

The work was supported by RSF project 15-12-30041 and RFBR project 15-32-20941.

[1] A.A. Tonkikh, V.I. Tsebro, E.A. Obraztsova, et al., *Carbon 94, 768-774, (2015).*

Direct Deposition of a Graphitic Film on a Dielectric Substrate by Nickel Nanocatalyst

Tommi Kaplas and Yuri Svirko
Institute of Photonics, University of Eastern Finland, Yliopistokatu 7, Joensuu, 80100, Finland
Tommi.kaplas@uef.fi

Chemical vapor deposition (CVD) process usually results in polycrystalline graphitic films [1,2], in which strong electron scattering and reduced group velocity of electrons suppressed the carriers mobility [3]. However, the grain boundaries do not necessarily affect optical properties of these materials because the film thickness is one or two order of magnitude smaller than the light wavelength. This makes development of the CVD process suitable for direct synthesis of graphene and graphitic films on dielectric substrates eagerly awaiting breakthrough in optics and photonics.

Here we demonstrate synthesis of the few tens of nanometer thick polycrystalline graphitic film deposited directly on a silica substrate by using a sacrificial nickel film as a catalyst. In the experiment, the nickel film with thickness of 10 nm was deposited on a smooth silica substrate and coated with a carbon based photoresist. Baking the sample at 800 °C resulted in the formation on the substrate surface a graphitic film with a thickness of a few tens of nanometers decorated with sub-micron Ni particles. By removing these particles by wet etching we arrive at a few tens of nanometer thick graphitic film directly deposited on a silica substrate.

The obtained graphitic film with and without Ni particles was characterized by Raman spectroscopy, optical transmission spectroscopy, multiphoton microscope and nonlinear optical pump-probe technique. We demonstrate that the properties of the fabricated ultrathin films resemble those of multilayer graphene. The proposed simple and versatile approach offers a tempting platform for a multilayer graphene film processing on dielectric substrates.

[1] H. Wang and G. Yu, *“Direct CVD Graphene growth on Semiconductors and Dielectrics for Transfer-Free Device Fabrication”*, Adv. Mater. DOI: 10.1002/adma.201505123 (2016).
[2] T. Kaplas, D. Sharma, and Y. Svirko, *Few-layer graphene synthesis on a dielectric substrate*, Carbon **50(4)**, 1503-1509, (2012).
[3] C.Y. Su, A.Y. Lu, C.Y. Wu, Y.T. Li, K.K. Liu, W. Zhang, et al. *“Direct Formation of Wafer Scale Graphene Thin Layers on Insulating Substrates by Chemical Vapor Deposition”,* Nano Letters 11, 3612–3616 (2011).

Triboelectricity Assisted Graphene Transfer for Flexible Graphene/ZnO UV Detector and Its Strain Modulated Performance

Shuo Liu[1], Qingliang Liao[1], Zheng Zhang[1], Li Wang[2] and Yue Zhang[1,*]

1 State Key Laboratory for Advanced Metals and Materials, School of Materials Science and Engineering, University of Science and Technology Beijing, Beijing 100083, People's Republic of China.

2 Department of Environmental Engineering, School of Civil and Environmental Engineering, University of Science and Technology Beijing, Beijing 100083, People's Republic of China.

E-Mail address (corresponding author): yuezhang@ustb.edu.cn

Graphene, firstly isolated in 2004 by Novoselov and Geim, had shown many remarkable properties, [1-5] which made graphene a promising building block in future flexible electronics and optoelectronics. In this work, a novel triboelectricity-assisted (TEA) graphene transfer method is demonstrated firstly. With the assistance of the electrostatic force from friction generated charges, graphene sheet was successfully transferred from copper foils to flexible substrates. Characterization results confirm the presence of high quality graphene with less defects and contaminations, as compared to the graphene transferred by the conventional PMMA-mediated transfer process. Then, a flexible graphene/ZnO nanorods (NRs) film hybridized PD is constructed. By utilizing the strain-induced piezo-polarization charges in the piezoelectric ZnO, the optoelectronic process initiated in the graphene/ZnO interface is effectively modulated. Experimental results indicate the device responsivity has been improved dramatically, from 71.61 A/W to 84.94 A/W, under -0.349% compressive strain and an interface energy band theory is proposed to explain these phenomena. This exploitation of strain provides a simple and feasible route to improve the optoelectronic devices performance based on graphene hybrid structure.

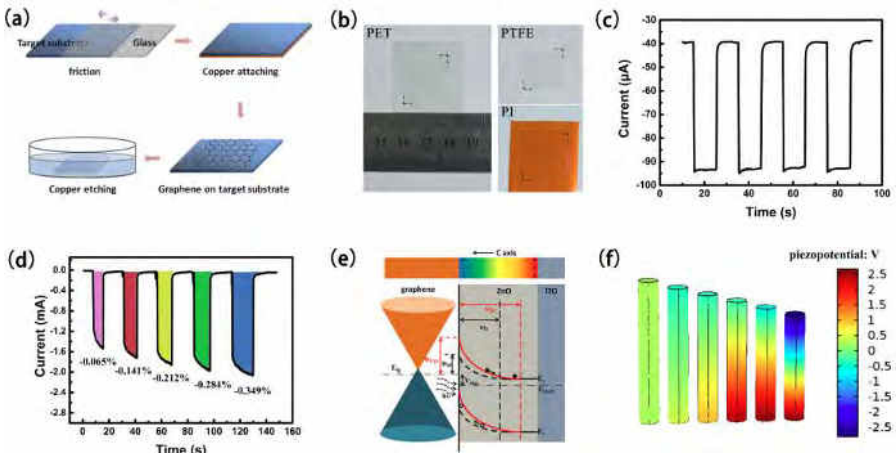

Figure1. (a) Schematic description of the TEA-transfer process. (b) The 2 cm×2 cm graphene films transferred on PET, PTFE and PI substrates respectively. (c) Time-resolved photoresponse of the graphene/ZnO PD under UV illumination. (d) The performance of the graphene/ZnO PD under different strain with a defined illumination density of 25.12 μW/cm^2. (e) Schematic band diagrams of graphene/ZnO Schottky junction with compressive strain. (f) Simulation results of piezoelectronic potential distribution (bottom panel) in the ZnO nanowire under different strain (from 0% to -1.0%, step size: -0.2%).

Acknowledgement

This work was supported by the National Major Research Program of China (No. 2013CB932602), the Program of Introducing Talents of Discipline to Universities (B14003), National Natural Science Foundation of China (No. 51527802 and 51232001), The Beijing Municipal Science & Technology Commission, the Fundamental Research Funds for Central Universities.

References

[1].Novoselov, K. S.; Geim, A. K.; Morozov, S. V.; Jiang, D.; Zhang, Y.; Dubonos, S. V.; Grigorieva, I. V.; Firsov, A. A. Science 2004, **306** (5696), 666-9.

[2].Du, X.; Skachko, I.; Barker, A.; Andrei, E. Y. Nat Nano 2008, 3, 491-495.

[3].Nair, R. R.; Blake, P.; Grigorenko, A. N.; Novoselov, K. S.; Booth, T. J.; Stauber, T.; Peres, N. M.; Geim, A. K. Science 2008, **320**, 1308.

[4].Lee, C.; Wei, X.; Kysar, J. W.; Hone, J. Science 2008, **321**, 385-8.

[5].Kim, K. S.; Zhao, Y.; Jang, H.; Lee, S. Y.; Kim, J. M.; Ahn, J. H.; Kim, P.; Choi, J. Y.; Hong, B. H. Nature 2009, **457**, 706-10.

Synthesis and characterization of hybrid graphene and ZnO nano/micro structures

W. Zhao[#1,2], M. Karlsson[#1,2], E. De Geer[1], Y. Zhao[2], Y. Fu[3], M. S. Toprak[2], and Q. Wang[*1]

[1]*Department of Sensor System, Acreo Swedish ICT, Box1070 164 25 Kista, Sweden*

[2]*Department of Materials and Nano Physics, KTH-Royal Institute of Technology, 164 40 Kista, Sweden*

3 SciLifeLab, KTH-Royal Institute of Technology, Box 1031, 171 21 Solna, Sweden

 # Authors have had equal contributions to this work

**qin.wang@acreo.se*

1. Introduction

Graphene is a ground-breaking two-dimensional material with extraordinary properties enabling a new generation of innovative devices. The most economical method to produce graphene is using chemical or thermal reduction of graphene oxide (RGO and GO). Both GO and RGO have efficient surface area and excellent capability of loading various biomolecules via chemical or physical interactions. In addition, nano-micro structured ZnO tetrapods (ZnO-Ts) have attracted significant attention due to its unique morphology consisting of four branches joined together and its multiple electron transfer paths, large surface-to-volume ratio and biocompatibility/biosafety. In our former work both the graphene-based and ZnO-Ts-based biosensors have been demonstrated for glucose detection [1-2]. In this work, we aim to address a new sensing platform by hybridization of the graphene-based structures and ZnO-Ts, which are expected to facilitate the use of large area graphene-based flakes with the high electrical conductivity of the ZnO to enhance the sensitivity of the sensors.

2. Results and Discussions

The GO was synthesized according to the modified Hummer's method. Afterwards the obtained GO was dispersed in DI water and reduced by L-ascorbic acid through vigorous stirring for 48 hours [1]. This turned the brown GO solution into characteristic black RGO. The nano-micro structured ZnO-Ts were synthesized by flame transport synthesis (FTS) [2]. The GO/ZnO-Ts composite was fabricated in two steps in sequence: 1) ZnO-Ts were modified with 3-aminopropyltriethoxysilane (APTES) to introduce amine groups. Thereafter, the ZnO-Ts-APTES were attached covalently with GO by carboxylic acid activation via ethyl (dimethylaminopropyl) carbodiimide/N-hydroxysuccinimide (EDC/NHS) [3]. 2) The EDC/NHS functioned to cross-link GO with ZnO-APTES, eventually formed the GO/ZnO-Ts composite.

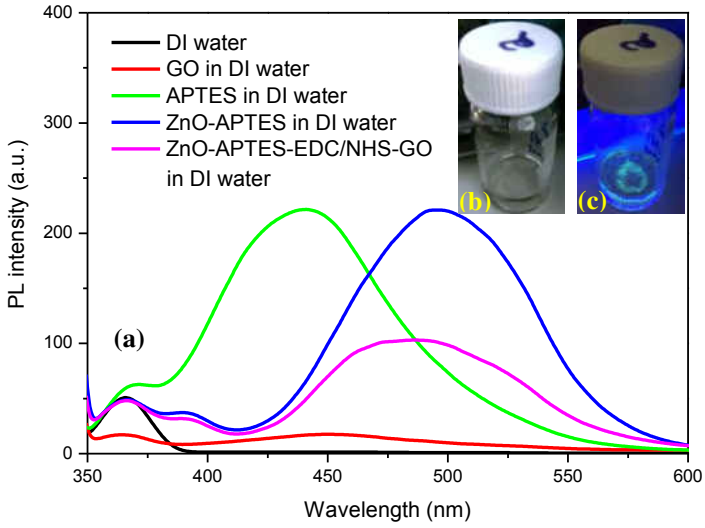

Figure 1 PL spectra of the GO/ZnO-Ts in synthesis sequence (a). Photos of GO/ZnO-Ts under normal (b) and UV light (c).

The PL spectra of GO/ZnO-Ts were measured using a fluorescence spectrometer (LS55, PerkinElmer) in conditions labeled in the insert of Fig. 1(a). The PL peak of the ZnO-APTES was appeared at about 490 nm, which might be mainly caused by ZnO-Ts although there was slightly shift compared to the PL peak of pure ZnO [2]. However its peak at about 430 nm was inhibited in comparison with APTES in DI water case. The emission of the ZnO-APTES-GO was quenched significantly at about 490 nm, and its shape became asymmetrical in correspondence with the spectrum of GO in DI water. The GO/ZnO-Ts in aqueous solution emit green photoluminescence, which is reveled and illustrated in Fig. 1 (b) and (c). Similar attempts to hybridize RGO and ZnO-Ts are still ongoing, and the results will be compared with the results of the GO/ZnO-Ts presented here.

3. Acknowledgements

The authors would like to thank Sweden's innovation agency (Vinnova) for financial support through the Graphene Strategic Innovations Program (SIO Grafen) under Grant Agreements 2014-05186 and 2016-01656.

4. References

[1] M. Karlsson, Q. Wang, Y. Zhao, W. Zhao, M. Toprak, SPIE Proc. 9668-122 (2015)
[2] W. Zhao, Y. Zhao, M. Karlsson, Q. Wang, M. Toprak, SPIE Proc. 9668-55 (2015)
[3] C. Guo, Y. Dong, H. Yang , C. Li, Adv. Energy Mater. 3, 997–1003 (2013)

Performance Comparison of ZnO UV Photodetector Based on Photoconductor and Photodiode

Zhi Yang, Minqiang Wang*

Electronic Materials Research Laboratory (EMRL), Key Laboratory of Education Ministry; International Center for Dielectric Research (ICDR), Xi' an Jiaotong University, Xi' an 710049, China

Corresponding author: mqwang@mail.xjtu.edu.cn

For decades, UV photodetectors have played the crucial role in a wide range of applications in fire monitoring, optical communications, and UV irradiation detections. Nanostructured photodetectors have two main structures: a photoconductor (PC) and a photodiode (PD) [1]. The PC type only conducts a single carrier type, making it unipolar, which usually has high gain and long response and recovery times. The surface trap and photo-generated carriers transporting efficiency are two main factors to limit photoresponse performance. The disadvantage of PC detector is long response and recovery times, resulting from large electrodes distance. In contrast, the PD type can extract both electron and hole through built-in potential, resulting in high responsivity and fast response speed. What's more, the nanostructured PD detector can work at a self-powered mode, meaning a huge current increase at 0 V employing photovoltaic property, which meets the requirement of low-energy consumption.

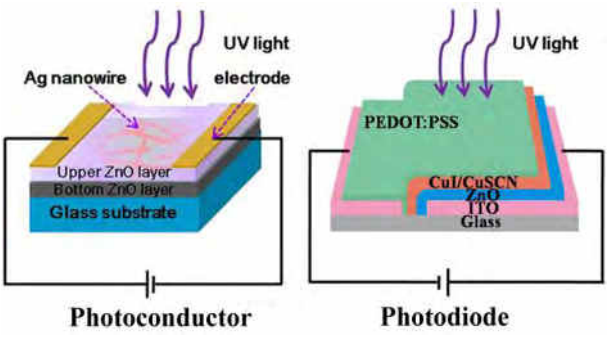

Fig.1 shows two different types of ZnO films photodetector. One is ZnO/Ag nanowires (NWs)/ZnO PC detector, the other is ZnO-CuI/CuSCN PD detector. For PC detector, sandwich structure was prepared by embedding Ag NWs between two layers ZnO NP thin films based on solution-processed method. For PD detector, inorganic p-type CuI/CuSCN composite films with compact morphology, high conductivity, and low surface state were adopted to build pn junction with ZnO films.

Fig.1 Two structured ZnO films UV photodetector

Based on two different structured photodetector, we obtained their photoresponse performance, as shown in Table 1, the results from ZnO NWs are also listed here as comparison. No doubt ZnO/Ag NWs/ZnO detector has better photoresponse performance than ZnO NPs film PD detector, resulting from Ag NWs not only greatly improve the extraction number of photoelectrons, but also shorten the extraction time in ZnO polycrystalline thin films [2]. In particular, ZnO/Ag NWs/ZnO detector has shorter recovery time compared with previous reported ZnO NWs detector. Compared with ZnO-CuI PD detector, ZnO-CuI/CuSCN detector has lower dark current and higher photocurrent, resulting from composite p-type films with compact morphology, high conductivity, and low surface state [4]. Moreover, the different performance advantage can be obtained by comparing two kinds of photodetector based on PC and PD. ZnO/Ag NWs/ZnO PC detector has higher photocurrent and On/off ratio, while ZnO-CuI/CuSCN PD detector has shorter recovery time. Their different performance can come from different photo-generated carriers transporting mode due to structure difference.

Table 1. Photoresponse parameters comparison of different structured ZnO films UV detectors

Devices	Type	J_d (μA/cm^2)	J_l (μA/cm^2)	On/off ratio	Voltage (V)	Recovery time (s)
ZnO NPs [2]	PC	0.01	0.4	40	1	74
ZnO/AgNWs/ZnO [2]	PC	0.08	225	2787	1	3.67
ZnO NWs [3]	PC	0.33	1000	3000	5	15.44
ZnO-CuI [4]	PD	0.24	9.8	41	0	<0.1
ZnO-CuI/CuSCN [4]	PD	0.1	13	130	0	<0.1
ZnO NWs-CuSCN [5]	PD	0.045	45	1000	0	6.7×10^{-6}

3. References

[1] G. Konstantatos, E. H.Sargent, Nature Nanotechnology, **5**, 391 (2010).
[2] Z. Yang, M. Q. Wang, X. H. Song, G. D. Yan, Y. C. Ding and J. B. Bai, Journal of Materials Chemistry C, **2**, 4312 (2014).
[3] Y. K. Su, S. Peng, L. Ji, C. Wu, W. Cheng and C. Liu, Langmuir, **26**, 603 (2010).
[4] Z. Yang, M. Q. Wang, J. J. Ding, Z. W. Sun, L. Li, J. Huang, J. Liu and J. Y. Shao, ACS Applied Materials and Interfaces, **7**, 21235 (2015).
[5] S. M. Hatch, J. Briscoe and S. A. Dunn, Advanced Materials, **25**, 867 (2013).

Poster session I

©E. Plotkin

Spin gap opening in graphene

A. Zyrianova[1], T. Makarova[1,2], E. Lahderanta[2], A. Okotrub[3], L. Bulusheva[3]

[1]Ioffe Physical Technical Institute, Polytechnicheskaya 26, 194021 St. Petersburg, Russia
[2]Lappeenranta University of Technology, FI-53851 Lappeenranta, Finland.
[3]Nikolaev Institute of Inorganic Chemistry SB RA3, 630060, Novosibirsk, Russia
Corresponding author e-mail: makaranya@gmail.comfi

Functionalizing graphene or confining the electrons in the graphene plane into one-dimensional graphene structures opens a charge gap them with the promises for technological applications. Here we speak about a quite a different phenomenon: a spin gap. Excitations in antiferromagnetic (AF) quantum chains and ladders are gapped because the simplest excitation above the ordered state would require one of the spins to flip costing $\Delta = 2J$ amount of energy, where J is the spin-spin coupling strength and Δ is the spin gap.. We show experimentally and confirm theoretically that the creation of confined graphene nanosegmens inside the functionalized graphene matrix brings graphene to an interesting class of magnetic materials for which the spectrum of magnetic excitations is characterized by a separation of the first excited state from the ground state by the spin gap [1]. We created narrow graphene nanoribbons embedded in the functionalized layer and possessing essentially the same electronic properties as freestanding nanoribbons, in particular, it has localized edge states, which give a sharp peak in the density of states at the Fermi energy. These states interact antiferromagnetically or ferromagnetically, depending on sublattice position. The observed spin ladder behaviour brings graphene to the class of Low-D magnetic materials for which the spectrum of magnetic excitations is characterized by a separation of the first excited state from the ground state by the spin gap. We demonstrate that spontaneously formed disordered embedded graphene nanosegments create the π-electron system with an antiferromagnetic ground state.

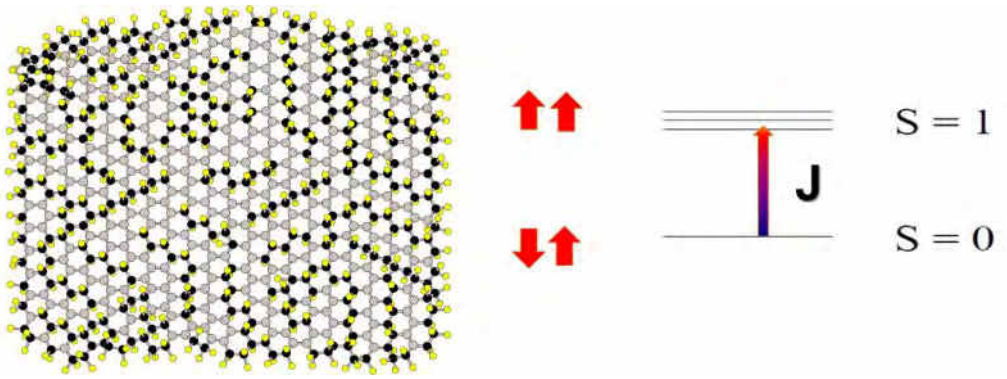

Fig. 1.The origin of the spin gapped behavior is in (i) sectioning graphene basal plane by functionalization which confines the electrons and (ii) the presence of zigzag interfaces as the spin sources

Acknowledgement.
Supported by FP7 MSCA project MagNonMag-295180"Magnetic order induced in nonmagnetic solids".

References

[1] T. Makarova, A. Shelankov, A. Zyrianova, A. Veinger, T. Tisnek, E. Lähderanta, A. Shames, A. Okotrub, L. Bulusheva, G. Chekhova, D. V. Pinakov, I. P. Asanov & Ž. Šljivančanin, Edge state magnetism in zigzag-interfaced graphene via spin susceptibility measurements, Scientific reports. 5 (2015) 13382.

Influence of PdO Content on the Helicity-Dependent Photocurrent in Resistive Ag/Pd Films

A. S. Saushin, R. G. Zonov, K. G. Mikheev, E. V. Alexandrovich, G. M. Mikheev
Institute of Mechanics of Ural Branch of RAS, 34 ul. T. Baramzinoy, Izhevsk, Russia
alex@udman.ru

1. Introduction

Recently, the helicity-dependent photocurrent which is generated in nanostructured film materials was studied. Such helicity-dependent photocurrent is named as a circular photocurrent (CPC).

In our studies [1–3] it was shown that in the porous silver-palladium (Ag/Pd) films, produced according to the thick-film technology, the CPC can be excited by nanosecond laser pulses in a wide spectral range. It was found out that the photocurrent appears in Ag/Pd films containing PdO nanocrystals [4]. However the nature of influence of PdO content on the CPC was not determined.

The aim of this work is to study influence of PdO content on the CPC in Ag/Pd resistive films.

2. Experimental and results

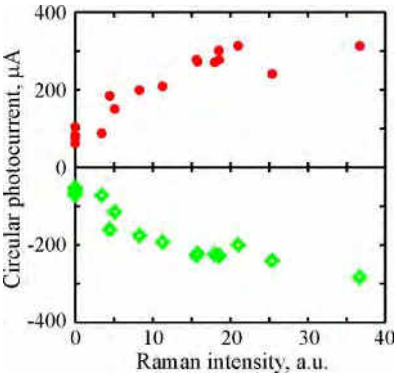

Fig. 1. The photocurrent induced by 1 MW pulsed laser radiation for (red circles) left-hand and (green rhombus) right-hand circularly polarized light vs. intensity of PdO Raman peak

Ag/Pd resistive films were produced in accordance to thick film technology [5] based on burning of a special paste on a ceramic substrate. The size of the film obtained was 12.5×11 mm. The thickness of the film was about ~10 μm. To measure the photocurrent the film was provided with two parallel film electrodes which were arranged along the opposite sides of the film between the dielectric substrate and the Ag/Pd-film.

To change PdO content in the films obtained we used a method based on chemical reduction of Pd from PdO [6] according to the following chemical reaction: $PdO + H \rightarrow Pd + H_2O$. To this end studying film was hydrogenated in the electrolytic sell filled with weak solution of sulfuric acid in distilled water. After some time gap t the film was taken out of electrolyte, washed in distilled water and dried. Further interelectrode resistance and photocurrent were measured (the measuring photocurrent is described in [1–3]), and the Raman spectra of the films were obtained. Then the processes of hydrogenating and measuring were repeated.

Fig.1 represents the dependences of the photocurrent on intensity of Raman-active mode B_{1g} of PdO crystals [7]. Raman intensity of PdO peak represents relative PdO content in the film surface layer. It can be seen that the decrease of PdO content on the film surface leads to the photocurrent decrease. However when PdO content reached zero, the photocurrent was still observable (Fig.1). In our case Raman scattering appears in the film within the skin depth h_R determined by the exciting wavelength of 632.8 nm. But the CPC induced by the light absorption appears in the skin depth h_{PD} determining by the exciting laser wavelength of 532 nm. Since $h_R > h_{PD}$, it is clear that the CPC can be excited in the film without PdO. Therefore the photocurrent appears in the porous structure consisting of Ag-Pd solid solution. The CPC decreasing due to PdO removing effect can be connected with disappearing of the enhancement effect which is possible in Schottky barriers into the film.

3. Conclusion

Thus in this work we showed that the decrease of PdO content in the film surface layer leads to the photocurrent decrease. Nevertheless, the photocurrent is observed at total PdO absence on the film surface. The porous structure of the Ag-Pd solid solution is responsible for the CPC generation.

3. Acknowledgement.

This study was supported by the RFBR (project no. 16-38-00552).

4. References

[1] G. M. Mikheev, V. A. Aleksandrov and A. S. Saushin, Tech. Phys. Lett., **37**(6), 551 (2011).
[2] G. M. Mikheev, A. S. Saushin, R. G. Zonov and V. M. Styapshin, Tech. Phys. Lett., **40**(5), 424 (2014).
[3] G. M. Mikheev, Saushin A, S. and V. V. Vanyukov, Quantum Electron, **45**(7), 635 (2015).
[4] G. M. Mikheev, A. S. Saushin, O. Yu. Goncharov, G. A. Dorofeev, F. Z. Gil'mutdinov and R. G. Zonov, Phys. Solid State., **56**(11), 2286. (2014).
[5] J. Larry, R. Rosenberg and R. Uhler, IEEE Trans. Components, Hybrids, Manuf. Technol., **3**(2), 211(1980).
[6] Y. T. Lee, J. M. Lee, Y. J. Kim, J. H. Joe and W. Lee, Nanotechnology, **21,** 165503 (2010).
[7] J. R. McBride, K. C. Hass and W. H., Phys. Rev. B, **44**(10), 5016 (1991).

Photopolymerization of doped fullerene films

A. Komlev[1,2,*], **M. Yesilbas**[3], **I. Zakharova**[4], **E. Lähderanta**[1], **T. Makarova**[1]
[1]*Lappeenranta University of Technology, Lappeenranta, 53851 Finland*
[2]*St. Petersburg State Electrotechnical University, St. Petersburg, 197376 Russia*
[3]*Umea University, Umea, 90187 Sweden*
[4]*State Technical University, St. Petersburg, 195251 Russia*
**e-mail: komlevanton@hotmail.com*

Irradiation of the fullerenes with visible light promote the transition of molecular oxygen from a triplet (with spin S=1) to a singlet state (S=0) [1, 2]. Singlet oxygen is a relatively long-lived species with very reactive behavior. In liquid phase it has many application in different areas, including photodynamic therapy, inactivation of the viruses and bacteria, lithography, photochemical degradation of harmful pollutants or oxidation in organic synthesis. Thus, creating materials with fullerenes, based on the production of singlet oxygen and connected effects can be beneficial.

The advantage of fullerenes compared to other singlet oxygen generators is that it can be activated under full-spectrum polychromatic light, similar to that under normal environmental conditions. However, the irradiation with light can also lead to the polymerization of fullerenes, decreasing the effectiveness of generation of singlet oxygen. Thus, the ways to suppress the photopolymerization have to be investigated.

In this work, the C_{60} fullerene films intercalated with tetraphenylporphyrin, CdS, CdTe, HNO_3, as well as the hydrogen plasma treated films were investigated. The polymerization process was examined by the Raman spectroscopy. It was shown that the polymerizing ability is tightly connected with the formation of charge transfer (Wannier-Mott) excitons which revealed in the absorption spectra measured with the help of spectroscopic ellipsometry. It was found, that the intercalated with the semiconductors fullerenes have reduced polymerization ability. The best results were obtained on hydrogen plasma treated fullerene films. Obtained results provide a technically feasible way to produce a photocatalytic material for the generation of singlet oxygen under atmospheric conditions.

Acknowledgements

This work was supported by European FP7 IRSES project 295180 MagNonMag.

References

[1] D. Guldi, M. Prato. Excited-state properties of C60 fullerene derivatives. Accounts of Chemical Research, 33, P. 695–703 (2000).
[2] D. M. McCluskey, T. N. Smith, P. K. Madasu, C. E. Coumbe, M. A. Mackey, P. A. Fulmer, J. H. Wynne, S. Stevenson, J. P. Phillips. Evidence for Singlet Oxygen Generation and Biocidal Activity in Photoresponsive Metallic Nitride Fullerene-Polymer Adhesive Films. ACS Appl. Mater. & Interfaces, 1, P. 882–887 (2009).

Scanning probe microscopy for in-situ analysis of carbon films growth by chemical vapor deposition.

A. B. Loginov, R. R. Ismagilov

M. V. Lomonosov Moscow State University, Department of Physics, Moscow 1119991, Russia

loginov.ab15@physics.msu.ru

The new in-situ scanning probe microscopy method of carbon materials deposition study during DC or "hot fiber" activation of the gas phase is described. This method should get the films of carbon materials assembling processes is showed with up to atomic resolution. Also it is possible to take electrical properties variation (conductivity, width of band gap, Fermi level) of carbon materials during deposition.

The development of various sectors of nanotechnology poses multiple problems to find, create and explore new nano-objects. To solve these problems more effectively, it is necessary to study the synthesis of nano-objects. The in-situ study of the nano-objects self-organization is especially relevant because in this study new rules of self-assembly process can be traced and identified to be applied to form new nano-structures with predetermined properties in future. Particularly this method can be applied for our research area of pyramidal shaped single crystal diamonds formation in chemical vapor deposition (CVD) [1].

The basis for this work is the experience of the successful creation of a scanning tunnel microscope (STM, one of the scanning probe microscopy mode) for in-situ study of graphite wall re-deposition process in a fusion reactor Tokamak T-10 [2]. The head of this STM (showed on figure) was entered into fusion facility into nuclear plasm at extreme temperature and electromagnetic fields. The head of STM was burned in 10 minutes, but it managed to make up to 100 successive frames describing the changing in the Tokamak’s graphite walls nanostructures. We decided to create the in-situ STM method for our CVD processes.

Piezo XYZ-scanner (1) is placed on the stainless steel body (2) with big heat capacity to avoid overheating and to make working time longer. Sample (4) lies on the plate (5) which protect scanner (1) from heat at the same time. Curved platinum STM-tip (3) comes from a top of the scanner, goes throw the hole in the plate (5) and comes close to the sample (4). To make coming heat lower the plate (5) is placed on two pointed columns (7). Sample approaches to the tip by linear motor (8) with pointed contact with the plate (5). The spring (6) presses plate (5) against the body to get rid of motor backlash. All the construction is placed on three pointed columns (10) inside the stainless steel heat shield (11).

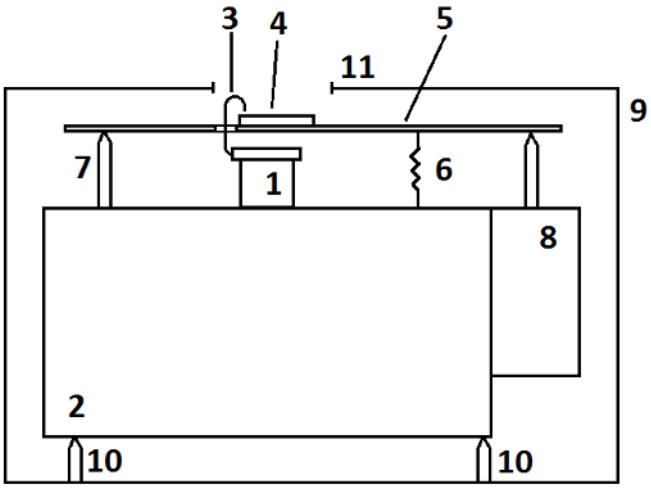

Sizes of XYZ-scanner’s piezo-tube were specially designed. Resonance frequency should be 14kHz at its length of 18mm, external diameter of 9mm and wall thickness of 0.5mm. It will protect from vibrations and should allow getting atomic resolution. Maximum field of view of this scanner at X/Y/Z is 2/2/0.5 microns. All of this should give possibility of observing the interesting initial stage of nucleation and evolution of carbon nano-objects from single atoms to 0.1-0.5 microns size.

[1] P.G. Kopylov, A.N. Obraztsov, M.A. Dolganov, and S.S. Abramchuk. Formation of pyramidal shaped single crystal diamonds in chemical vapor deposition. Protection of Metals and Physical Chemistry of Surfaces, 2009, V. 43, 5, pp. 553 – 557.

[2] L.N.Khimchenko, V.P.Budaev, M.I.Guseva, B.N.Kolbasov, A.M.Lebedev, B.A.Loginov, O.N.Makeev, K.A.Menshikov, V.G.Stankevich, N.J.Svechnikov, A.L.Suvorov. Investigation of TOKAMAK T-10 glogular films microstructure. 31st EPS Conference on Plasma Physics, 28 June - 2 July 2004, Imperial College, London.

A comparative study of field emission from pristine, annealed and CuCl-doped single-walled carbon nanotubes

Eugene V. Redekop[1], Victor I. Kleshch[1], Alexander A. Tonkikh[2,3], Elena D. Obraztsova[3], and Alexander N. Obraztsov[1,4]

[1]*Department of Physics, M.V. Lomonosov Moscow State University, 119991, Moscow, Russia*
[2]*Faculty of Physics, Southern Federal University, Rostov-on-Don, 344090 Russia*
[3]*A.M. Prokhorov General Physics Institute, RAS, 119991, Moscow, Russia*
[4]*Department of Physics and Mathematics, University of Eastern Finland, 80101, Joensuu, Finland*

A significant change in the electronic properties has been recently demonstrated for single-walled carbon nanotubes (SWCNTs), filled with CuCl by the gas phase method. The strong p-type doping induced by encapsulated CuCl crystals provides a possibility of modification of nanotubes work function and correspondingly their field emission (FE) characteristics. Here, we present a comparative study of FE characteristics of flat films composed of pristine, annealed and doped carbon nanotubes performed using a flat phosphor screen technique. A significant increase of the threshold field was observed after annealing or doping of SWCNTs films (Fig. 1). It can be caused by the selective oxidation of the small-diameter nanotubes. This explanation is confirmed by Raman spectroscopy (Fig. 2). Meanwhile FE characteristics of annealed and doped nanotubes coincided with each other, while the Raman spectra substantially changed due to the effective doping of CuCl. These results indicate that CuCl doping does not change the work function of the emitting tip of the carbon nanotubes.

The work was supported by Russian Science Foundation grant 15-12-30041

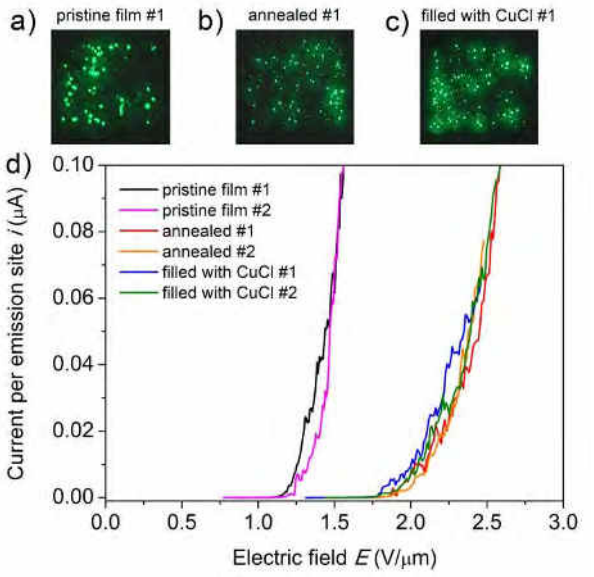

Fig. 1. (a-c) Field emission patterns at the current of 10 μA and cathode-to-anode distance of 500 μm for pristine, annealed and doped SWCNT films. Each pattern size is 1cm x 1cm. (d) The dependence of the current normalized on the number of the emission sites versus the electric field for the three types of SWCNT films. For each type of the film two experimental curves obtained for the two different samples are presented.

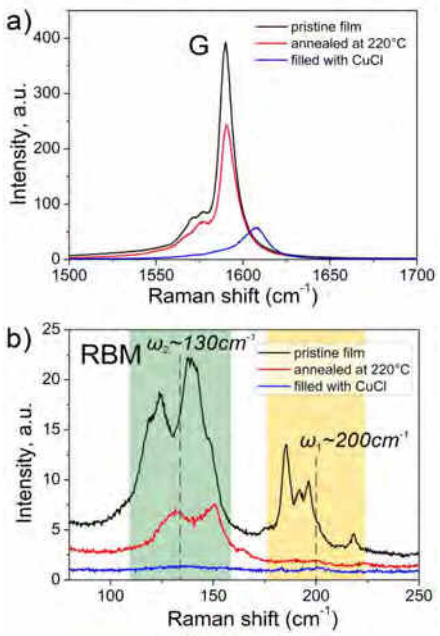

Fig. 2. The Raman spectra of pristine SWCNT film, annealed at 220 °C for 26 hours and film exposed to CuCl gas at 220 °C for 26 hours. The excitation wavelength is 633 nm.

Conductivity of nanomaterial layers at millimeter wave frequencies

I.I. Nefedova, D.V. Lioubtchenko, I.S. Nefedov, and A.V. Räisänen
Department of Radio Science and Engineering, Aalto University School of Electrical Engineering, FI-00076 Aalto, Finland
irina.nefedova@aalto.fi

Development of future millimeter wave components requires miniaturization of the integrated materials. Novel nanomaterials like carbon nanotubes (CNTs) and silver nanowires (AgNWs) offer new opportunities for applications at millimeter wave frequencies, e.g., in high speed and high data capacity electronics [1, 2]. The dielectric rod waveguide (DRW) is an effective technique for direct testing of nanomaterials in the frequency ranges up to 1 THz [3]. The propagation constant of nanomaterials can be estimated from S-parameters measurements of the DRW, connected to Vector Network Analyzer (Fig. 1).

A new approach to estimate a conductivity of the layer, consisting of CNTs or AgNWs, based on the measured propagation constant and followed by theoretical and numerical calculations is developed. The real part of conductivity for studied nanomaterials was calculated using the theory, which takes into account finite length of the CNTs and AgNWs, and the quantum conductivity of individual nano-wires/tubes. Calculated conductivity allows to perform the numerical simulations with Ansoft HFSS; a good agreement with experimental results is achieved (Fig. 2).

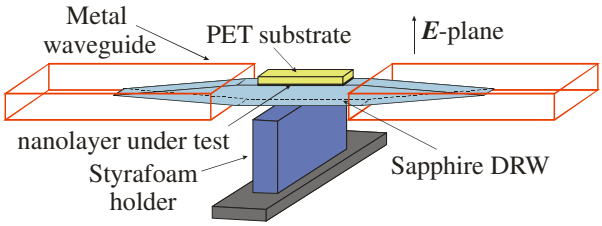

Figure 1. Measurement setup.

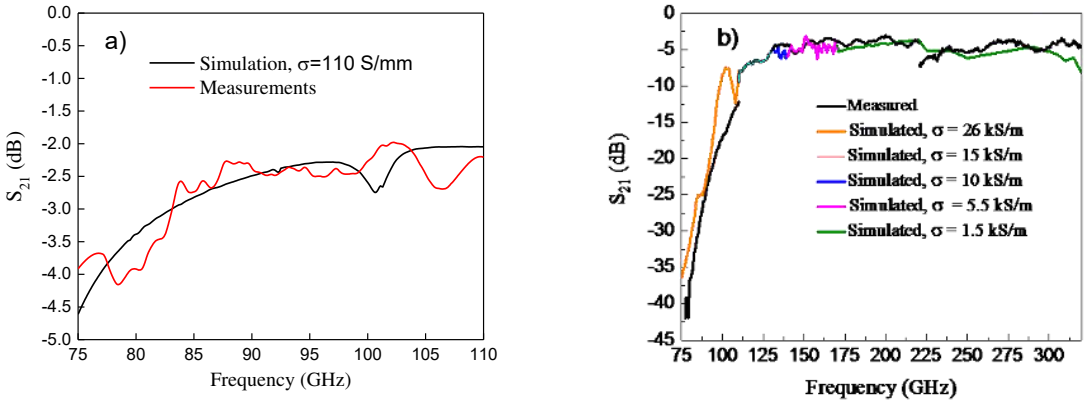

Figure 2. The measured and simulated S_{21} of DRW loaded with a) AgNW and b) CNT layers.

Analytical calculations and computer modeling indicate that the measured losses at low THz frequencies are mostly due to the conductivity of the nanomaterial layer. The observed rapid decrease of the conductivity with increasing frequency is related with finite lengths of nanomaterials.

This work was financially supported in part by the Academy of Finland for through the DYNAMITE project, Teknologiateollisuuden 100-vuotissäätiö Foundation, Nokia Foundation Corporation, and Aalto ELEC Doctoral School.

[1] H.-J. Song and T. Nagatsuma, “Present and future of terahertz communications,” IEEE Trans. on Terahertz Science and Tech., vol. 1, no. 1, pp. 256-263, 2011.
[2] Z. Zhong, D. Wang, Y. Cui, M. Bockrath and C.M. Lieber, “Nanowire crossbar arrays as address decoders for integrated nanosystems,” Science, vol. 302, no. 5649, pp. 1377-9, 2003.
[3] I.I. Nefedova, D.V. Lioubtchenko, I.S. Nefedov, and A.V. Räisänen, “Dielectric constant estimation of a carbon nanotube layer on the dielectric rod waveguide at millimeter wavelengths,” IEEE Trans. on Microwave Theory and Techniques, vol. 63, no. 10, pp. 3265 – 3271, 2015.

Electronic structure and optical properties $C_{60}O$ and $C_{120}O$ complexes

I.B. Zakharova[1], O.E. Kvyatkovskii[1,2], M.A. Elistratova[1], E. Lahderanta[3], T.L. Makarova [2,3]

[1]Peter the Great St.Petersburg Polytechnic University , Polytechnicheskaya 29, 195251, St. Petersburg, Russia
[2]Ioffe Physical Technical Institute, Polytechnicheskaya 26, 194021 St. Petersburg, Russia
[3]Lappeenranta University of Technology, FI-53851 Lappeenranta, Finland.

zakharova@rphf.spbstu.ru

Optical measurements on fullerene films, such as Raman or photoluminescence entails the use of laser excitation and are often held in the air atmosphere. It is known that fullerenes actively interact with oxygen, and in thin films this effect is especially notable. Still, the effect of oxygen on the fullerene oligomerization and therefore on the optical properties is not yet fully understood. We have previously determined that C_{60} fullerene thin film, depending on its structure and morphology, is almost entirely the oxygen-fullerene reaction products. It means that the results of optical measurements are related not to a pristine film, but to the photo-oxidation and photopolymerisation products.

Here we simulated these reactions considering normal environment. The role of oxygen in the formation of phototransformed fullerene phase is accounted on the basis of ab initio calculations of various oxygen energetics in C_{60} – O system. The optimized geometry and electronic structure of $C_{60}O$ isomers and C_{60}-O-C_{60} oligomers in singlet and triplet spin states are calculated using DFT/B3LYP method with 6-31G (2df, 2pd) basis set. The results of epoxide C_{60}-O optimization show that the dissociation of the oxygen molecule intercalated in the fullerene matrix into a pair of exohedrally attached ligands is energetically favorable. We calculated the energy gain under formation complex $C_{60}O(5,6)$ and cycloadduct dimer $C_{120}O$. We consider two possible scenarios of dimer formation: from pristine C_{60} and molecular O_2 and from epoxide $C_{60}O$ and C_{60}:

Eform(I) = 1/2Etot(O2) + 2Etot(C60) - Etot(C120O) = 1.384 eV
Eform(II) – Etot(OC60) + Etot(C60) - Etot(C120O) – 0.667 eV.

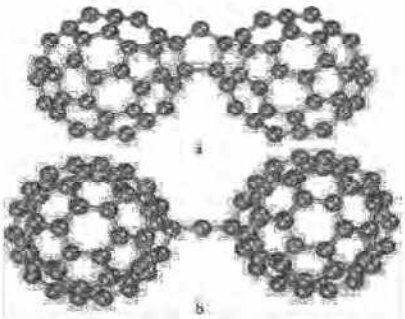

Fig. 1 $C_{120}O$ oligomers: a) [2+2] cycloadduct dimer C_{60}-O-C_{60} (CA/C_s); b)singly bonded dimer C_{60}-O-C_{60} (SB/C_i).

The calculations demonstrate the feasibility of the dimerization reaction involving oxygen. The corresponding reaction O_2+2C_{60}=>$2C_{60}O(5–6)$ can be hindered by an energetic barrier in pristine C_{60}. In photolyzed C_{60} a photolytic dissociation of molecular oxygen to atomic oxygen occurs, with a subsquent bonding to C_{60}. Thus, in fullerene matrix photolyzed in air, molecular oxygen prefers to be bound with fullerene molecule forming $C_{60}O$ and then the dimer $C_{120}O$ with singlet ground states; that is, the reaction changes the ground spin multiplicity.

We calculated the spectra of the exited singlet and triplet electron states by the TD DFT method for the dimer C_{60}-O-C_{60}. In contrast to pure fullerene, where the singlet optical transitions are forbidden by symmetry, the resolved singlet transitions in the dimer spectrum appear with the energies of E_{ex} = 1.92 eV, 2.12 eV, 2.18 eV, 2.30 eV. This leads to significant changes in optical properties of C_{60} thin films. The theoretical results are compared with the measurement of the photoluminescence spectra of the X-ray irradiated C_{60}.

Acknowledgements: Supported by FP7 MSCA project MagNonMag-295180"Magnetic order induced in nonmagnetic solids".

Paramagnetic anatase titania/carbon nanocomposites

I. Zakharchuk[1], T.L. Makarova[1,2], D.A. Zherebtsov[3], D.M. Galimov[3], E. Lähderanta[1]
[1]*Lappeenranta University of Technology, FI-53851, Lappeenranta, Finland*
[2]*Ioffe Physical Technical Institute, Polytechnicheskaya 26, 194021 St. Petersburg, Russia*
[3]*South Ural State University, pr. Lenina 76, 454080, Chelyabinsk, Russia*
ivan.zakharchuk@lut.fi

Nanostructured glassy carbon is a highly practical material with wide applications in adsorbents, molecular sieves, membranes, catalysts, supercapasitors, fuel cells, etc. Chemically resistant carbon matrix is a suitable electrical conducting media. Such porous carbon matrix combined with another intriguing material, titania (TiO_2), can be found useful for applications in electrochemical and photovoltaic devices.

The anatase nanoparticle/carbon composite was synthesized using furfuryl alcohol C_2H_5OH (FA), tetrabutyltitanate $Ti(C_4H_9O)_4$ (TBT) and nonionic surfactant polyethyleneglycol (10) ether of isooctylphenol (trade name OP-10). Starting solution was mixed in the following mass ratio 2 (FA): 4 (TBT): 1 (OP-10). The polymerization of FA was initiated by addition of a 0.2 ml of 36% toluenesulphonic acid solution in butyl alcohol. The reacting solution was held for 48 hours at each of the temperatures 20, 50, 70, 90, 110, and 150 °C successively. The resulted organic-inorganic polymer was slowly heated in inert atmosphere up to 970 °C and then annealed for 1 hour. The energy dispersive X-ray analysis yielded carbon, oxygen and titanium as main components. Also some contamination by 0.13 mass% Na, 0.10 mass% Al, 0.09 mass% S, and 0.08 mass% was found. The small angle X-ray scattering confirmed the presence of the TiO_2 crystals in anatase form with diameters of 5-15 nm.

The temperature evolution of susceptibility of the investigated TiO_2/carbon composites was found to obey the Curie law with minor irreversibility between the zero-field-cooled (red, Fig. 1a) and field-cooled curves (blue, Fig. 1a) at temperatures below 75 K. Whereas, the higher temperature region is dominated by diamagnetic contribution from the carbon matrix. The magnetic field dependences at low temperatures resemble paramagnetic behavior (see Fig. 1b). However, a small nonlinearity is observed in the curve measured at 3 K. This nonlinearity together with the irreversibility in temperature dependences points to the presence of a small magnetic ordering in the samples.

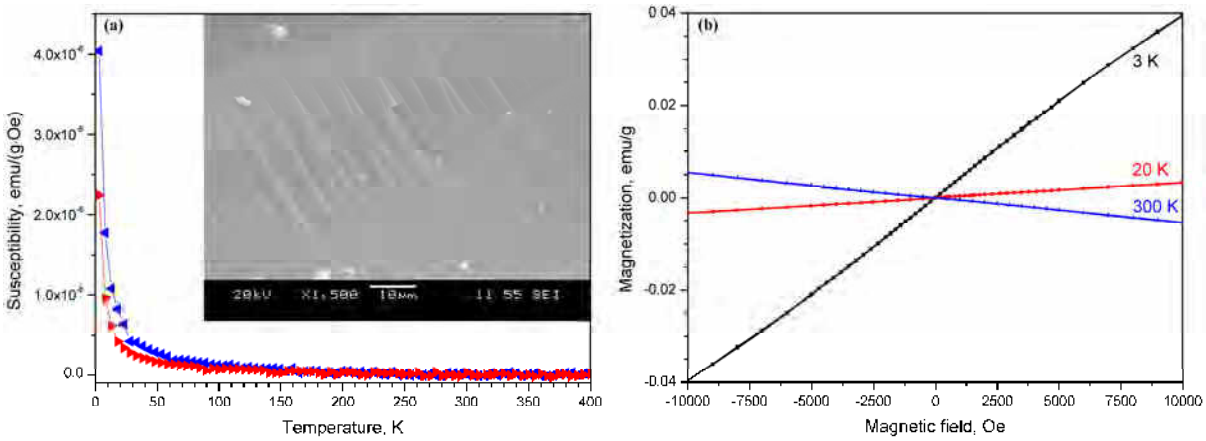

Fig. 1. (a) Temperature variation of susceptibility of one of the TiO_2/carbon samples. The inset presents a SEM image of the sample's surface. (b) Magnetic field dependences of the TiO_2/carbon sample at various temperatures.

Acknowledgement.

This work was supported by FP7 MSCA project MagNonMag-295180 "Magnetic order induced in nonmagnetic solids".

Frequency Tuned Cherenkov Laser Based on Graphene Structures

K. Batrakov
Institute for Nuclear Problems Belarus State University, Bobruiskaya 11, Minsk, Belarus
kgbatrakov@gmail.com

Graphene sheet supports surface electromagnetic waves which dispersion law differs from wave dispersion in three-dimensional systems [1]. Phase velocity of electromagnetic wave in graphene can be significantly less then speed of light, additional wave slowing down can be reached in the system of two spatial decoupled graphene monolayers [2]. All this can lead to Cherenkov radiation. This work studies Cherenkov generation by electron beam and frequency tuning of generated terahertz wave in graphene monolayer and spatial decoupled graphene monolayers systems. Frequency of generated wave depends on graphene chemical potential μ, which

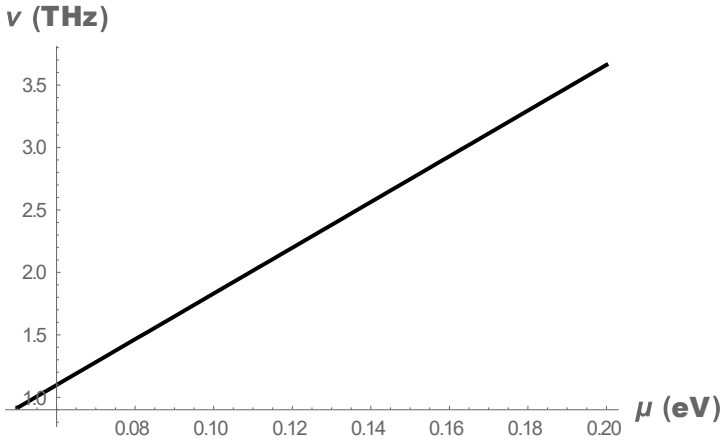

Fig. 1. Dependence of generated frequency on graphene chemical potential. Electron beam energy E=60 keV.

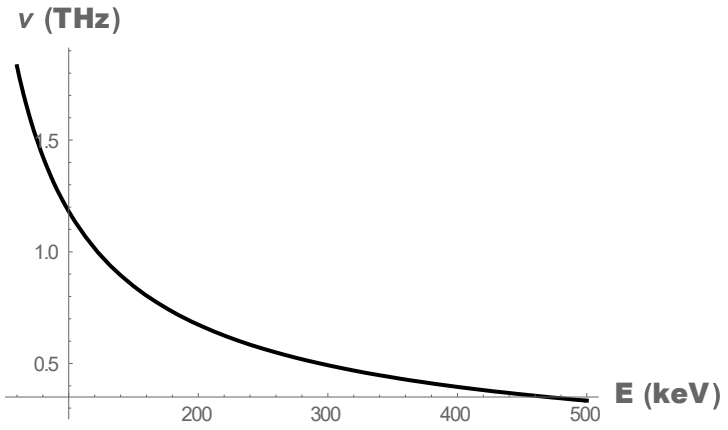

Fig. 2. Dependence of generated frequency on electron beam energy. Chemical potential $\mu = 0.1$ eV.

can be tuned electrostatically by external transverse electric field. Such type of dependence is presented on Fig.1. Fig.2 demonstrates frequency dependence on electron beam energy. Besides, frequency can be tuned by variation of distance between layers in decoupled graphene monolayers systems.

Acknowledgement.
The research leading to this work has received funding from the European Union Seventh Framework Program under Grant Agreement No. 604391 Graphene Flagship and Grant Agreement No. 318617 Marie Curie International Research Staff Exchange Scheme Fellowship (MC-IRSES FAEMCAR project), Call H2020-MSCA-RISE-2014 Programme H2020 CoExAN and U.S. Air Force through CRDF Global Agreement grant AF20-15-61804-1.

[1] S. Das Sarma and E. H. Hwang, Phys.Rev. Lett. **102**(20), 206412 (2009).
[2] K. Batrakov; V. Saroka, S. Maksimenko, Ch. Thomsen, Journal of Nanophotonics, **6**(1) 061719 (2012).

Optical limiting in suspension of detonation nanodiamonds in engine oil

K.G. Mikheev[1], R.Yu. Krivenkov[1], T.N. Mogileva[1], A.P. Puzyr[2], V.S. Bondar[2], G.M. Mikheev[1]
[1]*Institute of Mechanics UB RAS, 34, str. T. Baramzinoy, Izhevsk, 426067, Russia*
[2]*Institute of Biophysics Siberian Branch of RAS, Akademgorodok, Krasnoyarsk, 660036, Russia*
k.mikheev@udman.ru

Optical limiting (OL) is a nonlinear optical phenomenon at which the intensity of radiation passing through the medium under study nonlinearly decreases, with increasing the radiation power density. OL study is of interest in terms of creation of nonlinear optical filters aimed to protect the eyes and photosensor devices. Earlier it was shown that aqueous suspensions of detonation nanodiamonds (DND) can be used as optical limiters over a wide wavelength range [1-3]. It was established that the nonlinear light scattering is one of the main mechanisms of OL in aqueous DND suspensions. It was shown that OL efficiency in aqueous DND suspensions increases with increasing of the nanoparticles clusters average size D_{aver} [4]. Thereupon, it is of interest to obtain time stable supensions of DND with high values of D_{aver}.

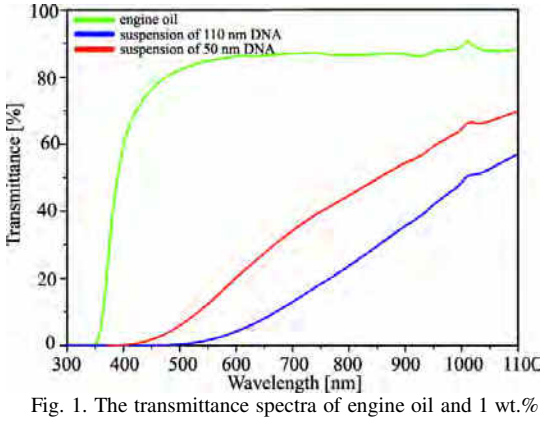

Fig. 1. The transmittance spectra of engine oil and 1 wt.% DND suspensions with D_{aver} = 50 and 110 nm in engine oil relative to air measured in a 1.5 mm-thick optical cell

According to our previous studies aqueous suspensions of DND with average nanoparticles clusters size of 110 and 320 nm are less time stable than those with D_{aver} = 50 nm. One of the ways to increase the stability of the suspensions is to use a viscous dispersion medium, e.g. engine oil. Our experiments showed that the DND suspensions in engine oil with the average nanoparticles clusters size of 50 and 110 nm obtained in 2009 are still stable with no signs of dispersed phase layering. Besides that, engine oil is a low-freezing liquid. All mentioned above makes study of OL in DND suspensions in engine oil relevant in terms of creation non-freezing optical limiters.

In our experiments DND were synthesized by the technique described in [4]. OL study was carried out by z-scan technique. Experiments were carried out on automatized setup allowing one to obtain the nonlinear transmittance and the nonlinear refraction in a single pass scanning simultaneously. First harmonic (1064 nm) and second harmonic (532 nm) radiation of YAG:Nd^{3+}-laser with passive Q-switching were used as an excitation source.

In Fig.1 the transmittance spectra of engine oil and 1 wt.% DND suspensions with D_{aver} = 50 and 110 nm in engine oil relative to air are presented. One can see that the engine oil is transparent in a wide wavelength range, while transmittance of DND suspensions decreases in the short wavelength range.

In Fig.2 the normalized transmittance of the DND suspension with D_{aver} = 50 nm at 532 and 1064 nm as a function of pulse energy density are shown. One can also see the normalized transmittance of the DND suspensions with D_{aver} = 50 and 110 nm as a function of z/z_0 in the inset of Fig.2. The efficiency of OL in the DND suspensions is higher at 532 nm excitation and it is higher in the suspension with D_{aver} = 110 nm comparing to that with D_{aver} = 50 nm. This result is in agreement with the study of wavelength influence to the OL in infrared wavelength range [3,4].

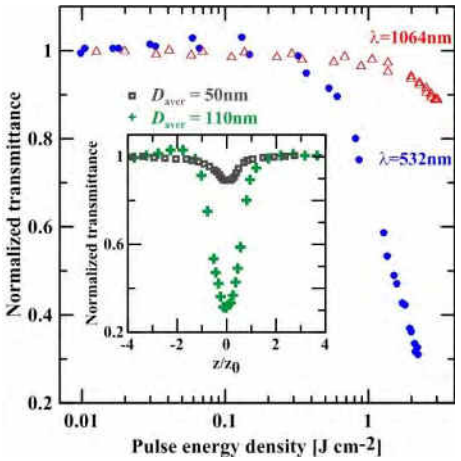

Fig. 2. The normalized transmittance of the DND suspension in engine oil with D_{aver} = 50 nm at 532 and 1064 nm. The normalized transmittance of the DND suspensions in engine oil with D_{aver} = 50 and 110 nm (inset)

Other interesting features of OL in DND suspensions in engine oil are also studied in this work.

Acknowledgement
This work was financially supported by RFBR (project No 16-38-00553).

References

[1] G.M. Mikheev, A.P. Puzyr, V.V Vanyukov, K.V. Purtov, T.N. Mogileva, V.S. Bondar. Tech. Phys. Lett., **36**, 358 (2010).
[2] V.V. Vanyukov, G.M. Mikheev, T.N. Mogileva, A.P. Puzyr, V.S. Bondar, Yu.P. Svirko. JOSA B, **31**, 2990 (2014).
[3] V.V. Vanyukov, G.M. Mikheev, T.N. Mogileva, A.P. Puzyr, V.S. Bondar, Yu.P. Svirko. Applied Optics, **54**, 3290(2015).
[4] V.V. Vanyukov, T.N. Mogileva, G.M. Mikheev, A.P. Puzyr, V.S. Bondar, Yu.P. Svirko.Applied Optics, **52**, 4123 (2013).

Tailoring electronic and optical properties of graphene by functionalization

Maxim G. Rybin, Elena D. Obraztsova
A.M. Prokhorov General Physics Institute, Moscow, Russia
rybmaxim@gmail.com

Functional materials are very attractive for studying and exploring new applications, and on the other hand graphene is one of the most promising materials which can be applied in a variety of areas from biomedicine to optics and electronics. But in some cases the pristine graphene cannot be used and the functionalization can provide a new type of graphene based materials with modified electronic and optical properties which enlarge the opportunity of graphene applications.

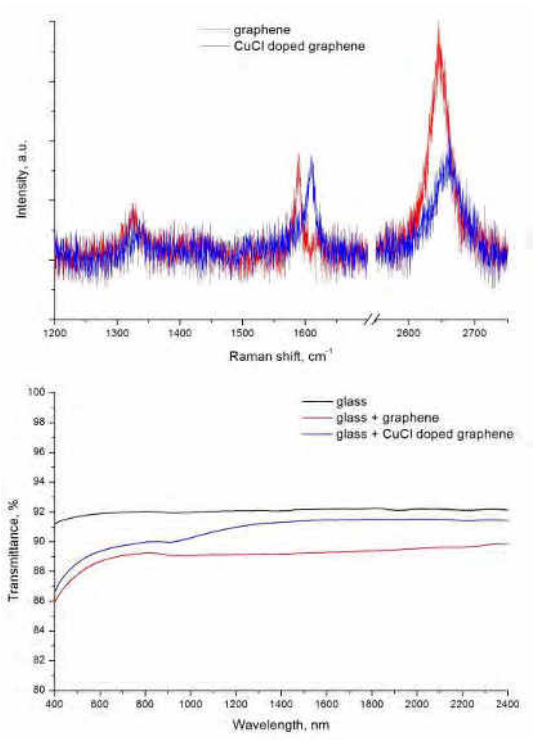

Figure 1. Raman spectra of pristine graphene and CuCl doped graphene (top). Optical transmission spectra of pristine graphene and CuCl doped graphene (bottom).

The changes of graphene properties rise from either changes of atomic structure of graphene lattice or adding new compounds to graphene structure. Previously we demonstrated the effective approach for adjusting electronic structure of graphene by doping with nitrogen atoms using plasma treatment [1, 2]. It results in slightly changed electronic structure, namely the shift of Fermi level in conduction zone by 0.2 eV.

Here we present stronger tailoring of electronic properties by functionalization of the pristine graphene by deposition of copper chloride or iron chloride on the surface of graphene by gas-phase adsorption. The interaction between the graphene and the molecules results in charge transfer due to strong acceptor characteristics of molecules. The changing of electronic structure was confirmed by Raman spectroscopy, the shift of G-peak of doped graphene from 1587 cm^{-1} to 1605 cm^{-1} corresponds to strong p-doping effect of graphene electronic structure. Moreover the optical transmission measurements shown the opening of the band gap of doped graphene around 1 eV this results in increasing of transmittance of doped graphene to almost 100% from 97% around 1-1.2 μm (see Fig. 1).

Demonstrated results open new perspectives for graphene applications in nano- and microelectronics.

The work was supported by 15-12-30041 of the Russian Scientific Foundation. Maxim Rybin gives thanks to RFBR № 16-32-60203.

[1] M. Rybin, A. Pereyaslavtsev, T. Vasilieva, V. Myasnikov, I. Sokolov, A. Pavlova, E.A. Obraztsova, A. Khomich, V. Ralchenko, E.D. Obraztsova "Efficient nitrogen doping of graphene by plasma treatment", ***Carbon*** 96 (2016) 196-202.
[2] A. Pereyaslavtsev; M. Rybin; T. Vasilieva; V. Miasnikov and I. Sokolov "Experimental study of nitrogen-doped graphene by spectroscopic and probe methods of surface analysis", ***J. Nanophoton.*** 10(1), 012521.

Reduced graphene oxide humidity sensor

Vinokurov P.V., Timofeev V.B., Smagulova S.A.
North-Eastern Federal University, 677000,Belinskogo str., Yakutsk, Republic of Sakha (Yakutia), Russia
pv.vinokurov@s-vfu.ru

Unique physical and optical properties make graphene oxide (GO) a versatile material for fabrication of various sensing devices [1]. In particular, a pronounced dependence of the GO conductivity on the adsorbed water can be employed in humidity sensors. Conductivity of the GO can be improved by its reduction via thermal treatment, photoreduction, functionalization in gases etc. The films of the reduced graphene oxide (rGO) are flexible and can be used sd electrodes for supercapacitors and sensor elements [2]. One of the attractive methods to obtain rGO film is reduction of the GO under irradiation with an intense laser beam [3]. This method possesses spatial selectivity allowing one to create a prescribed conductive rGO pattern on the surface of the non-conductive GO film. We demonstrate that such a patterned GO film can be employed as an efficient humidity sensor.

In the experiment we used GO dispersion, which was synthesized from graphite powder using a conventional Hummers technique [4]. The GO films were prepared by coating a transparent polyester film with dispersion and drying at room temperature. Space-selective reduction of the GO film was performed by using a semiconductor laser of the DVD player with LightScribe technology [5]. The photographic image of the “comb-like” electrodes formed on the GO film surface is shown in Fig.1(a). The dependence of the resistance between electrodes on the amount of the adsorbed water allows us to measure the ambient humidity (RH).

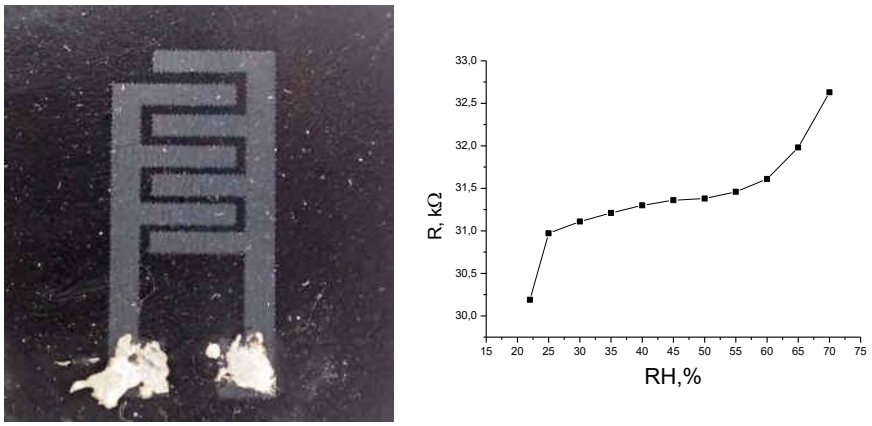

Fig.1. (a) Image of the GO film with rGO pattern obtained by laser irradiation. (b) Dependence of the resistance between rGO electrodes of the relative humidity.

The air humidity during the experiment was controlled by conventional humidity sensor, which was placed in a measurement chamber. Figure 1b shows that the higher the humidity the bigger the resistance between electrodes. Conductance of rGO film decreased when humidity was increasing from 20% RH to 70%. We also observed a weak hysteresis in the dependence of the resistance on humidity when the measurements were performed by increasing and decreasing RH. The possible mechanisms of interaction of water molecules with the GO surface resulting in an increase of conductivity of the films were discussed.

Acknowledgement

This study was financially supported in part by Russian Foundation of Basic Research (Grant No. 15-08-01977)

References

[1] Y-L. Zhang, L. Guo, H. Xia, Q-D. Chen, J. Feng, H-B. Sun, Advanced Optical Materials, **2,** 1 (2014)
[2] H. Tian, Y. Yang, D. Xie, Y-L. Cui, W-T. Mi, Y. Zhang and T-L. Ren, Scientific Reports **4**, 3598 (2014)
[3] M.F. El-Kady, V. Strong, S. Dubin, B. R. Kaner Science, **335**, 6074 (2012)
[4] W.S. Hummers, R.E. Offeman, Journal of the American Chemical Society **80 (6)**, 1339 (1958)
[5] D.E. Anderson, M.P. Gore, P.J. McClellan, Hewlett-Packard Development Company, U.S. Patent 7172991 B2 (2001)

Z-scan technique modernization to study the saturable absorption in nanocarbon materials

R.Yu. Krivenkov[1], K.G. Mikheev[1], T.N. Mogileva[1], A.V. Okotrub[2], G.M. Mikheev[1]
[1]*Institute of Mechanics UB RAS, 34, str. T. Baramzinoy, Izhevsk, 426067, Russia*
[2]*Nikolaev Institute of Inorganic Chemistry SB RAS, 3, Acad. Lavrentiev Ave., Novosibirsk, 630090, Russia*
roman@udman.ru

Saturable absorption (SA) is one of interesting nonlinear-optical phenomena in nanocarbon materials[1, 2]. SA is the effect of an optical medium bleaching which is due to the electron transition between two energy levels. SA in nanocarbon materials is usually accompanied by the increase of the transmittance in the medium studied in the range of a few tenths to a few percent.

Z-scan is one of the techniques of SA investigation that is measuring the optical transmittance of the sample while it is being scanned along the axis of the focused laser beam [3, 4]. However during z-scan measurements using of a monochromatic laser pump, uncontrolled change of the reflectance from the sample due to the interference of the beams reflected from the front and back side of the sample can occur. This fact can significantly misinterpret the results of the z-scan experiments.

It is shown that the z-scan of the uncoated optical cuvette inclined relatively to the optical axis of the narrow laser beam allows one to obtain nonlinear transmittance of the sample as a function of intensity with high accuracy. We demonstrate the opportunity of measuring the linear transmittance of the nanocarbon materials suspension with the data scattering less than 0.17%. At the same time it is possible to obtain the data to calculate the nonlinear transmittance and nonlinear refraction of the suspension in a single pass scanning.

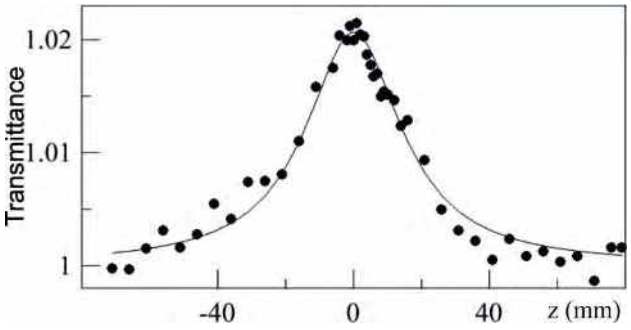

Fig.The nonlinear transmittance of the 0.01 wt. % MWNTs suspension as a function of z, measured by an open aperture z-scan

The possibilities of the technique developed are demonstrated by the example of the observation of weak SA and weak nonlinear refraction in the suspension of multi-wall carbon nanotubes (MWNTs). The nonlinear transmittance of the 0.01 wt % MWNTs suspension as a function of z, measured by an open aperture z-scan is shown in the Fig. as an example. The suspension was placed into a 1 mm-thick optical cuvette. Single-frequency pulsed 532 nm laser was used as a laser pump. The laser pulse duration was 13.6 ns, the M^2parameter characterizing the beam quality was equal to 1.03, the laser pulse energy was 11 μJ, and the laser beam diameter in the waist was 102.6 μm. The laser beam was focused by a collecting lens with a focal length of 192 mm. One can see from the Fig. that the nonlinear transmittance measured at the beam waist increases by up to 2%. Thus, the SA in the aqueous suspension of MWNTs is confidently observed. The high measurements accuracy reached allows to reliably approximate the experimental dependence and to calculate the saturation parameter, characterizing the SA, I_{sat} = 2.7 MW/cm^2.

Acknowledgement
This work was financially supported by RFBR (project No 16-42-180147) and the Finnish Academy of Sciences (Grant No.288547).

References

[1] T. Hasan, Z. Sun, F. Wang, F. Bonaccorso, P. H. Tan, A. G. Rozhin, A. C. Ferrari, Adv. Mater., **21**, 38 (2009).
[2] Z. Sun, T. Hasan, A. C. Ferrari, Phys. E, **44**, 1082 (2012).
[3] M. Sheik-Bahae, A. A. Said, T. H. Wei, D. J. Hagan, E. W. Van Stryland, IEEE J. Quantum Electron., **26,** 760 (1990).
[4] M. George, C. I. Muneera, C. P. Singh, K. . Bindra, S. M. Oak, Opt. Laser Technol., **40**, 373 (2008).

Increase in transmittance of nanodiamond dispersions by femtosecond laser excitation

V.V. Vanyukov[1,2], G.M. Mikheev[3], T.N. Mogileva[3], A.P. Puzyr[4], V.S. Bondar[4], A.L. Chuvilin[5,6], D.A. Lyashenko[7], and Y.P. Svirko[1]

[1]Institute of Photonics, University of Eastern Finland, Joensuu 80101, Finland
Hypermemo Oy, Joensuu 80101, Finland
[3]Institute of Mechanics, Russian Academy of Sciences, Izhevsk 426067, Russia
[4]Institute of Biophysics, Russian Academy of Sciences, Krasnoyarsk 660036, Russia
[5]CIC nanoGUNE Consolider, 20018 Donostia−San Sebastián, Spain
[6]IKERBASQUE, Basque foundation for science, 48013 Bilbao, Spain
[7]Texas State University, Materials Science, Engineering, and Commercialization, San Marcos, USA
[*]viatcheslav.vanyukov@uef.fi

Advances in fabrication of graphene and carbon nanotubes along with their exciting optical properties overshadowed the nanodiamond (ND), a nanomaterial with sp3 hybridization of carbon orbitals. NDs are known from 1960s and possess a number of unique properties, which give rise to their application in various areas of industry, science, technology and medicine [1-3]. In our previous study, we have shown that aqueous ND dispersions possess a strong nonlinearity that was successfully employed for the optical limiting (OL) in the nanosecond (ns) time scale [4]. We report the results of the nonlinear optical studies in the ND dispersions in the femtosecond (fs) time domain. Contrary to the ns, the fs Z-scan measurements revealed an increase of transmittance in aqueous ND dispersions. The transmittance increase is originated from the saturation of light absorption in ND dispersions.

We have experimentally studied aqueous dispersions of detonation ND clusters with an average size of 49.6 nm. The ND clusters were suspended in water with mass concentration of 0.75%, 1%, 1.5%, and 2%. In the experiments, we employed Ti: sapphire laser operating at the wavelength of 795 nm with the repetition rate of 1 kHz and the pulse duration of 120 fs. Measurements were performed using an open-aperture Z-scan configuration.

In the Z-scan measurements we have found that the transmittance of the ND dispersions increase as the cell with NDs approaches the focal point, i.e. z=0. In particular, for the 2% ND dispersion the transmittance increase riches 3.3% and 3.8%, at the laser pulse excitations of 53.4 GW/cm^2 and 89 GW/cm^2, respectively. Importantly, the transmittance dependence presents an even function with respect to z=0, and hence, one may expect that the light-induced bleaching does not occur.

In order to demonstrate this we measured the transmittance by placing the samples in the focal point (z=0) and at the distance of z=15 mm from it. The dispersions with ND concentrations of 1% and 2% were exposed to more than 30 thousands fs laser pulses with pulse energies of 150 nJ and 200 nJ, which corresponded to intensities of 133 GW/cm^2 and 178 GW/cm^2, respectively. Since the transmittances of both samples did not change, no light-induced irreversible transparency occurs independently on the pulse energy. This implies that the transmittance increase originates from the saturation of the light absorption in the ND. Additional experiments with ND samples with average cluster sizes of 34 nm and 110 nm also revealed the saturation of light absorption in ND.

In conclusion, we observed an increase of the transmittance in aqueous ND dispersions for fs laser pulses at the wavelength of 795 nm. The observed nonlinear optical effect is reversible, i.e. it is not associated with light-induced modification of the ND clusters. The observed phenomenon originates from the electronic nonlinearity of the ND clusters and manifests itself as a suppression of the absorption coefficient of the dispersion under irradiation with fs pulses with photon energy of 1.56 eV. We demonstrated experimentally that the saturable absorption takes place in a wide range of ND cluster sizes and concentrations.

[1] V.N. Mochalin, O. Shenderova, D. Ho, Y. Gogotsi, Nat. Nanotechnol. Nature Publishing Group, **7**, 1 (2012).
[2] A.E. Aleksenskiy, E.D. Eydelman, A.Y. Vul', Nanosci. Nanotechnol. Lett. **3**, 1 (2011).
[3] V.S. Bondar, A.P. Puzyr, Phys. Solid State. **46**, 4 (2004).
[4] V.V. Vanyukov, "Effects of nonlinear light scattering on optical limiting in nanocarbon suspensions", PhD Thesis, *publication of the University of Eastern Finland* №182, (2015).

Thursday, August 4

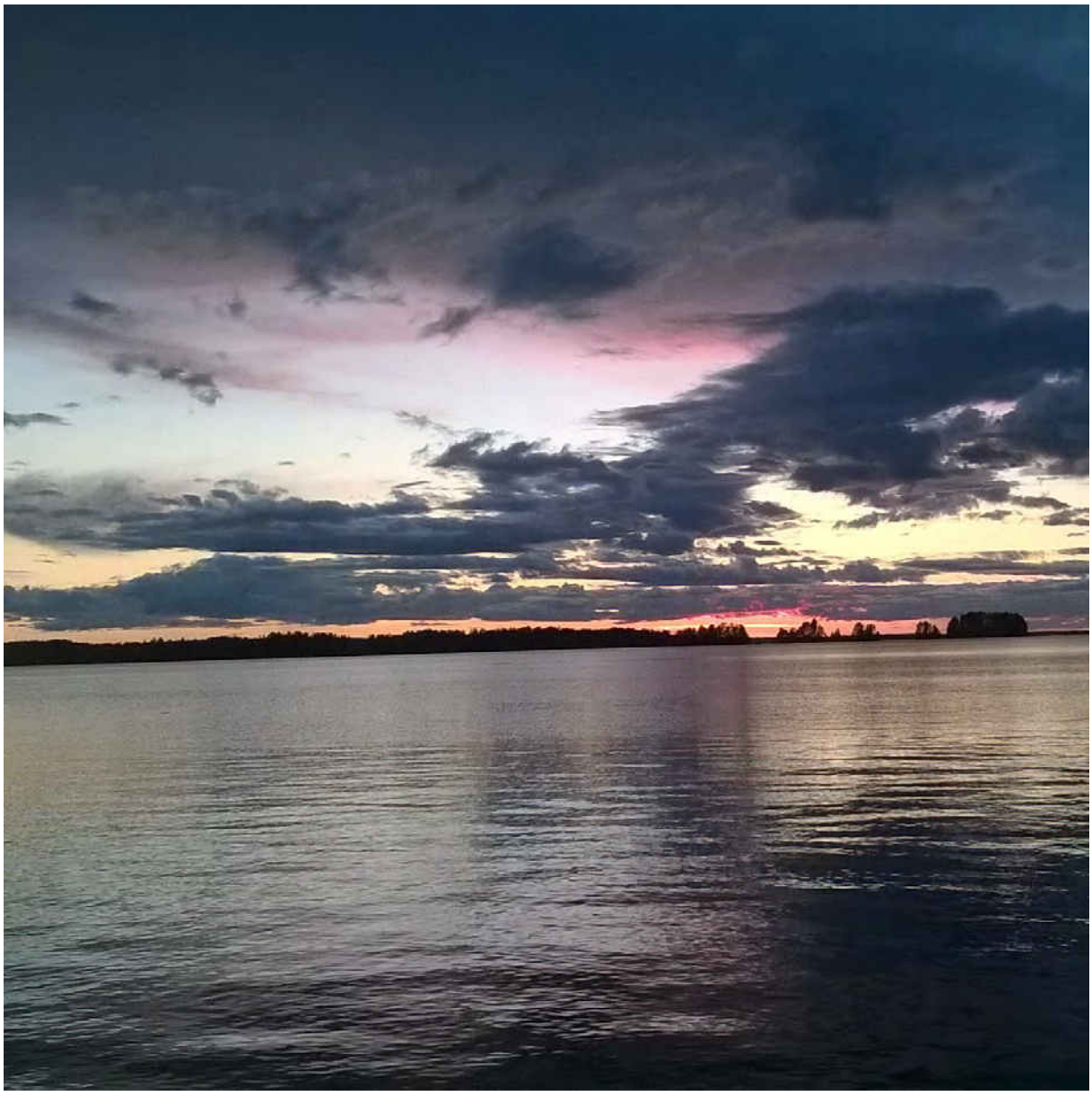

©Y. Svirko

Single-Walled Carbon Nanotube Films as Electron-Blocking-Layer and Transparent Electrode for Various Solar Cells

Shigeo Maruyama
Department of Mechanical Engineering, The University of Tokyo, 7-3-1 Hongo, Bunkyo-ku, Tokyo 113-8656, Japan
Energy NanoEngineering Lab., National Institute of Advanced Industrial Science and Technology, 1-2-1 Namiki, Tsukuba 305-8564, Japan
maruyama@photon.t.u-tokyo.ac.jp

1. CNT-Si and graphene-Si solar cells

It was found that a film of single-walled carbon nanotubes (SWNTs) can be dual-functional as electron-blocking-layer and transparent electrode through studies of nanotube-silicon heterojunction solar cells [1-3]. We have demonstrated efficient SWNT/Si solar cells using dry-deposited high-quality SWNTs [1] and honeycomb-structured SWNTs [2]. The SWNT/Si solar cells using the dry deposited SWNT film demonstrated the air-stable power conversion efficiency (PCE) of 11.6 % before any intentional doping process. With the stable copper oxide based doping, the PCE can be more than 13.5 %. Another long-term air-stable doping using boron-based molecular super Lewis acid is also introduced [4]. Adequately doped mm scale single crystal graphene [5] also exhibited the similar performance [3]. Even though the film of SWNTs composed of mixture of semiconducting and metallic tubes should be naively metallic, however, it can behave as an electron blocking layer.

2. Organic thin film and Perovskite solar cells

The dual functionality is also demonstrated for organic thin film and perovskite-type solar cells. For organic thin film solar cells, the SWNT/MoOx/PEDOT:PSS layer (normal structure) was demonstrated as a dual functional layer replacing ITO and organic electron-blocking-layer. Using PTB7/PC71BM mixture as active materials, the PCE of 6 % was obtained for glass substrate and 3.9 % on flexible PET substrate [6]. Window-like semi-transparent solar cells are demonstrated by replacing the electron blocking layer and metal electrode in inverted structure organic solar cell.

The SWNT film was also applied to normal and inverted organic-inorganic hybrid perovskite ($CH_3NH_3PbI_3$) solar cells. The dual-functional feature was demonstrated in double-sided illumination perovskite solar cells using SWNT film instead of electron-blocking-layer and gold electrode (shown in Figure 1) with over 9 % PCE [7]. Another perovskite solar cell structure using SWNTs instead of ITO is also proposed [8].

3. Acknowledgments

A part of this work was financially supported by Grants-in-Aid for Scientific Research (25107002, 15H05760) and IRENA Project by JST-EC DG RTD, Strategic International Collaborative Research Program, SICORP.

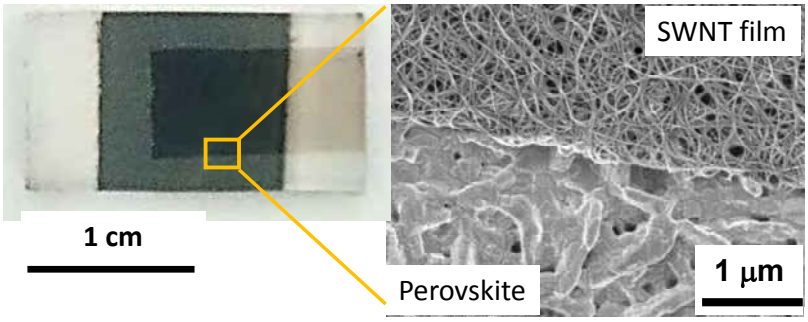

Fig. 1. Photograph and SEM image of a perovskite solar cell using SWNT film as electron-blocking-layer and transparent electrode.

4. References

[1] K. Cui, T. Chiba, S. Omiya, T. Thurakitseree, P. Zhao, S. Fujii, H. Kataura, E. Einarsson, S. Chiashi, S. Maruyama, J. Phys. Chem. Lett., 4 (2013), 2571.
[2] K. Cui, A. S. Anisimov, T. Chiba, S. Fujii, H. Kataura, A. G. Nasibulin, S. Chiashi, E. I. Kauppinen, S. Maruyama, J. Mater. Chem. A, 2 (2014) 11311.
[3] K. Cui, S. Maruyama, IEEE Nanotechnology Magazine, 10 (2016) 34.
[4] Y. Shoji, N. Tanaka, K. Mikami, M. Uchiyama, T. Fukushima, Nature Chem., 6 (2014) 498.
[5] X. Chen, P. Zhao, R. Xiang, S. Kim, J. Cha, S. Chiashi, S. Maruyama, Carbon, 94 (2015) 810.
[6] I. Jeon, K. Cui, T. Chiba, A. Anisimov, A. Nasibulin, E. Kauppinen, S. Maruyama, Y. Matsuo, J. Am. Chem. Soc., 137 (2015) 7982.
[7] T. Chiba, T. Sakaguchi, A. G. Nasibulin, E. I. Kauppinen, R. Xiang, S. Chiashi, S. Maruyama, to be submitted.
[8] I. Jeon, T. Chiba, C. Delacou, Y. Guo, A. Kaskela, O. Reynaud, E. I. Kauppinen, S. Maruyama, Y. Matsuo, Nano Lett., 15 (2015) 6665.

The photophysics of hybrid lead halide perovskites

Alex J. Barker
Center for Nano Science and Technology@PoliMi, Istituto Italiano di Tecnologia, via Giovanni Pascoli 70/3, 20133, Milan, Italy.
alex.barker@iit.it

Hybrid lead halide perovskites (‘perovskites’) – such as $CH_3NH_3PbI_3$ – are a family of solution-processible semiconductors first reported in 1978. Since 2012, they have received enormous attention as the active material in solar cells, with record power-conversion efficiencies of over 20% being achieved after only a few years of development. The possibility of distrupting existing solar technologies using abundant materials and simple, low-temperature manufacturing methods has driven rapid advances in our understanding of these materials over the last four years.

While their semiconducting characteristics are reminiscent of direct-bandgap semiconductors such as GaAs, the ionic nature of perovskites results in an intrinsic softness, giving rise to phenomena such as ionic conduction that must be understood and controlled to enable widespread implementation. Furthermore, the bandgap of perovskites is tunable throughout the entire visible spectrum, an attractive feature for use in multi-junction solar, light emitting, and lasing devices.

In this talk I will present an overview of the photophysics of perovskites, with particular focus on the spectroscopic investigations conducted by our group at CNST in Milan. This includes investigations of the relation between microstructure and electronic response,[1,2] the role of excitons,[3] the origin and nature of static and photoinduced trap states,[in preparation] and studies of nanocrystalline and confined structures.[4]

Acknowledgements
My colleagues at CNST, including principal investigator Annamaria Petrozza and director Guglielmo Lanzani. The research leading to these results has received funding from the European Union Seventh Framework Programme (FP7/2007-2013) under grant agreement no. 604032 of the MESO project.

References

[1] V. D’Innocenzo, A. R. Srimath Kandada, M. De Bastiani, M. Gandini and A. Petrozza. *J. Am. Chem. Soc.* (2014).
[2] G. Grancini, A. R. Srimath Kandada, J. M. Frost, A. J. Barker, M. De Bastiani, M. Gandini, S. Marras, G. Lanzani, A. Walsh and A. Petrozza. *Nat. Photonics* **9,** 695–701 (2015).
[3] V. D’Innocenzo, G. Grancini, M. J. P. Alcocer, A. R. S. Kandada, S. D. Stranks, M. M. Lee, G. Lanzani, H. J. Snaith and A. Petrozza. *Nat. Commun.* **5,** 1–6 (2014).
[4] Q. A. Akkerman, S. G. Motti, A. R. Srimath Kandada, E. Mosconi, V. D’Innocenzo, G. Bertoni, S. Marras, B. A. Kamino, L. Miranda, F. De Angelis, A. Petrozza, M. Prato and L. Manna. *J. Am. Chem. Soc.* **138,** 1010–1016 (2016).

High-resolution patterning of Organohalide Lead Perovskite Photovoltaic films for optical photodetectors applications

Dmitry Lyashenko[1,2], Aureliano Perez[1], Dr. Alex Zakhidov[1,2]
1. Physics Department, Texas State University, 601 University Dr., San Marcos, Texas, 78666, USA
2. Materials Science, Engineering, and Commercialization, Texas State University, 601 University Dr., San Marcos, TX 78666, USA

Organohalide lead perovskites are an emerging class of materials that have garnered significant consideration for applications in high-performance, low-cost photovoltaic devices including solar cells[1] and photodetectors.[2] Recent reports show that perovskite phototransistors are capable of achieving a photoresponsivity of 320 A W^{-1}, ranking among the highest values ever reported[3] (for comparison, Si photodetectors average <0.5 A W^{-1} in the visible spectrum). Most importantly, it is a highly absorptive (absorbance≈10^5 cm^{-1} in UV-visible range)[4] direct band-gap (1.6 eV) semiconductor with high carrier mobilities[5], long carrier diffusion lengths,[6] and shallow defect levels.[7] Low-temperature solution processing of absorbing perovskite and compatible organic transport layers, such as PEDOT:PSS and PCBM, enables monolithic, cost-effective integration of these photodetectors on complementary metal oxide semiconductor (CMOS) backplanes. Combination of high-sensitivity perovskite light absorbers with mature silicon technology may result in novel cost-efficient hybrid imagers with improved sensitivities and shorter response times.

Fig. 1. Solvency tests of CH3NH3PbI3 in various solvents with different polarity. Photographs of the samples were taken after 10 min immersion (10 seconds in case of acetone).

There is, however, a need for high-resolution structuring of the perovskite film to minimize cross-talk between neighboring detectors (pixels) for imaging purposes. $CH_3NH_3PbI_3$ films cannot be patterned by conventional photolithography as they are highly soluble in the polar solvents utilized in photoresist processing, such as water-based developers (tetramethylammonium hydroxide, sodium hydroxide, acetone, isopropanol (IPA), and N-methyl-2-pyrrolidone (NMP)). This point is further illustrated in **Fig. 1**, which shows perovskite films on glass substrates immersed half-way into various liquids.

Results

This work presents a method to develop $CH_3NH_3PbI_3$ thin films possessing high-resolution patterning, using lithography processing with hydrofluoroether solvents. The results presented herein confirm that, unlike the majority of traditional solvents utilized in conventional photolithography, hydrofluoroethers do not adversely affect $CH_3NH_3PbI_3$ films, enabling photolithographic processing (see Fig 2).

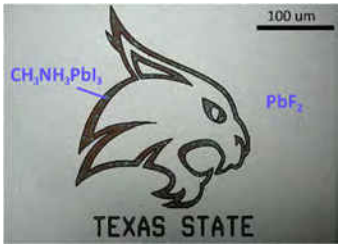

Fig. 2. High-Resolution Patterning of Organohalide Lead Perovskite Pixels for photodetectors using Orthogonal Photolithography

Transfer of the resist pattern is achieved using a SF6 plasma functionalization process, which extracts the iodine and organic components from the film, converting the perovskite into insulating PbF2. This work also demonstrates that the isolation of perovskite photodetecting pixels with a 20 µm-wide strip of PbF2 oxide leads to a 4.5-fold reduction in the cross-talk between neighboring pixels. It is believed that the presented method will facilitate simple monolithic integration of perovskite photodiodes to the silicon backplane chip utilized in active-pixel sensor and charge-coupled device applications.

Acknowledgements

This work was supported by ACS Petroleum Research Fund #56095-UNI6 (Program Manager Askar Fahr) and the REP program at Texas State University.

References

[1] J.-H. Im, C.-R. Lee, J.-W. Lee, S.-W. Park, N.-G. Park, Nanoscale 2011, 3, 4088.
[2] Y. Fang, Q. Dong, Y. Shao, Y. Yuan, J. Huang, Nat. Photonics 2015, 9, 679
[3] F. Li, C. Ma, H. Wang, W. Hu, W. Yu, A. D. Sheikh, T. Wu, Nat. Commun. 2015, 6:8238, 1
[4] M. A. Green, A. Ho-Baillie, H. J. Snaith, Nat. Photonics 2014, 8, 506.
[5] C. C. Stoumpos, C. D. Malliakas, M. G. Kanatzidis, Inorg. Chem. 2013, 52, 9019.
[6] Q. Dong, Y. Fang, Y. Shao, P. Mulligan, J. Qiu, L. Cao, J. Huang, Science 2015, 347, 967.
[7] W.-J. Yin, T. Shi, Y. Yan, Appl. Phys. Lett. 2014, 104, 063903/1.

Graphene heterostructures: peculiarities of microwave and THz response

Polina Kuzhir [1], Konstantin Batrakov [1], Alesia Paddubskaya [1,2], Sergey Maksimenko [1], Rumiana Kotsilkova [3], Tommi Kaplas [4], Yuri Svirko [4], Philippe Lambin [5]

[1] Research Institute for Nuclear Problems, Belarusian State University, Belarus
[2] Center of Physical Science and technology, Vilnius, Lithuania
[3] Open Laboratory on Experimental Micro and Nano Mechanics, Institute of Mechanics, Bulgarian Academy of Sciences, Bulgaria
[4] Institute of Photonics, University of Eastern Finland, Finland
[5] Physics Department, University of Namur, Belgium
Corresponding author e-mail: polina.kuzhir@gmail.com

Recently, we demonstrated that graphene can provide an efficient far-field shielding against microwave radiations [1,2] allowing one to achieve up to 50% absorption of the incident radiation, depending on the number of graphene sheets and doping level. Here we discuss different possibilities to enhance graphene/polymer absorption ability in wide frequency range, from microwaves to THz, up to perfect, 100%, absorption. For that substrate of proper thickness and dielectric properties supported graphene sample, as well as an optimal incidence angle of electromagnetic radiation can be used. We demonstrate both theoretically [3,4] and experimentally that the increase of the grain size of the CVD graphene from 20 to 400 microns does not affect the electromagnetic interference shielding performance of graphene/polymer heterostructure. The possibilities to tune electromagnetic response of graphene/polymer sandwich by changing the incidence angle for s-polarized wave in THz range, by electrostatic doping as well as mechanical strengths and deformations are also addressed in this communication.

The work was carried out within the framework of the FP7- FET Flagship 604391 Graphene and H2020 project 696656 Graphene Core1, and supported by H2020 project 644076 CoExAN.

[1] K. Batrakov et al, Scientific Reports 4, Article number: 7191 (2015)
[2] K. Batrakov, et al, Appl.Phys. Lett. 108, 123101 (2016)
[3] M. Lobet et al Nanotechnology 26, 285702 (2015)
[4] Ph. Lambin, et al, Electrodynamics of graphene/p olymer multilayers in the GHz frequency domain, Fundamental and Applied ElectroMagneticsA. Maffucci and S. Maksimenko (edits) Springer NATO Science for Peace and Security Series B: Physics and Biophysics, 2015

Tunable Metal-Graphene and Graphene-GaSe Devices

Harri Lipsanen
Department of Micro and Nanosciences, Aalto University, Espoo, Finland
harri.lipsanen@aalto.fi

Graphene and other 2D materials have unique properties that have made them hot topics not just in scientific research but also in the development of new types of applications in photonics and electronics. Unlike most 2D materials semimetallic graphene lacks bandgap needed in a number of applications. Especially interesting for devices are hybrid materials based on different 2D materials, such as graphene/GaSe [1] and BN/MoS_2, which combine the benefits and possibilities of dissimilar materials. These ultrathin, transparent devices open new opportunities, e.g., for flexible sensing and displays.

In this presentation studies of tunable 2D materials based on metal-graphene interface [2,3] and graphene–GaSe–graphene heterojunction device [1] will be shown. Our graphene-GaSe device configuration uses multilayer 2D materials with CVD graphene as a contact material. The gate electrodes placed on top of the graphene contacts on GaSe modulate only the Fermi energy of graphene allowing tunable contact. Transport measurements revealed promisingly strong current rectification and a high on/off ratio in the devices. In addition, GaSe and GaTe are attractive 2D materials for optoelectronics as demonstrated by recent SHG and THG measurements [4,5].

[1] W. Kim, C. Li, F. A. Chaves, D. Jiménez, R. D. Rodriguez, J. Susoma, M. A. Fenner, H. Lipsanen, and J. Riikonen, *Tunable Graphene-GaSe Dual Heterojunction Device*, Advanced Materials **28**, 1845 (2016).
[2] F. Chaves, D. Jimenez, A. Sagade, W. Kim, J. Riikonen, H. Lipsanen, D. Neumaier, *A physics based model of gate tunable metal-graphene contact resistance benchmarked against experimental data,* 2D Materials **2**, 025006 (2015).
[3] W. Kim, C. Li, N. Chekurov, S. Arpiainen, D. Akinwande, H. Lipsanen, J. Riikonen, *All-graphene Three-terminal Junction Field-Effect Devices as Rectifier and Inverter*, ACS Nano **9**, 5666 (2015).
[4] L. Karvonen, A. Säynätjoki, S. Mehravar, R. Rodriquez, S. Hartmann, D. Zahn, S. Honkanen, R. Norwood, N. Peyghambarian, K. Kieu, H. Lipsanen, J. Riikonen, *Investigation of Second-, Third- and Fourth-Harmonic Generation in Few-Layer Gallium Selenide by Multiphoton Microscopy*" Scientific Reports **5**, 10334 (2015).
[5] J. Susoma, L. Karvonen, A. Säynätjoki, S. Mehravar, R. A. Norwood, N. Peyghambarian, K. Kieu, H. Lipsanen, and J. Riikonen, *Second and Third Harmonic Generation in Few-Layer Gallium Telluride Characterized by Multiphoton Microscopy*, Applied Physics Letters **108**, 073103 (2016).

Sensing in the Shortwave Infrared using Carbon Nanotube

Lian-Mao Peng
Department of Electronics, Peking University, Beijing 100871, China
Corresponding author e-mail: lmpeng@pku.edu.cn

Carbon nanotubes (CNTs) are direct band gap materials that are not only useful for nanoelectronic applications, but also have the potential to make significant impact on the developments of nanoscale optoelectronic devices. In particular CNTs have been investigated for various electronic and optoelectronic device applications, such as light-emitting diodes [1,2], photodetectors and photovoltaic (PV) cells [3,4]. Semiconducting single-wall CNTs (SWCNTs) can efficiently absorb and emit light. The unique band structure of SWCNT suggests that multiple subbands absorptions can contribute to optoelectric properties. By combining sufficient nanotubes with different diameters, it was also demonstrated that it is possible to gain a nearly continuous absorption response within a broad spectral range (from UV to infrared) to match the solar spectrum [5]. In addition, extremely efficient carrier multiplication (CM) effect has been observed [6], which may potentially lead to a higher energy conversion efficiency than that defined by the Shockley-Quiesser limit. More recently, efficient photovoltage multiplication was realized via introducing virtual contacts in CNTs, making the output photovoltage of CNT based solar cells a tunable quantity via choosing the diameter of the tube and the number of virtual contacts introduced in the device [7]. This technique has been utilized to build high performance infrared photodetectors [8-10] and sensors for shortwave infrared [11], and for developing optoelectronic communications between nanoelectronic circuits using carbon nanotube based optoelectronic devices [12].

References

[1] Mueller T et al. (2010), Nature Nanotech, 5:27-31.
[2] Wang S et al. (2011), Nano Lett., 11: 23.
[3] Lee JU, Gipp PP and Heller CM (2004), Appl. Phys. Lett., 85:145.
[4] Wang S et al. (2009), J. Phys. Chem. C, 113(17): 6892.
[5] Lehman J, Sanders A, Hanssen L, Wilthan B, Zeng J and Jensen C (2010), Nano Lett., 10, 3261.
[6] Gabor, N.M., Zhong, Z.H., Bosnick, K., Park, J. & McEuen, P.L. (2010), Science 325, 1367.
[7] Yang LJ, Wang S, Zeng QS, Zhang ZY, Pei T, Li Y and Peng LM (2011), Nature Photonics, 5:672.
[8] Zeng Q.S. et al. (2012), Optical Materials Express 2(6): 839
[9] Yang L.J., Wang, S., Zeng, Q.S., Zhang, Z.Y. and Peng, L.-M. (2013) Small 8:1225.
[10] Yu, D.M. et al. (2014) Small 10:1050.
[11] Liu, Y et al. (2015) Advanced Optical Materials 4:238-245
[12] Liu, Y et al. (2015) unpublished

From bulk crystals to nanowires: investigating $CH_3NH_3PbI_3$ photovoltaic perovskite

László Forró
Laboratory of Physics of Complex Matter Ecole Polytechnique Fédérale de Lausanne CH-1015 Lausanne, Switzerland
laszlo.forro@epfl.ch

Recently, it has been shown by the Snaith [1] and Graetzel [2] groups that $CH_3NH_3PbI_3$ is very promising material in photovoltaic devices reaching light conversion efficiency (η) up to 21%. A strong research activity has been focused on the chemistry of the material to establish the most important parameters which could further improve η and to collect photons from a broad energy window. The major trend in this field is in photovoltaic device engineering although the fundamental aspects of the material are not yet understood.

In my lab we have devoted considerable effort to the growth of high quality single crystals at different length scales, ranging from large bulk crystals (up to 100 mm^3) through nanowires [3,4] down to quantum dots of tens of nanometers of linear dimensions. The structural tunability of the material allows to study a broad range of physical phenomena including electrical and thermal transport, magnetism and optical properties which will be reported in this presentation together with some device applications [5].

Acknowledgement: The work has been performed in collaboration with Endre Horvath, Massimo Spina, Balint Nafradi, Alla Araktcheva, Andrea Pisoni, Jacim Jacimovic and the Van der Marel group. This work was partially supported by the ERC Advanced Grant (PICOPROP#670918).

References:
[1] Lee, M. M. et al.,Science **338**, 643-647 (2012)
[2] Stranks, S. D. et al.. Science, **342**, 341−344, (2013)
[3] Horvath et al., Nano Letters ***14*****,** 6761, (2015)
[4] Spina et al., Scientific Reports, **6**, 1 (2016)
[5]Spina et al., Small, **11**, 4823(2015)

Thermal conductivity of single-walled carbon nanotubes

M. V. Avramenko, S. B. Rochal
Department of Nanotechnology, Faculty of Physics, Southern Federal University, Rostov-on-Don, 5 Zorge Str., 344090, Russia
avramenko.marina@gmail.com

Since their discovery [1], carbon nanotubes (CNTs) are investigated due to their unique physical properties [2–4]. Recent finding of extremely high thermal conductivity of graphene [5] has stimulated a new wave of interest to the theory of thermal properties of low-dimensional graphene-related systems [6,7] including CNTs. Their thermal conductivity is one of those important thermal characteristics, which has been a matter of intense debate for a long time.

To measure thermal conductivity of a single CNT is a very complicated task, so experiments are often performed with the CNTs bundles. Nevertheless, the existing theories of CNTs thermal conductivity do not take into account an interaction between an individual nanotube and its environment. Moreover, both theoretical and experimental results presented in a number of different papers are quite contradictory.

In our work we continue developing a recently proposed theory [8], in the frame of which a single-walled CNT is considered as an object constructed by a graphene monolayer of one-atom thickness. Taking into account the interaction between a CNT and its environment results in losing Goldstone degrees of freedom by the CNT and essential reconstruction of its low-frequency phonon spectrum. Finally, it turns out that heat capacity of a CNT decreases significantly: from several times to more than one order of magnitude at ultra-low temperatures [9]. We demonstrate that the environment can influence on CNTs thermal conductivity in a similar way. Using the continuous theory described and the classical methods of condensed matter physics, we calculate low-temperature thermal conductivity of CNTs both with and without taking in account the interaction between CNTs and their environment. We suppose that heat transport in such systems is ballistic: phonon mean free path is comparable to the nanotubes mean length and phonons are scattered only at the ends of nanotubes. Despite the predictions of authors [10, 11, 12] and many others, we demonstrate that, firstly, thermal conductivity coefficient of single-walled CNTs is of the same order of magnitude as the ones of graphite and diamond, and secondly, unusually high values of CNTs thermal conductivity coefficient cannot be reached unless phonon mean free path is at least 500 μm. From the practical point of view, it is possible for a composite material consisting of defectless CNTs of 500 μm mean length.

The results of the approach proposed can be applied to the analysis of other thermodynamic properties of single- and multi-walled CNTs (for instance, heat capacity and thermal conductivity), which are also determined by the phonon spectrum and peculiarities of its reconstruction when the complex system is formed and influenced by the environment.

This work was supported by the RSF grant No. 15-12-10004.

[1] S. Iijima, Nature, **354**, 56 (1991).
[2] R. Saito, G. Dresselhaus and M.S. Dresselhaus, *Physical Properties of Carbon Nanotubes* (Imperial College Press, London, 1998).
[3] S. Reich, C. Thomsen and P. Ordejon, *Elastic Properties and Pressure-induced Phase Transitions of Single-walled Carbon Nanotubes*, Vol. 235 (Wiley Online Library, 2003).
[4] A. Jorio, M.S. Dresselhaus and G. Dresselhaus, *Carbon Nanotubes: Advanced Topics in the Synthesis, Structure, Properties and Applications*, Vol. 111 (Springer, Berlin, 2008).
[5] A. A. Balandin, S. Ghosh, W. Bao, I. Calizo, D. Teweldebrhan, F. Miao, Ch. N.Lau, Nano Lett., **8**, 902 (2008).
[6] A. A. Balandin, Nat. Mater., **10**, 569 (2011).
[7] D. L. Nika, A. A. Balandin, J. Phys.: Condens. Matter, **24**, 233203 (2012).
[8] S. B. Rochal, V. L. Lorman and Yu. I. Yuzyuk, Physical Review B, **88**, 235435 (2013).
[9] M. V. Avramenko, I. Yu. Golushko, S. B. Rochal, A. E. Myasnikova, Physica E, **68**, 133 (2015).
[10] S. Berber, Y.-K. Kwon, D. Tománek, Physical Review Letters **84**, 4613 (2000).
[11] M. Mir, E. Ebrahimnia-Bajestan, H. Niazmand, M. Mir, Computational Materials Science **63**, 52 (2012).
[12] M. Grujicic, G. Cao, B. Gersten, Materials Science and Engineering B **107**, 204 (2004).

Single or not?
SWNTs studied by photoluminescence and Raman microscopy

Kerstin Müller, Friedrich Schöppler, Tobias Hertel
Institut für Physikalische und Theoretische Chemie, Julius-Maximilians-Universität Würzburg
kerstin.mueller@uni-wuerzburg.de

Abstract

Single-particle studies and single-particle microscopy aim to explore and study individual nanoparticles. However, single-walled carbon nanotubes (SWNTs) often come in the form of bundles and telling isolated SWNTs apart from small aggregates is by no means trivial. Here, we present a systematic spectroscopic investigation of different batches of semiconducting SWNTs using photoluminescence and Raman microscopy in an attempt to identify spectroscopic signatures which allow to clearly distinguish isolated SWNTs 'singles' from interacting 'couples' or assemblies of SWNTs. In doing so this study will facilitate further exploration of the intrinsic photophysical and spectroelectrochemical properties of isolated SWNTs.

In total we have accumulated PL and Raman spectra from 150 semiconducting individual or aggregated SWNTs dropcast from a solution of PFO-BPy dispersed SWNTs in toluene. A PL microscope image, PL spectrum and Raman spectrum of an individualized SWNT are shown in Figure 1. Prior to dropcasting this sample was prepared by gentle shear mixing of home grown nanotube soot prepared by the alcoholic CVD process (ACVD). Such samples show an abundance of individualized, long and brightly-fluorescent SWNTs as well as some smaller bundles.

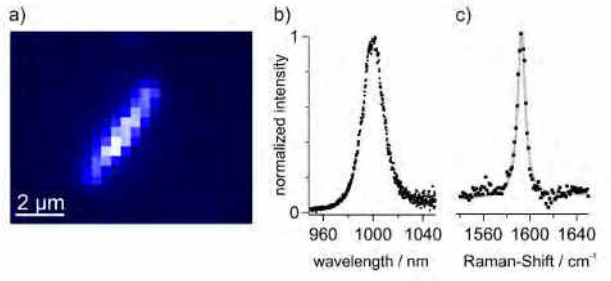

Fig. 1. PL image (a), spectra (b) and Raman spectra (c) showing the G^+ band of an individual (6,5)-SWNT obtained from the CVD sample with the dispersant PFO:BPy

Next we compare the relative PL-QYs by normalizing the PL intensity of the S_1 exciton to the intensity of the Raman G^+ band. The latter is used as a measure of the SWNTs photoabsorption. In addition we find that SWNTs emitting at smaller wavelengths and with narrower line widths, tend to have higher PL-QY (Figure 2) and are therefore more likely to be individual SWNTs than smaller bundles.[1]

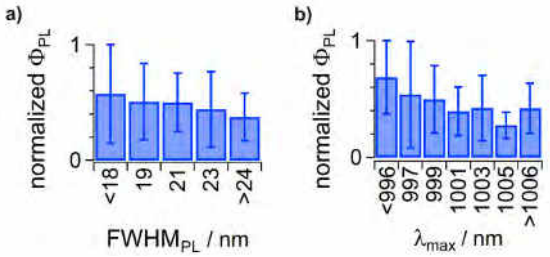

Fig. 2. normalized PL-QY as a function of FWHM (a) and emission peak (b) of the S_1 exciton

The combination of PL microscopy with PL and Raman spectroscopic investigation thereby allows for a reliable identification of individual SWNTs and of small bundles.

Acknowledgement
We thank Matthias Kastner for preparation of CVD-samples.

[1] J. Crochet, M. Clemens, T. Hertel, J. Am. Chem. Soc., **129**, 8058-8059 (2007).

Polarization-Sensitive Photoresponse of Nanostructure Films

G.M. Mikheev
Institute of Mechanics UB RAS, 34, str. T. Baramzinoy, Izhevsk, Russia 426067
mikheev@udman.ru

One of interesting features of laser radiation interaction with nanostructured conductive film materials is the generation of surface currents caused by different mechanisms. Among them a special place is occupied by the surface photogalvanic effect (SPGE) [1], circular photogalvanic effect (CPGE) [2] and photon drag effect (PDE) [3] which may lead to the generation of a photocurrent dependent on the incidence angle and polarization of the laser beam.

Here we present a review of our investigations [4-8] on the polarization-sensitive photoresponse of nanographite films, single-walled nanocarbon tubes films and nanostructured resistive Ag/Pd films due to the SPGE and PDE under the obliquely incident nanosecond laser radiation in a wide spectral range of 266-3000 nm. Particular attention is paid to the generation of circular photocurrent in resistive Ag/Pd films due to PDE.

Resistive Ag/Pd films used in our experiments were manufactured by the well-known thick-film technology. This technique has allowed us to obtain ~20-mm-thick 20×20 mm resistive Ag/Pd films on a ceramic substrate. By means of the X-ray analysis, it has been found that the films consist of the phases AgPd, PdO and Ag_2O with a mass ratio of 80.3 : 18.7 : 1.0 respectively. The minimum sizes of crystallites of the phase components AgPd and PdO are 39 and 28 nm, respectively. Studies carried out by the scanning electron microscope have shown that the resistive Ag/Pd films obtained represent a porous material.

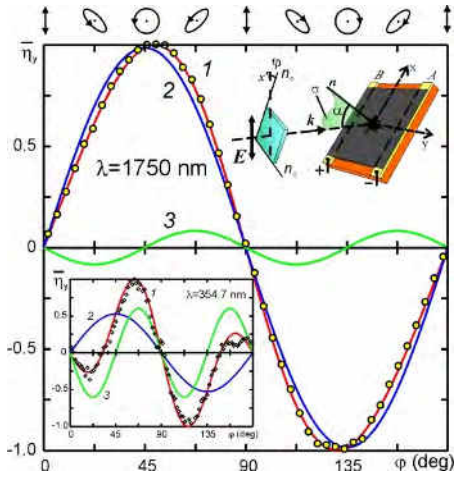

Fig. Dependences of the normalised factor of the laser power conversion into the trunsverse photocurrent on the angle φ (dots), obtained for the excitation wavelengths of 1750 and 354.7 nm (inset). Curves (1) show approximating dependences, curves (2) and (3) – dependences of circular and linear contributions, respectively. Polarisation ellipses of radiation for different angles φ are shown at the top. The top right inset shows the experimantal geometry

We have studied the effect of ellipticity and sign of circular polarization of incident radiation on the value of transverse photocurrent in a wide spectral range of 266-3000 nm. It was found that for the wavelength λ=1750 nm the factor of the laser power conversion into the transverse photocurrent, $\overline{\eta_y}$, is positive for circular polarization with the positive sign (0<φ<90°) and negative for circular polarization with the negative sign (0<φ<180°) (see the Fig.). The conversion factor $\overline{\eta_y}$ depends considerably on the degree of ellipticity of light polarization, i.e. on the angle φ. The resultant normalized experimental dependence can be well approximated by the function:

$$\overline{\eta_y} = \eta_{02} sin2\varphi - \eta_{04} sin4\varphi,$$

where η_{02} and η_{04} are the amplitudes of the circular and linear contributions, respectively. Curves (2) and (3) in Fig. describe circular (η_{02}sin2φ) and linear (-η_{04}sin4φ) contributions, which are, respectively, dependent and independent on the sign of circular polarization. The similar results were obtained for wavelengths range of 529-3000 nm.

We have shown that for λ<529 nm the conversion factor $\overline{\eta_y}$ can take on both positive and negative values for one and the same sign of circular polarization of light. This fact is demonstrated by the dependence $\overline{\eta_y}(\varphi)$ obtained for λ=354.7 nm (inset in the Fig.).

The results obtained allow one to use resistive Ag/Pd films for the development of innovative sensors of the sign of circular polarization of pulsed laser radiation, operating in a wide spectral range.

References

[1] V. L. Al'perovich, V. I. Belinicher, V. N. Novikov, and A. S. Terekhov, Sov. Phys. JETP, **6**, 1201 (1981).
[2] E. L. Ivchenko, Physics-Uspekhi., **45**, 1299 (2002).
[3] V. L. Gurevich, R. Laiho, Phys. Solid State, **42**, 1807 (2000).
[4] G. M. Mikheev, V. M. Styapshin, P.A. Obraztsov, E. A. Khestanova, S.V. Garnov, Quantum Electron, **40**, 425 (2010).
[5] P. A. Obraztsov, G. M.Mikheev, S. V. Garnov, A. N. Obraztsov, Y. P. Svirko, Appl. Phys. Lett., **98**, 091903 (2011).
[6] G. M. Mikheev, A. G. Nasibulin, R. G. Zonov, A. Kaskela., E. I. Kauppinen, Nano Lett., **12**, 77 (2012).
[7] G. M. Mikheev , A. S. Saushin, V. V. Vanyukov, Quantum Electron., **45**, 635 (2015).
[8] K. G. Mikheev, A. S. Saushin, R. G. Zonov, A. G. Nasibulin, G. M. Mikheev, Journal of Nanophotonics, **10**, 0125051 (2016).

Determine the Structure Information of Horizontal Carbon Nanotube Arrays by Optical Imaging

Jin ZHANG
Center for Nanochemistry, College of Chemistry and Molecular Engineering, Peking University, Beijing 100871, China.
E-mail: jinzhang@pku.edu.cn

Up to now, many methods have been used to characterize the structure of nanotubes in different aspects and scales. Transmission electron microscopy (TEM) and scanning tunnelling microscopy (STM) can provide atomic resolution images for nanotubes while the analytical area is quite limited (typically tens of nanometer). Scanning electron microscopy (SEM) and atomic force microscopy (AFM) are two most used methods to "count" the numbers of nanotubes, but they lack the ability of metallic/semiconducting (M/S) recognition and they even meet great challenges at lateral resolution as the density of nanotubes increases. Generally, conventional methods are hard to provide statistical structure information with high-throughput which is necessary for development of carbon nanotubes now.

Optical imaging and spectroscopy were widely used to monitor the structure of massive bulk materials. Here we utilize optical imaging to achieve high-throughput measurement on structure information of massive nanotubes on substrates. The high-throughput ability is realized by direct use of the multicolour information in optical image with contrast enhanced over 10 folds. We successfully employ this technique to characterize carbon nanotube arrays on their line density and M/S ratio in a statistical way for submillimeter view field with integration time less than one second.

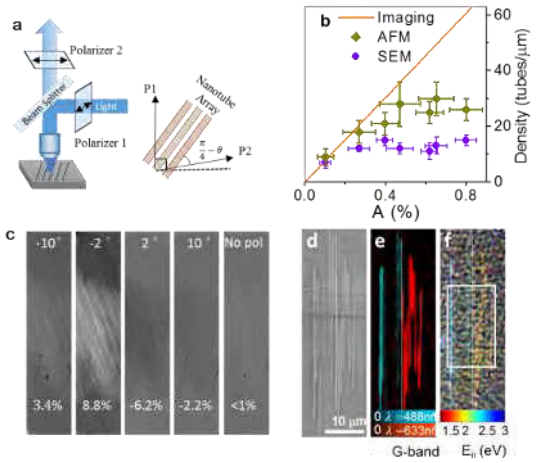

Figure 1 Optical multicolour imaging is used as a high-throughput statistical tool to determine the structure information of horizontally aligned carbon nanotube arrays on various substrates and in diverse environments.

References

[1] S B Deng, J Y Tang, L X Kang, Y Hu, F R Yao, Q C Zhao, S C Zhang, K H Liu, J Zhang, High-throughput Determination of Statistical Structure Information for Horizontal Carbon Nanotube Arrays by Optical Imaging, ***Adv. Mater.*** **28,** 2018 (2016).

Length effect on terahertz permittivity of thin films comprising carbon nanotubes

M. V. Shuba[1], A.G. Paddubskaya[2], G. Valusis[2], and S. A. Maksimenko[1]
[1]*Institute for Nuclear Problems, Belarus State University, Bobruiskaya 11, 220030 Minsk, Belarus*
[2]*THz Photonics Laboratory, Center for Physical Sciences and Technology, Saulėtekio st. 3, Vilnius LT-10222, Lithuania*
mikhail.shuba@gmail.com

Typical carbon nanotubes are conductive nanoparticles with high aspect ratio (10^2-10^3). Their electromagnetic response depends on their length [1-3]. Due to localized plasmon resonance in finite-length single-walled CNTs, broad peak occurs in terahertz conductivity spectra of SWCNT based composites [3]. The peak frequency typically lies in the range 3-30 THz and it depends on the length and diameters of CNT bundles [4]. There are three regimes of CNT interaction with alternative field: quasi-static, intermediate (or resonance) and dynamical [2]. Quasi-static regime is realized at low frequencies bellow localized plasmon resonance. CNT has high real and low imaginary parts of the polarizability in this regime. Both real and imaginary parts of the CNT polarizability are high in resonance regime, whereas imaginary part is higher than the real one for CNT polarizability in dynamical regime which occurs at frequencies above localized plasmon resonance.

In order to demonstrate different regimes of CNT interaction with terahertz field we studied experimentally the effective permittivity of thin films comprising short (~200 nm) and long (~1000 nm) CNTs in the range from 0.1 to 1 THz. Three different materials were used in the experiment: single-, double-, and multi-walled CNTs. For film preparation, long-length CNTs were used as purchased; whereas short-length CNTs were obtain by soft cutting procedure [5]. The films were prepared by filtration method and their thicknesses were in the range from 300 to 1000 nm. Some single-walled CNT films were doped by nitric acid to estimate the influence of the doping effect. The measurements of complex transmission for CNT films were conducted under normal incidence in the frequency range from 0.2 to 1 THz by means of time domain terahertz spectrometer (EK-SPLA, Vilnius, Lithuania).

In experiment, we have demonstrated that quasi-static regime is realized for all the short-length CNT samples in considered terahertz range. In contrast to that, the dynamical regime occurs for long-length CNT films. Doping effect leads to an increase of both the real and imaginary parts of the permittivity of single-walled CNT film, but it does not change the regime of CNT interaction with terahertz field.

The effective medium theory has been applied to calculate the effective permittivity of CNT-base composite material. The calculation has been done for composite comprising doped and undoped individual and bundled single-walled CNTs and multi-walled CNTs as well. The comparative analysis has shown that among the all types of tubes, the individual single-walled CNTs give the maximal contribution to value of effective permittivity.

Thus, both theoretically and experimentally we have demonstrated that terahertz parameters of CNT film can be tune in wide range by means of variation of CNT length and CNT type.

Acknowledgement.

This research was supported by the H2020 project ID 644076 Call H2020-MSCA-RISE-2014 Programme H2020 CoExAN, EU FP7 under projects FP7-612285 CANTOR, AGP is thankful to FP7-316633, POCAONTAS.

References

[1] G. Y. Slepyan, M. V. Shuba, S. A. Maksimenko and A. Lakhtakia, Phys. Rev. B **73**, 195416 (2006).
[2] M. V. Shuba, A. V. Melnikov, A. G. Paddubskaya, P. P. Kuzhir, S. A. Maksimenko, and C. Thomsen, Phys. Rev. B, **88**, 045436 (2013).
[3] M. V. Shuba, A. G. Paddubskaya, A. O. Plyushch, P. P. Kuzhir, G. Y. Slepyan, S. A. Maksimenko, V. K. Ksenevich, P. Buka, D. Seliuta, I. Kasalynas, J. Macutkevic, G. Valusis, C. Thomsen, and A. Lakhtakia, Phys.Rev. B, **85**, 165435 (2012).
[4] M. V. Shuba, A. G. Paddubskaya, P. P. Kuzhir, G. Y. Slepyan, D. Seliuta, I. Kasalynas, G. Valusis, and A. Lakhtakia, Journal of Nanophotonics, **6**, 061707 (2012).
[5] M. V. Shuba, A. G. Paddubskaya, P. P. Kuzhir, S. A. Maksimenko, V. K. Ksenevich, G. Niaura, D. Seliuta, I. Kasalynas, and G. Valusis, Nanotechnology, **23**, 495714 (2012).

Carbon nanotube based devices for terahertz applications.

G. Fedorov[1,2], I. Gayduchenko[1,3], B. Voronov[1], V. Ryzhii[5], M. Ryzhii[5], V. G.Leiman[2] and G. Goltsman[1,4]

1Physics Department, Moscow State Pedagogical University, Moscow, 119991, Russia
E-mail: gefedorov@mail.ru
2 Moscow Institute of Physics and Technology (State University), Dolgoprudny, 141700, Russia
3 National Research Centre "Kurchatov Institute", Moscow, 123128, Russia
4Moscow Institute of Electronics and Mathematics, National Research University Higher School of Economics, Moscow, 109028, Russia
5Research Institute of Electrical Communication, Tohoku University, Sendai, Japan

Increased sensitivity of detection of terahertz (THz) signals can be achieved by reducing the size of the sensitive element. Therefore, it is expected that recent advances in nanotechnology may result in cost-effective solutions for new THz detectors. Most attractive are solutions, which can be based on chemically processed nano-scale objects, minimizing the use of relatively expensive fabrication procedures. One particular route is the use of carbon nanotubes (CNTs) that can be easily synthesized in a chemical vapor deposition (CVD) system using inexpensive precursors for the growth. This talk will be devoted to the prospects of using asymmetric CNT devices as a basic element of THz detectors.

We studied response of such devices to terahertz radiation [1, 2]. It was maintained that photothermoelectric effect under certain conditions results in strong response of such devices to terahertz radiation even at room temperature. The asymmetry which is crucial for the observation of the DC voltage response to the radiation has been implemented in our devices in different ways. In most cases devices different metals are used to contact the CNT network of a uniform morphology at the source and drain electrodes. Such devices show the most promising results with room temperature resposnivity of up to 100V/W. Analysis of the experimental data shows that the response contains two components. One is thermal reflecting different increase in temperature in the areas of the nanotube/metal interfaces. The second is a response due to the non-linearity of the current-voltage characteristic of the device at zero bias. The rectification of the signal leads to a DC component, which contributes to the observed signals.

Our recent theoretical work [3] has shown excitation of two-dimensional plasmons by incoming THz radiation the detector responsivity can exhibit sharp resonant peaks at the signal frequencies corresponding to the plasmonic resonances in case of devices with lateral CNT networks forming the channel. The prospects opened by this result will be discussed in the talk as well.

This work was supported by the Grant of Ministry of Education and Science of Russian Federation under Contract No. 14.586.21.0003 (project ID RFMEFI58614X0003).

[1] G. Fedorov, A. Kardakova, I. Gayduchenko, I. Charayev, B. M. Voronov, M. Finkel, T. M. Klapwijk, S. Morozov, M. Presniakov, I. Bobrinetskiy, R. Ibragimov and G. Goltsman, Appl. Phys. Lett. 103, 181121 (2013)
[2] I. Gayduchenko, A. Kardakova, G. Fedorov, B. Voronov, M. Finkel, D. Jimenez, S. Morozov, M. Presniakov, and G. N. Goltzman, J. Appl. Phys. 118, 194303 (2015).
[3] V. Ryzhii, T. Otsuji, M. Ryzhii, V. G. Leiman, G. Fedorov, G. N.Goltzman, I. A. Gayduchenko, D. Coquillat, D. But, W. Knap. V. Mitin, and M. S. Shur (submitted).

Black phosphorus based anisotropic saturable absorber for ultrafast pulse generation

Diao Li[1,2], Henri Jussila[1], Lasse Karvonen[1], Guojun Ye[3,4], Harri Lipsanen[1], Xianhui Chen[3,4,5], and Zhipei Sun[1]

1 Department of Micro- and Nanosciences, Aalto University, Tietotie 3, FI-02150 Espoo, Finland
2 Institute of Photonics & Photo-Technology, Northwest University, Xi'an, 710069, China
3 Hefei National Laboratory for Physical Science at Microscale and Department of Physics, University of Science and Technology of China, Hefei, 230026, China
[4] Key Laboratory of Strongly-coupled Quantum Matter Physics, University of Science and Technology of China, Chinese Academy of Sciences, Hefei, 230026, China
5 Collaborative Innovation Center of Advanced Microstructures, Nanjing, 210093, China
Corresponding author e-mail: diao.li@aalto.fi

Black phosphorus (BP), a rediscovered layered 2D material with anisotropic atomic alignment, has drawn increasing attention in photonics and electronics community due to its novel physical properties [1,2]. Unlike other commonly studied 2D materials, BP is the first layered semiconductor presenting a strong intrinsic anisotropy [3]. The benefits gained from this crystal anisotropy has been demonstrated for electronic and photonic devices [1,2]. However, very few studies have been implemented to reveal the polarization dependent nonlinear optical properties in BP flakes. The thickness dependent band gap variation of layered BP (from ~0.3 eV in bulk to ~1.5 eV in monolayer) covers the wavelengths from the visible to mid-infrared region [4], which makes BP a suitable material for the fabrication of optical components at the infrared spectral region.

In this work, we study both the linear and nonlinear optical absorption properties of layered BP [5]. The mechanically exfoliated BP flakes show strong thickness and polarization dependent absorption, different with the optical properties presented in graphene [6,7,8] and other 2D materials (e.g., transition metal dichalcogenides [9,10]). The polarization dependent BP flakes were subsequently used as a saturable absorber (SA) at 1.55 μm Erbium doped fiber laser for pulsed laser operation (shown in Fig. 1). Large energy Q-switching and ultrafast mode-locking pulse trains can be obtained according to different flake thicknesses and cavity lengths. The highest output pulse energy in Q-switching and the shortest pulse duration in mode-locking were 18 nJ and 786 fs (Fig. 1c), respectively. However, both the large energy pulses and the ultrafast pulses are strongly linearly polarized, showing a degree of polarization (DOP) of 99% in Q-switching (Fig.1b) and 98% in mode-locking (Fig. 1d), respectively. These results are attributed to the polarization dependent nonlinear optical absorption caused by intrinsic crystal anisotropy of BP atoms. Our study demonstrates the strong thickness and polarization dominant optical nonlinearity of mechanically exfoliated BP flakes, paving the way for BP based nonlinear and ultrafast photonics application such as ultrafast all-optical polarization switches, modulators and frequency converters.

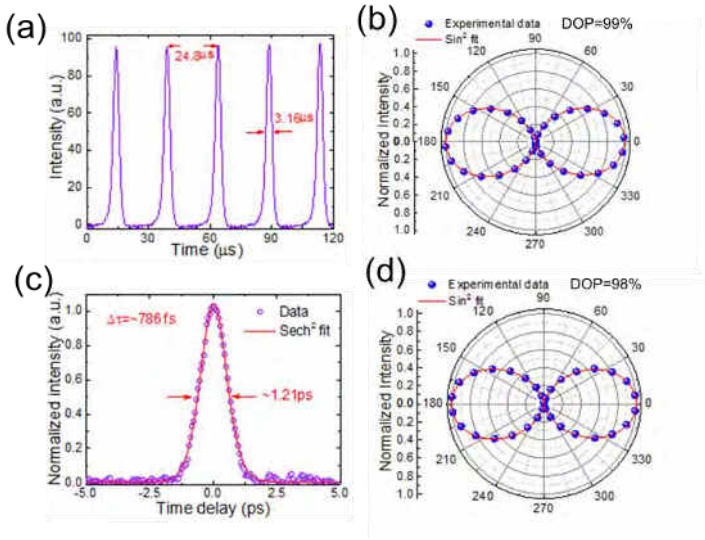

Figure 1 (a) Q-switching pulse train; (b) Polarization characterization (DOP = 99%); (c) Mode-locking autocorrelation trace; (d) Polarization characterization (DOP = 98%).

References

[1] F. Xia, H. Wang and Y. Jia, Nature Communications, **5**, 4458 (2014).
[2] L. Li, Y. Yu, G. J. Ye, Q. Ge, X. Ou, H. Wu, D. Feng, X. H. Chen and Y. Zhang, Nature Nanotechnology, **9**, 372 (2014).
[3] X. Wang, A. M. Jones, K. L. Seyler, V. Tran, Y. Jia, H. Zhao, H. Wang, L. Yang, X. Xu and F. Xia, Nature Nanotechnology, **10**, 517 (2015).
[4] V. Tran, R. Soklaski, Y. Liang, and L. Yang, Physical Review B, **89**, 235319 (2014).
[5] D. Li, H. Jussila, L. Karvonen, G. Ye, H. Lipsanen, X. Chen and Z Sun, Scientific Reports, **5**, 15899 (2015).
[6] A. Martinez and Z. Sun, Nature Photonics, **7**, 842 (2013).
[7] Z. Sun, T. Hasan, A. C. Ferrari, Physica E, **44**, 1082 (2012).
[8] A. C. Ferrari et al., Nanoscale, **7**, 4598 (2015).
[9] Z. Luo, D. Wu, B. Xu, H. Xu, Z. Cai, J. Peng, J. Weng, S. Xu, C. Zhu, F. Wang, Z. Sun and H. Zhang, Nanoscale, **8**, 1066 (2016).
[10] Z. Sun, A. Martinez and F. Wang, Nature Photonics, **10**, 227 (2016).

Graphene oxide deposited microfiber knot resonator for gas sensing

Cai-Bin Yu[1], Yu Wu[1, 3*] Xiao-Lei Liu[1], Fei Fu[2], Yun-Jiang Rao[1] and Yuan-Fu Chen[2]
[1]*Key Laboratory of Optical Fiber Sensing and Communications (Education Ministry of China), University of Electronic Science and Technology of China, Chengdu 610054, China*
[2]*State Key Laboratory of Electronic Thin Films and Integrated Devices, University of Electronic Science and Technology of China, Chengdu 610054, China*
[3]*Center for Information in BioMedicine, University of Electronic Science and Technology of China, Chengdu 611731, China*
[*]*wuyu@uestc.edu.cn*

1. Abstract: Graphene and its derivative graphene oxide (GO) have been the focus of attention in the field of chemical and biological sensing. In this paper, we report a fiber-optic sensor for chemical gas sensing by using graphene oxide coated microfiber knot resonator (GMKR). The refractive index of GO was changed when the gas molecules were adsorbed to the surface of GO, and the gas concentration varying induced refractive index change can be detected by measuring the interference fringes shift of the GMKR. The experimental results show the sensitivities of ~0.35pm/ppm for NH_3 and ~0.17pm/ppm for CO detection, due to the different adsorption energy and charge transfer ability between the gas molecules and GO. Experimental results show GO is a promising candidate for gas sensing and can be combined with various fiber-optic devices due to the easy transfer process.

2. Gas sensing experiment

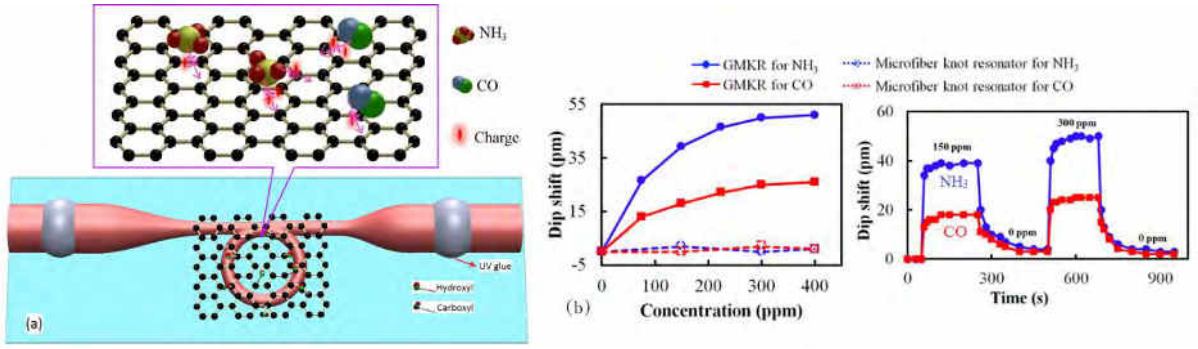

Fig. 1. (a) Schematic diagram of the GMKR and the sensing mechanism (inset). (b) Dip shift of GMKR as a function of the gas concentration change and the recoverability of the GMKR.

The schematic GMKR structure is shown in Fig. 1(a). A microfiber knot resonator is attached tightly onto the MgF_2 substrate, which are further covered by the transferred GO sheet. The sensing mechanism is based on the charge transfer due to gas molecules adsorbed on the GO sheet that act as donors [1]. When GO adsorbed the gas molecules, the "free electrons" were transfer from gas molecules to carbon atoms of GO [2]. The conductivity of the GO result in the refractive index changed [3] as shown in the inset of Fig. 1(a).

Two sets of experiments have done in order to investigate the relationship among refractive index of GO and the different gases. For the NH_3 and CO gases, the resonant dip shifts of the GKNR in the gases sensing experiments are shown in the Fig. 1(b). For NH_3 gas sensing, the sensitivity is about 0.35pm/ppm, and about 0.17pm/ppm for CO in the range of 0ppm to 150ppm. Experimental results indicate that the good reversibility of GKNR sensor is also obtained.

3. Acknowledgement

This work was supported by the National Natural Science Foundation of China (NSFC) under Grants 61290312, 61475032, and 61575039. It was also supported by the Program for Changjiang Scholars and Innovative Research Team in University (PCSIRT, IRT1218), and the 111 Project (B14039).

4. References

[1] O. Leenaerts, B. Partoens and F. M. Peeters, "Adsorption of H2O, NH3, CO, NO2, and NO on graphene: A first-principles study," Phys. Rev. B 77(12), 125416 (2008).
[2] B. C. Yao, Y. Wu, Y. Cheng, A. Q. Zhang, Y. Gong, Y. J. Rao, Z. G. Wang, Y. F. Chen, "All-optical Mach–Zehnder interferometric NH3 gas sensor based on graphene/microfiber hybrid waveguide," Sens. Actuators, B 194, 142-148 (2014).
[3] B. C. Yao, Y. Wu, A. Q. Zhang, Y. J. Rao, Z. G. Wang, Y. Cheng, Y. Gong, W. L. Zhang, Y. F. Chen, Y. R. Li, and K. S. Chiang, "Graphene enhanced evanescent field in microfiber multimode interferometer for highly sensitive gas sensing," Opt. Express **23**(23), 28154-28162 (2014).

Poster session II

©E. Plotkin

Diameter-dependent encapsulation of graphene nanoribbons inside single-walled carbon nanotubes

Alexander I. Chernov[1,2], Pavel V. Fedotov[1], Vladimir L. Kuznetsov[3,4], Andrei L. Chuvilin[5], Elena D. Obraztsova[1,2]

[1]*Prokhorov General Physics Institute, RAS, 38 Vavilov str., 119991, Moscow, Russia*
[2]*National Research Nuclear University MEPhI (Moscow Engineering Physics Institute), Kashirskoe hwy. 31, 115409, Moscow, Russia*
[3]*Boreskov Institute of Catalysis SB RAS, Lavrentieva ave. 5, 630090, Novosibirsk, Russia*
[4]*Novosibirsk State University, Pirogova 2, 630090, Novosibirsk, Russia*
[5] *CIC nanoGUNE Consolider, Tolosa Hiribidea 76, 20018 Donostia-San Sebastian, Spain*

Corresponding author e-mail al.chernov@nsc.gpi.ru

Single-walled carbon nanotubes (SWCNTs) can serve as nanoscale chemical reactors [1]. Molecules placed inside the SWCNTs are well protected from the external environment and can form one-dimensional structures, which may be thermodynamically unstable in the absence of encapsulating template. Recently it has been demonstrated that polycyclic aromatic hydrocarbon molecules, for instance, coronene can easily enter the SWCNTs [2]. Transferring the thermal energy to the molecule – nanotube system leads to polymerization reaction inside SWCNT. As a result, hydrogen-terminated graphene nanoribbons (GNRs) can be formed [3].

In this work we demonstrate that the properties of formed GNRs strongly depend on the host SWCNTs. The diameter dependent filling is studied by spectroscopy, HRTEM microscopy and additionally confirmed by calculations. The photoluminescence excitation (PLE) mapping (Fig. 1) together with the additional Raman and optical absorption spectroscopies allow discriminating between the encapsulated and not encapsulated aggregates, and reveal their electronic properties [4,5,6]. Nanotube confinement determines type of the encapsulated structures. Optical properties are accessed by spectroscopy techniques. According to the PLE mapping the largest GNRs possess the smallest band gap values. Control over the electronic properties of the encapsulated structures via the nanotube confinement shows the way to implement the GNR inside the nanotube shell as the robust light emitter in the visible spectral range or as the basic component for the optoelectronic devices.

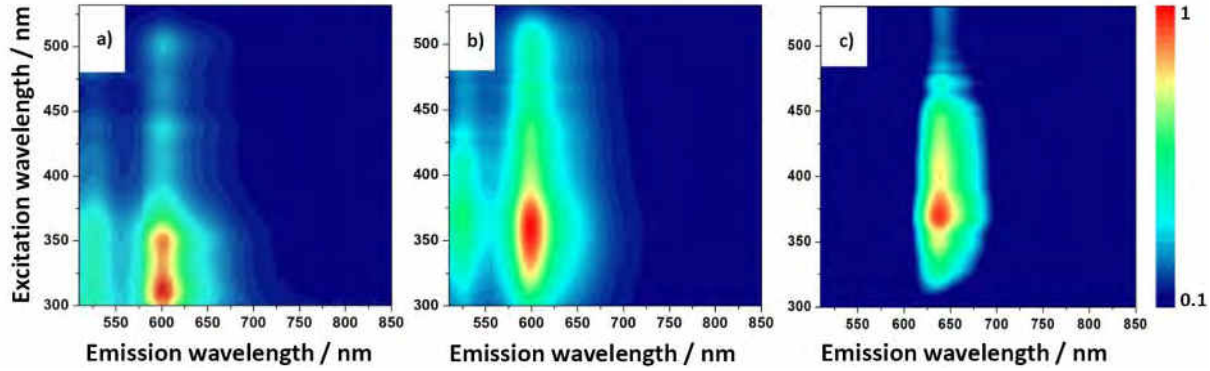

Fig. 1. The PLE maps of the GNRs formed inside SWCNTs with an average diameter: a) –1.4 nm, b) – 1.5 nm and c) – 1.9 nm.

Acknowledgements

The work was supported by RFBR projects: 14-02-00777, 15-32-70005 mol_a_mos, 15-32-20941_mol_a_ved and IRSES-612577.

References

[1] A. N. Khlobystov, *ACS Nano*, **5**, 9306 (2011).
[2] T. Okazaki, Y. Iizumi, S. Okubo, H. Kataura, Z. Liu, K. Suenaga, Y. Tahara, M. Yudasaka, S. Okada, S. Iijima, *Angew. Chem. Int. Ed.* **50**, 4853 (2011).
[3] A. V. Talyzin, I. V. Anoshkin, A. V. Krasheninnikov, R. M. Nieminen, A. G. Nasibulin, H. Jiang, E. I. Kauppinen, *Nano Lett.* **11**, 4352 (2011).
[4] A. I. Chernov, P. V. Fedotov, A. V. Talyzin, I. Suarez Lopez, I. V. Anoshkin, A. G. Nasibulin, E. I. Kauppinen, E. D. Obraztsova, *ACS Nano* **7**, 6346 (2013).
[5] A. I. Chernov, P. V. Fedotov, A. G. Nasibulin, I. V. Anoshkin, E. I. Kauppinen, V. L. Kuznetsov, E. D. Obraztsova, *Phys. Stat. Sol. (B)* **251**, 2372 (2014).
[6] A. I. Chernov, P. V. Fedotov, A. S. Krylov, A. N. Vtyurin, E. D. Obraztsova, *Journal of Nanophotonics* **10 (1)**, 012504 (2016

Quasi-two-dimensional diamond produced by chemical vapour deposition

A.M. Alexeev[1,2], R.R. Ismagilov[1,2], E.E. Ashkinazi[2], A.S. Orekhov[1,3], S.A. Malykhin[1], A.N. Obraztsov[1,4]
[1]*Department of Physics, Lomonosov Moscow State University, Moscow, Russia*
[2]*A.M. Prokhorov General Physics Institute, Russian Academy of Sciences, Moscow, Russia*
[3]*A.V. Shubnikov Institute of Crystallography, Russian Academy of Sciences, Moscow, Russia*
[4]*Department of Physics and Mathematics, University of Eastern Finland, Joensuu, Finland*
am.alekseev@physics.msu.ru

Polycrystalline diamond films consisting of platelet crystallites were obtained by DC PECVD from hydrogen and methane gas mixture. Thickness of the platelet diamond crystallites was in nanometer scale and their lateral size was of about few micrometers. TEM and electron diffraction examinations revealed their six-fold rotational symmetry and composition of stacked (111) atomic planes. The experimental data and theoretical considerations predict existence of several lamellar twins in the crystallites' structure. The structure and possible growth mechanisms of the quasi-2D diamond crystals in the case of DC PECVD are explained by existence of re-entrant corners on the edges, twin boundaries and of extremely low growth rate in direction perpendicular to the platelets [1].

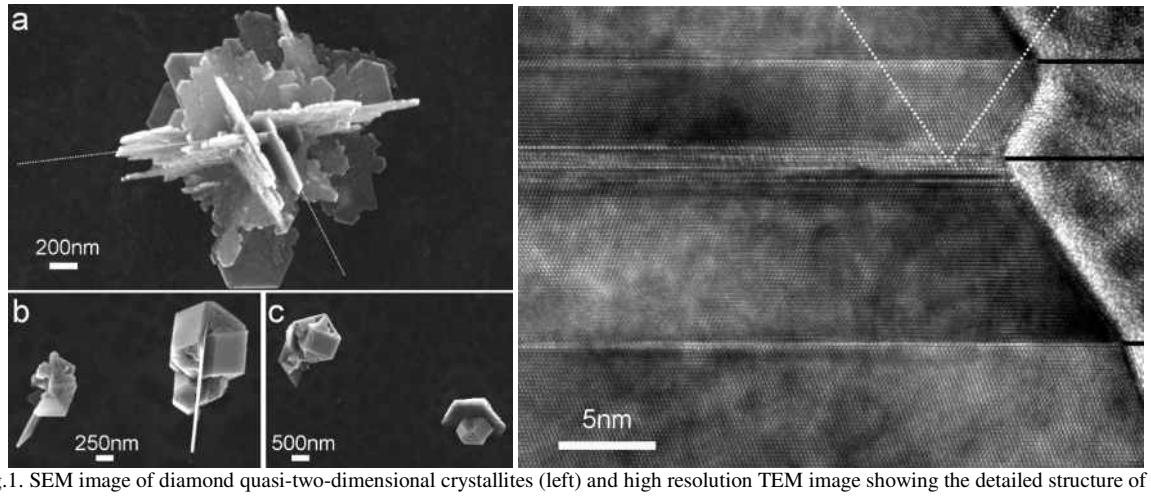

Fig.1. SEM image of diamond quasi-two-dimensional crystallites (left) and high resolution TEM image showing the detailed structure of the individual platelet (right).

This work was supported by Russian Science Foundation (Grant №15-19-00279)

[1] A.M. Alexeev, R.R. Ismagilov, E.E. Ashkinazi, A.S. Orekhov, S.A. Malykhin and A.N. Obraztsov, Diamond and Related Materials, **65**, 13-16 (2016)

Structure Simulation of One-Dimensional CuCl Crystals Inside Single-Walled Carbon Nanotube

Andrey Orekhov[1, 2], Andrey Chuvilin[3, 4], Alexander Tonkikh[5], Vladimir Kuznetsov[6], Elena Obraztsova[5]

[1] *University of Eastern Finland, Joensuu, FINLAND*
[2] *National Research Center «Kurchatov Institute», Moscow, RUSSIA*
[3] *CIC nanoGUNE Consolider, Donostia - San Sebastian, SPAIN*
[4] *IKERBASQUE Basque Foundation for Science, Bilbao, SPAIN*
[5] *Prokhorov General Physics Institute of Russian Academy of Sciences, Moscow, RUSSIA*
[6] *Boreskov Institute of Catalysis SB RAS, Novosobirsk, Russia*
Andrey.orekhov@gmail.com

The type and structure of encapsulated crystals and their interaction with parent carbon nanotube determines the electronic properties of entire system. Change in the local crystal chemistry of incorporated crystals can be observed directly by High-Resolution Transmission Electron Microscopy (HRTEM). Therefore, the precise composition and structure data of encapsulated crystal is important for a correct interpretation of the filled carbon nanotube electronic properties.

In this study, the structure of encapsulated CuCl@SWCNT was simulated according to experimental HRTEM images. The TEM measurements were performed on a Titan 60-300 TEM/STEM microscope (FEI, The Netherlands) at acceleration voltage of 80 kV equipped with monochromator and Cs spherical aberration corrector. The chemical composition was estimated by X-ray Energy Dispersion Spectroscopy (EDS) technique.

A series of HRTEM images with different orientations of encapsulated CuCl crystal inside the nanotubes was obtained and analyzed. It is shown that the composition ratio of copper and chlorine is 1:1. The interplanar distances, angles between the vectors of reciprocal lattice and relative intensity distribution were estimated. Experimental data were compared with known CuCl polytypes for bulk crystals. The good agreement between the calculated and experimental values of interplanar distances was observed for CuCl phase with NaCl type deformed along the [110] direction. A fragment of filled CuCl@SWCNT is shown in Fig. 1. The crystal lattice was deformed at the tube direction perpendicular to its long axis. The simulation of CuCl@SWCNT HRTEM images revealed a good correspondence of calculated and experimental data. The data obtained by simulation were confirmed with molecular dynamic results. The possibility of lattice distortions of encapsulated CuCl was estimated. The distance increase between cupper and chlorine atoms due to interaction with carbon nanotube walls is in good agreement with HRTEM data.

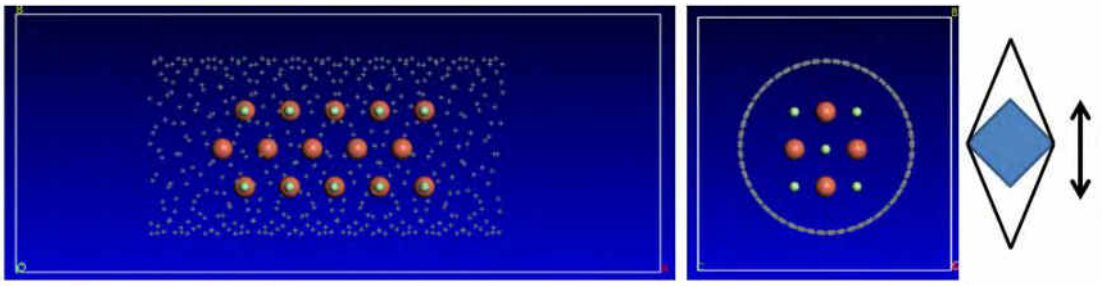

Fig. 1. The model of CuCl with distortions inside the single-walled carbon nanotube.

Acknowledgements.
The work was supported by RSF-15-12-30041.

Hydrocarbon-based Floating Catalyst CVD Synthesis of SWCNTs using Nitrogen as Carrier Gas

Aqeel Hussain, Antti Kaskela, Ying Tian, Hua Jiang, Patrik Laiho, Esko I. Kauppinen
NanoMaterials Group, Department of Applied Physics, School of Science, Aalto University, Puumiehenkuja 2, Espoo 02150, Finland
esko.kauppinen@aalto.fi

The single-walled carbon nanotubes (SWCNT) thin film stands as a strong candidate for replacement of indium-tin oxide (ITO) in transparent electrodes. The length of nanotubes is critical to achieve high conductivity SWCNTs transparent conducting films (TCF) due to smaller number of resistive junctions with the longer tubes [1]. The synthesis process of using carbon monoxide (CO) as carbon source is limited to produce longer SWCNTs owing to its thermodynamically limited, i.e. rather low synthesis temperature. Moreover, the CO process has usually low yield, and CO is expensive and challenging to operate safely. In this contribution, we demonstrate high yield synthesis of SWCNTs in floating catalyst CVD (FC-CVD) using C_2H_4 hydrocarbon as the carbon source and nitrogen with small amount of hydrogen as the carrier gas. The nitrogen environment makes the SWCNT growth process operation safer and also largely cuts the running cost. Our results show that the C_2H_4-N_2-H_2 FC-CVD reactor operated at 1050 ^oC and using ferrocene vapor based Fe catalyst particles produced relatively long bundles with an average length up to 16 µm, while the similar reactor operated at CO produced tubes with just 4 µm average length. This ethylene process produced long SWCNTs while keeping mean diameter below 1.5 nm. Highly conductive transparent films were achieved, with the sheet resistance of 200 ohm/sq. at 90% transmittance at a wavelength of 550 nm without doping. The doping of the film with gold chloride ($AuCl_3$) in acetonitrile solution further reduced the sheet resistance down to 60 ohm/sq. at 90% transmittance at 550 nm. TEM diffraction analysis was carried out with 0.75 ccm C_2H_4, 35 ccm H_2 and 100 ccm N_2 through the ferrocene cartridge at 1050 ^oC. TEM diffraction results show 73% semiconducting and 27% metallic nanotubes. We also present (n,m) distributions based on TEM/ED. Very low sheet resistance of 60 ohm/sq at 90% T was achieved even with higher ratio of semiconducting tubes. It can be assumed that the length of the nanotubes is the major factor to lower the sheet resistance even with the higher ratio of semiconducting tubes than metallic ones.

References

[1]A. Kaskela, A. G. Nasibulin, M. Y. Timmermans, B. Aitchison, A. Papadimitratos, Y. Tian, Z. Zhu, H. Jiang, D. P. Brown, A. Zakhidov, and E. I. Kauppinen, Nano Letters, **10**, 4349 (2010).

Growth of Morphology-Controllable Carbon Nanomaterials from Catalyst Prepared by Spray-coating Method

Er-Xiong Ding[1], Hong-Zhang Geng[2], Hua Jiang[1], Esko I. Kauppinen[1,*]

[1] NanoMaterials Group, Department of Applied Physics, School of Science, Aalto University, Puumiehenkuja 2, Espoo 02150, Finland, [2] School of Material Science and Engineering, Tianjin Polytechnic University, Tianjin 300387, PR China

esko.kauppinen@aalto.fi

Conventional catalyst preparation for growth of carbon nanomaterials (CNMs) mainly consists of atomic layer deposition (ALD) and sol-gel method, among which ALD can control the size of metal catalyst though it is time- and energy-consuming with high cost, while sol-gel method is always accompanied with much undesirable metal impurities as a result of powder catalyst, making the purification of products troublesome. Spray-coating method, which is newly developed for catalyst preparation for synthesis of CNMs, has been demonstrated to be a more feasible alternative with low cost and high quality products [1].

Herein, controllable growth of CNMs by substrate chemical vapor deposition (CVD) is presented, spray-coating method was adopted for catalyst preparation. Metal catalyst nanoparticles were obtained by decomposition and reduction of catalyst precursor film on SiO_2/Si substrate fabricated by spray-coating method. Acetylene and gas mixture of Ar/H_2 were used as carbon source and carrier gas, respectively. With the increase of number of spray-coating time for catalyst preparation, the helicity of as-prepared carbon nanocoils (CNCs) increases whereas the average line diameter and coil pitch decrease. Compared with dip-coating, spray-coating method can prepare more uniform catalyst nanoparticles, resulting in more CNCs and carbon nanomaterials [2]. Moreover, via optimizing experimental parameters, various kinds of Y-junction CNCs were obtained [3]. Additionally, hierarchical chrysanthemum-flower-like carbon nanomaterials were synthesized directly by thermal CVD method. The flower looks like a blooming chrysanthemum with a stem instead of a spheral flower reported in literatures [4]. Formation mechanisms of Y-junction CNCs and flower-like carbon nanomaterials were elaborated detailedly.

References

[1] R. Xiang, H. Zeng, Y. Su, X. Gui, T. Wu, E. Einarsson, S. Maruyama and Z. Tang, Carbon, **64**, 537 (2013).

[2] E.-X. Ding, H.-Z. Geng, W.-Y. Wang, L. Mao, Y. Wang, Z.-C. Zhang, Z.-J. Luo, J. Wang, H.-J. Yang and L. Pan, Carbon, **82**, 604 (2015).

[3] E.-X. Ding, J. Wang, H.-Z. Geng, W.-Y. Wang, Y. Wang, Z.-C. Zhang, Z.-J. Luo, H.-J. Yang, C.-X. Zou, J. Kang and L. Pan, Scientific Reports, **5**, 11281 (2015).

[4] E.-X. Ding, H.-Z. Geng, J. Wang, Z.-J. Luo, G. Li, W.-Y. Wang, L.-G. Li, H.-J. Yang, S.-X. Da, J. Wang, H. Jiang and E. I. Kauppinen, Nanotechnology, **27**, 085602 (2016).

Structure And Raman Spectra Peculiarities Of Monocrystalline Diamond Needles

Andrey S. Orekhov[1,2], Feruza T. Tuyakova*[1,3] , Ekaterina A. Obraztsova[4,5], Artem B. Loginov[6], Andrey L. Chuvilin[7,8], Alexander N. Obraztsov[1,6]

[1]University of Eastern Finland, Department of Physics and Mathematics, Joensuu 80101, Finland

[2] National Research Center «Kurchatov Institute», 123182, Moscow, Russia

[3]Moscow University of Technology, Moscow 119454, Russia

[4]M.M. Shemyakin and Yu.A. Ovchinnikov Institute of Bioorganic Chemistry, Russian Academy of Sciences, Moscow 117997, Russia

[5]A.M. Prokhorov General Physics Institute, Russian Academy of Sciences, Moscow 119991, Russia

[6]M.V. Lomonosov Moscow State University, Department of Physics, Moscow 119991, Russia

[7]CIC nanoGUNE Consolider, San Sebastian 20018, Spain

[8]IKERBASQUE, Basque Foundation for Science, Bilbao 48013, Spain

feruza.tuyakova@uef.fi

Diamond is known for its unique properties: high thermal conductivity, outstanding optical and mechanical properties. One possible application of a diamond needles is a probes for scanning optical microscopy. Single crystal diamond needles have high aspect ratio geometry of the sides, as well as a sharp apex, which are well suited for optical sensors. Pyramidal diamond needles have a length of from 10 to 160 micrometers and the apex angle of the tip 2 - 200 nm were obtained by chemical vapor deposition on a silicon substrate. In this work we were examined defects on the surface and inside the diamond monocrystals. It was found that during the CVD growth surface of single-crystal needles enriches extended defects, whereas in the volume needle point defects such as sp3 are formed. It has been shown that the addition of nitrogen increases the concentration of sp3 defects, and also increases the growth rate on (001) the surface.

Thermostable polyimide films with dispersed SWNTs for optics

Natalia R. Arutyunyan[1], Valentina A. Eremina[2], Elena P. Kharitonova[2], Der-Jang Liaw[3], Wei-Hung Chiang[3], Elena D. Obraztsova[1]

[1]*A.M.Prokhorov General Physics Institute RAS, Vavilova 38, Moscow 119991, Russia*
[2]*M.V.Lomonosov Moscow State University, Faculty of Physics, Vorob'evy gory 1, Moscow 119991, Russia*
[3]*National Taiwan University of Science and Technology, 43 Keelung Road, Section 4 Taipei 106-07, Taiwan*
Corresponding author e-mail: natalia.arutyunyan@gmail.com

Single-wall carbon nanotubes (SWNTs) are very efficient saturable absorbers in near IR range due to the fast relaxation of electronic excitations. For realization of mode locking regime with femtosecond duration of output pulses in fiber lasers, the polymer films with embedded nanotubes are convenient to use [1-3]. However, one of the main obstacles is a low threshold of thermal destruction of polymer matrix. Due to this the output power of laser beam is low. Polyimides are known as thermally stable polymers, so they could be a good candidate for solution of this problem. Here, we present the results on fabrication of composite SWNTs/polyimide films for laser applications.

The characteristics of more than 25 polyimides, synthesized in National Taiwan University of Science and Technology (NTUST), were compared with each other. Their optical properties, solubility in various solvents and ability to disperse nanotubes were analyzed. The main absorption bands of all types of polyimides were in UV range (<400 nm). For the efficient operation of saturable absorbers it is necessary to minimize the polymer matrix absorption at the working wavelength of lasers. Several most acceptable samples were selected. They were transparent in the range 1000-2000 nm, being characteristic for Er^{+}, Tm, Yb, fiber lasers.

The temperature dependences of the mass losses (thermogravimetry) and of the heat flow (differential scanning calorimetry) were measured to estimate the thermal threshold of the polymer stability. For all the samples the thermal destruction starts at 500-540^{0}C.

The procedure of fabrication of SWNTs/polyimide composites was developed. The films were formed on the transparent substrates (quartz and glass). The uniform suspension of SWNTs and polyimide in NMP (or another solvent) was prepared. In order to disrupt the nanotube bundles, the suspension was ultrasonicated. Then, the suspension has been centrifuged. The supernatant, containing isolated individual nanotubes, was deposited layer by layer on the substrate at elevated temperature. To avoid the aggregation of the nanotubes, the suspension was re-sonicated each time before deposition of a new layer. The final composite SWNTs/polyimide films are presented in Fig.1.

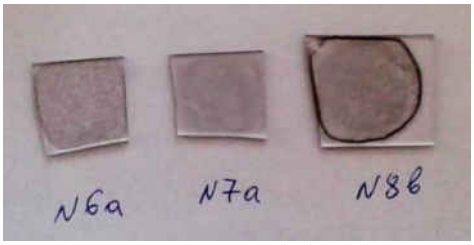

Fig. 1. Composite SWNTs/polyimide films

This work was supported by the project RFBR 15-59-31817 RT-omi.

[1] A.A. Krylov, S. G. Sazonkin, N.R. Arutyunyan, V.V. Grebenyukov, A.S. Pozharov, D.A. Dvoretskiy, E.D. Obraztsova, and E.M. Dianov, JOSA, **33** 134 (2016).
[2] M.A. Chernysheva, A.A. Krylov, P.G. Kryukov, N.R. Arutyunyan, A.S. Pozharov, E.D. Obraztsova, and E.M. Dianov, Optics express, **20**, B124 (2012).
[3] M.A. Chernysheva, A.A. Krylov, A.A. Ogleznev, N.R. Arutyunyan, A.S. Pozharov, E.D. Obraztsova, E.M. Dianov, Optics express, **20**, 23994 (2012).

Tuning the Diameter of SWNTs from Ferrocene-CO Floating Catalyst Chemical Vapor Deposition by Carbon Dioxide

Nguyen Ngan Nguyen, Ying Tian, Patrik Laiho, Hua Jiang, Esko I. Kauppinen
NanoMaterials Group, Department of Applied Physics, Aalto University, School of Science, PO Box 15100, FI-00076 AALTO, Finland

Floating catalyst chemical vapor deposition has been well known the stable and effective method to produce single wall carbon nanotubes (SWNT).[1] For commercialized products, the yield as well as the quality of the nanotube thin films must be comparable to indium tin oxide thin films. Here, SWNTs were grown from the ferrocene-based catalyst and carbon monoxide as the carbon source. By tuning the synthesising temperature and the amount of carbon dioxide, the diameter of SWNTs is finely controlled,[2] improving also conductivity-optical transparency of SWNT thin films. Moreover, the yield of SWNTs is also increased significantly by adding small amount of carbon dioxide.

[1] A. G. Nasibulin , A. Moisala, D. P. Brown, H. Jiang and E. I. Kauppinen, Chemical Physics Letters, 402, 227 (2005).
[2] Y. Tian, A. G. Nasibulin, B. Aitchison, T. Nikitin, J. v. Pfaler, H. Jiang, Z. Zhu, L. Khriachtchev, D. P. Brown and E. I. Kauppinen, J. Phys. Chem. C 115, 7309 (2011).

Bending of individual carbon nanotubes in PeakForce AFM

Pavel Geydt[1], Tatiana Makarova[1,2], Erkki Lähderanta[1], Mikhail Kanygin[3] and Aleksander Okotrub[3,4]
1 Laboratory of Solid State Physics, Lappeenranta University of Technology, 53851 Lappeenranta, Finland
2 Laboratory of Physics for Cluster Structures, Ioffe Institute, 194021 Saint Petersburg, Russia
3 Laboratory of Nanomaterials, Nikolaev Institute of Inorganic Chemistry, SB RAS, Novosibirsk 630090, Russia
4 Novosibirsk State University, Novosibirsk 630090, Russia
Corresponding author: pavel.geydt@lut.fi

Carbon nanotubes (CNTs) demonstrate remarkably high stiffness in the order of hundreds of gigapascals [1-3]. Due to the outstanding rigidity of these nanostructures, CNTs are proposed for such polar applications as ultra-hard reinforced composites or flexible wearable electronics etc.

Assessment of their elastic properties is laborious, so artificial techniques [2,3] were proposed during latest two decades. Therefore, necessity to arrange easy and fast methods of control of parameters of CNTs still exists.

Our starting point was that it is possible to measure the elastic modulus of CNTs with help of an accurate probe in common bending experiment. Furthermore, the most consistent variant is carrying out scanning probe microscopy. With recent advances allowing precise force control, it is possible to establish and record the applied force with preciseness of tens of piconewtons.

CNTs in our experiments were fixed in two-contact geometry [4], when only the middle area is protruding from the substrate (See Fig. 1). Substrate has been represented by a matrix of polysterene (PS) polymer, which was stretched or rolled during the preparation cycle of PS/CNTs composite. We could measure the elastic properties in advanced PeakForce Quantitative NanoMechanical mode of AFM [5].

Thus, simplified technique can be proposed to quantify the dependence between the deformation (in surface topography) and the applied force. Amount of the layers enclosed into the multi-walled CNT becomes recognized from the reported parameters of elasticity [2]. However, when the probe station is coupled with RAMAN or infra-red laser, then it also becomes possible to measure the shift of the spectra of the strained PS/CNT system and its relaxation in dependence from the force applied. This leads to the understanding of the phenomena of physical-chemical attachment between these two materials, which can lead to advances in fabrication procedure.

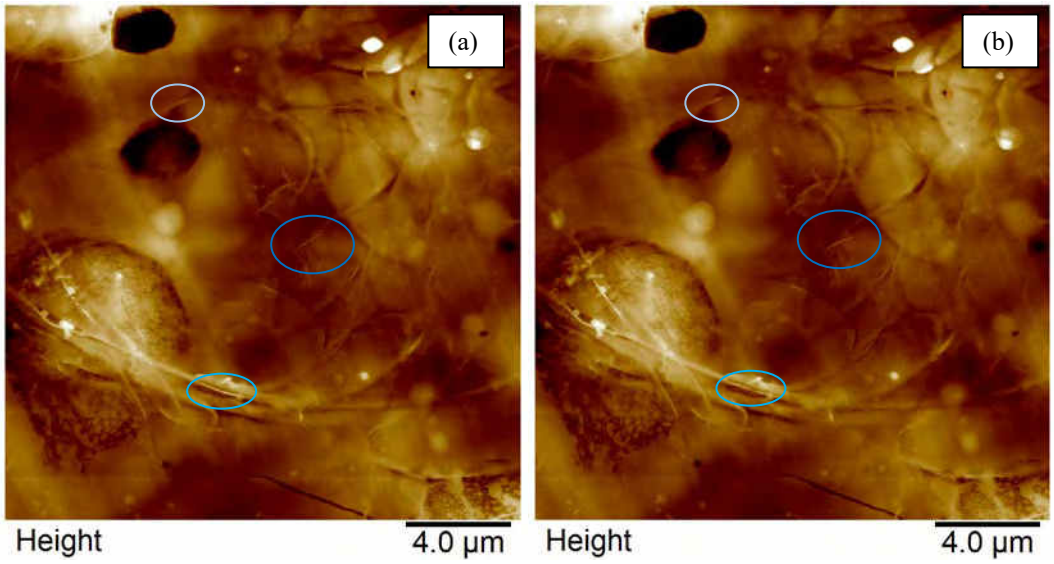

Fig. 1. Surface of the PS/MWCNTs composite comprising 5% of CNTs by weight. Bending of individual NTs is visible even from different directions of AFM probe movements: from right to left (a) and backwards (b).

References

[1] N. Silvestre, Advanced Computational Nanomechanics, (Wiley, 2016).
[2] L. Deng, S.J. Eichhorn, Ch.-Ch. Kao and R.J. Young, ACS Appl. Mater. Interfaces, **3**, 433, (2011).
[3] J.-P. Salvetat, A.J. Kulik, J.-M. Bonard, G.A.D. Briggs, Th. Stöckli, K. Méténier, S. Bonnamy, F. Béguin, N.A. Burnham and L. Forró, Adv. Mater., **11**, 161, (1999).
[4] E.T. Thostenson and T.-W. Chou, J. Phys. D: Appl. Phys., **36**, 573, (2003).
[5] T.L. Makarova, P. Geydt, I. Zakharchuk, E. Lahderanta, A.A. Komlev, A.A. Zyrianova, M.A. Kanygin, O.V. Sedelnikova, V.I. Suslyaev, L.G. Bulusheva and A.V. Okotrub, Comp. B: Eng., **91**, 505, (2016).

Quasi-two-dimensional diamond: structure and mechanical properties

I.P. Kudarenko[1], A.M. Alexeev[1], R.R. Ismagilov[1], E.A. Korznikova[2], S.V. Dmitriev[2], A.N. Obraztsov[1,3]

[1]Department of Physics, Lomonosov Moscow State University, Moscow, Russia
[2]Institute for Metals Superplasticity Problems of Russian Academy of Sciences, Ufa, Russia
[3]Department of Physics and Mathematics, University of Eastern Finland, Joensuu, Finland

ismagil@polly.phys.msu.ru

Diamond platelets of sub-micrometer size were obtained by chemical vapor deposition technique from CH_4/H_2 gas mixture activated by a direct current discharge [1]. Comprehensive characterization of the diamond platelets was performed with use of scanning and transmission electron microscopy. According to experimental results isolated hexagonal platelets are composed of stacked (111) well-ordered atom planes with a few number of twin planes. Thickness of the platelet diamond crystallites was in nanometers scale and their lateral size of few micrometer.

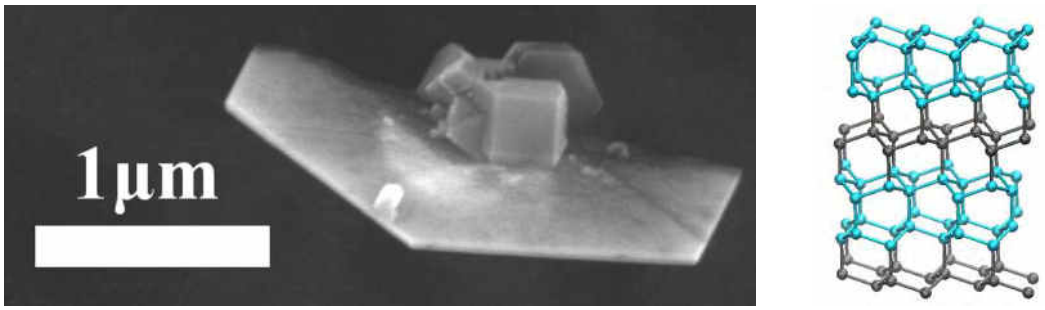

Fig.1. SEM image of isolated diamond platelet (left) and fraction of the modeled atomic structure (right).

Mechanical (elastic) properties of diamond platelets were estimated by means of atomistic modeling. Large-scale Atomic/Molecular Massively Parallel Simulator (LAMMPS) and the adaptive intermolecular REBO potential were used for molecular dynamics experiments. Uniaxial strain ε_{xx} were applied to the material followed by the material relaxation. Simulation results explicitly demonstrated expected symmetry reduction and provided helpful stiffness constants for such type of diamond materials.

This work was supported by Russian Foundation for Basic Research (project no. 16-32-50103-nr)

[1] A.M. Alexeev, R.R. Ismagilov, E.E. Ashkinazi, A.S. Orekhov, S.A. Malykhin and A.N. Obraztsov, Diamond and Related Materials, **65**, 13-16 (2016)

Cathodoluminescent Properties of Needle-like Single Crystal Diamond

S. A. Malykhin[1,2], R. R. Ismagilov[1,2], A. S. Orekhov[3], A. N. Obraztsov[1,4]
[1]*Department of Physics, Lomonosov Moscow State University, Moscow, Russia*
[2]*Prokhorov General Physics Institute, Russian Academy of Sciences, Moscow, Russia*
[3]*Russian Research Centre Kurchatov Institute, Moscow, Russia*
[4]*Department of Physics and Mathematics, University of Eastern Finland, Joensuu, Finland*
sermal92@mail.ru

Diamond micrometer-size crystallites shaped as pyramids with rectangular base were produced by combination of chemical vapor deposition (CVD) and selective oxidation. CVD process was made with use hydrogen-methane gas mixture to achieve (100) textured growth of polycrystalline films composed of needle like diamond crystallites embedded into nano-diamond and disordered carbon material. Oxidation at temperature about 600C in air allowed selective elimination of the smallest carbon species and thus remaining material consist only from the needle like diamond crystallites having shape of geometrically perfect pyramids [1]. Cathodoluminescent (CL) studies for the diamond pyramids were performed with use JEOL JSM-7001F instrument equipped by cathodoluminescent attachment GATAN MonoCL3.

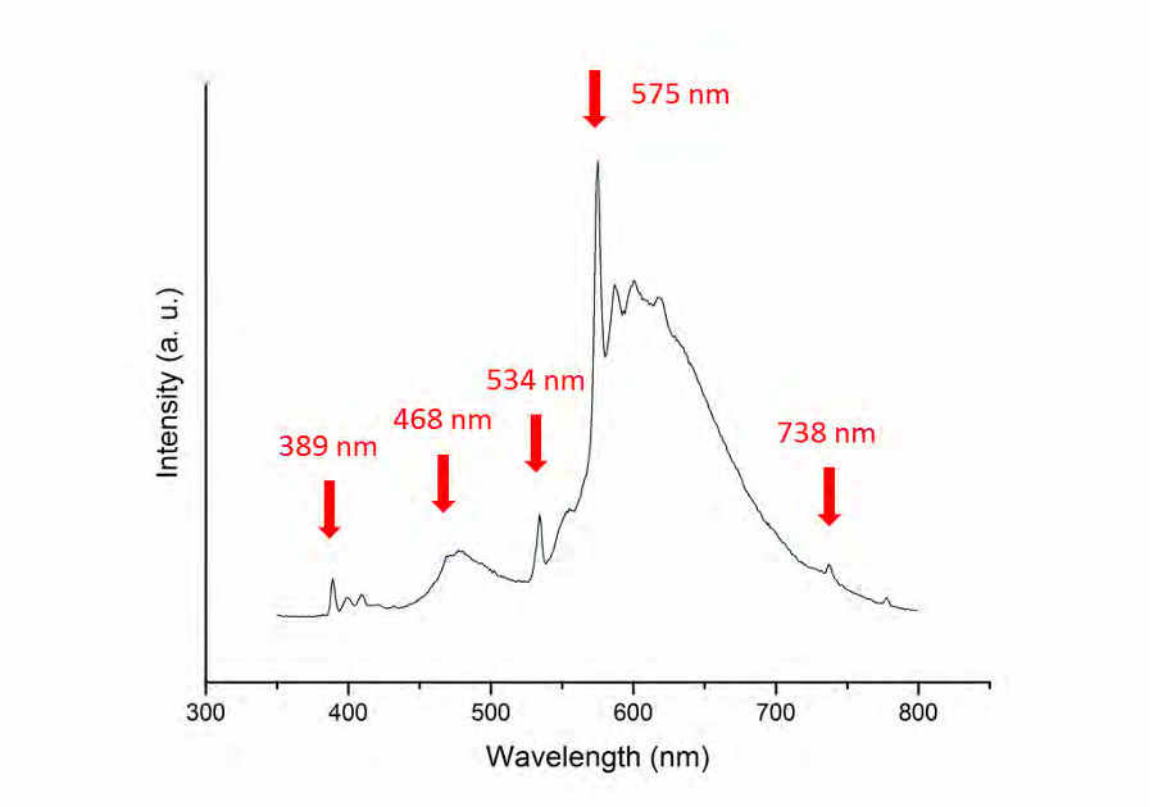

Fig. 1. Typical CL spectra of individual needle-like diamond crystal

Fig. 1 shows typical example of measured CL spectra. The main components of common CL spectra are: 389 nm, 468 nm, 534nm, 575 nm and 738 nm. Some of these components have typical vibronic structure. Presence of these components gives us information about monocrystal structure with substitutional or/and interstitial nitrogen atoms that contains NV^0 and SiV colour centres [2,3]. Intensity of these components is different in different points of needle like diamond crystal.

This work was supported by Russian Science Foundation (Grant № 15-19-00279).

[1] A. A. Zolotukhin, M. A. Dolganov, A. M. Alekseev, A. N. Obraztsov, Diamond and Related Materials, **42**, 15 (2014)
[2]A. M. Zaitsev, *Optical Properties of Diamond. A Data Handbook*, (Springer Science & Business Media, 2001)
[3] B. Dischler, *Handbook of Spectral Lines in Diamond,* (Springer Science & Business Media, 2012)

Suspending of single-walled carbon nanotubes doped with CuCl

T.V. Eremin[1,2], P.V. Fedotov[2], A.A. Tonkikh[2], E.D. Obraztsova[1,2]
[1]*Physics Department of M.V. Lomonosov Moscow State University, Moscow, Russia*
[2]*A.M.Prokhorov General Physics Institute, RAS, Moscow, Russia*
timaeremin@yandex.ru

Filling of single-walled carbon nanotubes (SWCNTs) with CuCl leads to suppression of the first and the second semiconducting optical transitions (S_{11} and S_{22}) in optical absorption spectra and also to a blue shift of the tangential modes in Raman scattering spectra. It is assumed that such phenomena are induced by the charge transfer between nanotubes and CuCl molecules inside nanotubes, which leads to the downshift of the Fermi level to the valence band [1,2]. Whereas the gas-phase filling technique allows filling of nanotubes in films or powder, there is an actual task to obtain material with a significant concentration of individual SWCNTs filled with CuCl. The aim of this work is to obtain such material via suspending of the doped SWCNTs.

Pre-purified powder of SWCNTs, synthesized with arc-discharge method, was filled with CuCl via the gas-phase filling technique at 230 °C with the exposition time of 13 hours. After the filling procedure, the sample was annealed in air for 2 hours at the same temperature in order to remove molecules adsorbed on the external surfaces of SWCNT bundles.

Fig.1 shows the Raman spectra of pristine (black line) and filled (red line) SWCNTs in the G-mode frequency range. Significant shift of the G-mode after filling (1594,5 cm^{-1}→1611,5 cm^{-1}) indicates a strong charge transfer between SWCNTs and CuCl molecules. In order to test influence of solvents on the doped SWCNTs, two different powder samples were placed in water or NMP for 24 hours. After that, solvents were evaporated and Raman spectra were measured. The treatment of doped SWCNTs via NMP (green line at Fig. 1) results in the shift of the G-mode to the original position (1594,5 cm^{-1}), while the treatment via water (blue line at Fig. 1) leads to the G-mode shift to some intermediate position (1600 cm^{-1}). This indicates of the charge transfer remaining, though not so strong as before the water treatment. Therefore, water was used in further experiments as more appropriate solvent.

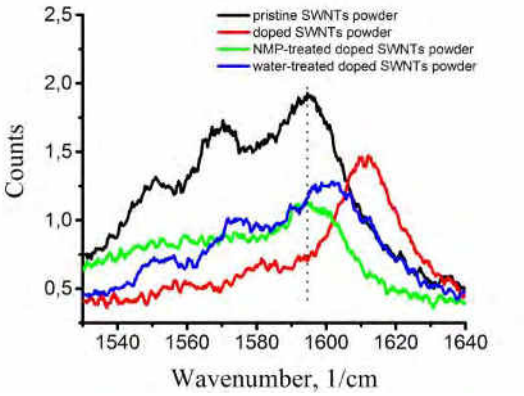

Fig.1. The illustration of solvent influence on the Raman spectra of doped SWCNTs

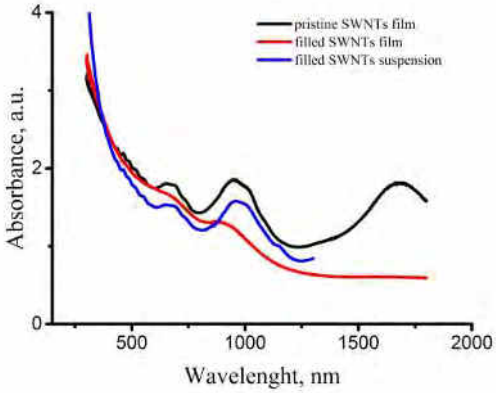

Fig.2. The illustration of ultrasonication influence on absorption spectra of doped SWCNTs

In order to break bundles and nets of SWCNTs into individual nanotubes, ultrasonication and intensive mechanical agitation in water was applied. However, such treatment leads to the shift of the G-mode to the original position and emergence of the S_{22} optical transition band to the initial absorbance units (Fig.2).

Such results can indicate, that unfilled nanotubes in the powder are doped due to contacts with filled SWCNTs even at low percentage of filled SWCNTs in the sample. Also, an assumption that applied treatments lead to the removing of CuCl molecules from internal channels of SWCNTs can explain the obtained results.

This work is supported by RSF 15-12-30041 project.

References

[1] Fedotov P. V. et al. " Optical properties of single-walled carbon nanotubes filled with CuCl by gas-phase technique", *Physica Status Sol. B 251 (2014) 2466-2470.*

[2] Eliseev A. A. et al. "Interaction between single walled carbon nanotube and 1D crystal in CuX@ SWCNT (X= Cl, Br, I) nanostructures", *Carbon, 50 (2012)4021-4039.*

Separation of semiconducting and metallic large diameter single-walled carbon nanotubes via aqueous two-phase extraction

V.A. Eremina[1,2], P.V. Fedotov[2], E.D. Obraztsova[1,2]
[1]Physics Department of M.V. Lomonosov Moscow State University, 1 Leninskie gori, Moscow, Russia
[2]A.M. Prokhorov General Physics Institute, RAS, 38 Vavilov street, 119991 Moscow, Russia
erjomina@physics.msu.ru

Single-walled carbon nanotubes (SWNTs) demonstrate a wide variety of promising features due to their unique physical, electronic, optical and other properties [1,2]. According to their geometrical structure, SWNTs may have different types of conductivity - metallic or semiconducting [3]. Extraction of one particular type of nanotubes is very desirable for studies and applications [4,5]. In our work we have achieved the separation of novel brand of nanotubes with an average diameter of 1.8 nm produced by "OCSiAl" company. Using aqueous two phase extraction technique [6,7] we have obtained the exceptional results of separation: up to 98% purity of semiconducting nanotubes and up to 98% of metallic ones at the first stage of treatment. We used UV-vis-NIR optical absorption spectroscopy to characterize the extracted samples (Fig.1).

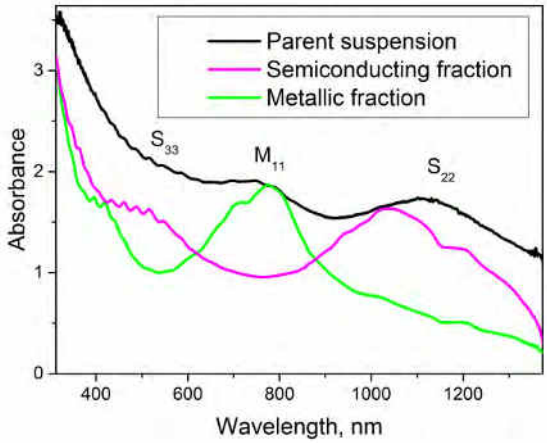

Fig.1. UV-vis-NIR optical absorbance spectra for parent suspension (black line), semiconducting fraction (magenta line) and metallic fraction (green line).

Acknowledgements

The work was supported by RSF-15-12-30041 and RFBR-16-52-540003 projects.

We are grateful to company OCSiAl for providing large diameter single-walled carbon nanotubes.

References

[1] Baughman, Ray H., Anvar A. Zakhidov, and Walt A. de Heer. "Carbon nanotubes-the route toward applications." *Science* 297.5582 (2002): 787-792.
[2] Ouyang, Min, Jin-Lin Huang, and Charles M. Lieber. "Fundamental electronic properties and applications of single-walled carbon nanotubes." *Accounts of Chemical Research* 35.12 (2002): 1018-1025.
[3] Dresselhaus, Mildred S., et al. "Carbon nanotubes" (2000) *Springer Netherlands*.
[4] Blackburn, Jeffrey L., et al. "Transparent conductive single-walled carbon nanotube networks with precisely tunable ratios of semiconducting and metallic nanotubes." *Acs Nano* 2.6 (2008): 1266-1274.
[5] Islam, Ahmad E., John A. Rogers, and Muhammad A. Alam. "Recent Progress in Obtaining Semiconducting Single-Walled Carbon Nanotubes for Transistor Applications." *Advanced Materials* 27.48 (2015): 7908-7937.
[6] Khripin, Constantine Y., Jeffrey A. Fagan, and Ming Zheng. "Spontaneous partition of carbon nanotubes in polymer-modified aqueous phases." *Journal of the American Chemical Society* 135.18 (2013): 6822-6825.
[7] Eremina, Valentina A., Pavel V. Fedotov, and Elena D. Obraztsova. "Copper chloride functionalization of semiconducting and metallic fractions of single-walled carbon nanotubes." *Journal of Nanophotonics* 10.1 (2016): 012515-012515.

Optical Spectrum of Single-Walled Carbon Nanotubes by Hydrocarbon Based Floating Catalyst Chemical Vapor Deposition

Yongping Liao, Er-Xiong Ding, Ying Tian, Hua Jiang, Esko I. Kauppinen
NanoMaterials Group, Department of Applied Physics, Aalto University, Puumiehenkuja 2, 00076 AALTO, Finland
esko.kauppinen@aalto.fi

Single-walled carbon nanotubes (SWCNTs) have been drew great attention in recent years since its potential in future electronics. Normally, the SWCNTs are synthesized by chemical vapor deposition (CVD) method, where the catalysts are deposited on silicon substrate, however, the yield of SWCNTs by this traditional method is quite low. In our floating catalysts CVD [1], the catalysts which should be preheated before coming to the reactor are always floating in the gas phase and the SWCNTs are also grown in the gas phase. What's more, here the hydrocarbon such as CH_4 or C_2H_4 were used as the carbon source, which can be reacted on the surface of catalysts more effectively, and the reactor is vertical so the reaction could be continuous, so in this way, the yield can be increased remarkably.

The Raman and ultraviolet-visible-near infrared (UV-Vis-NIR) are effective ways to analyze the properties of SWCNTs [2]. In this work, the SWCNTs were directly deposited a filter film, and then the SWCNTs film were transferred on a quartz substrate for further characterization. The Raman spectrum was used to check the chirality and quality of SWCNTs, it was found that the as-prepared SWCNTs had both metallic and semiconducting nanotubes with good quality. And the UV-Vis-NIR was used to determine the diameter of SWCNTs, and it can be concluded that our SWCNTs had a mean diameter of 1.9 nm. Further formation should be identified by TEM images and electron diffraction. In the future work, more delicate reactor should be designed, in which the catalysts precursor can be controlled more precisely, and diameter and chirality of SWCNTs should be controlled.

References

[1] A. G. Nasibulin , A. Moisala, D. P. Brown, H. Jiang and E. I. Kauppinen, Chemical Physics Letters, **402,** 227 (2005).
[2]Y. Tian, A. G. Nasibulin, B. Aitchison, T. Nikitin, J. v. Pfaler, H. Jiang, Z. Zhu, L. Khriachtchev, D. P. Brown and E. I. Kauppinen, J. Phys. Chem. C, **115**, 7309 (2011).

Friday, August 5

©Y. Svirko

Large Scale Separation of Single Chirality SWCNTs and Their Application to Near Infrared Vascular Imaging

Hiromichi Kataura, Yohei Yomogida, Minfang Zhang, Masako Yudasaka, Xiaojun Wei, and Takeshi Tanaka
Nanomaterials Research Institute (NMRI), AIST, Tsukuba, Japan
h-kataura@aist.go.jp

Recently, single-wall carbon nanotubes (SWCNTs) have attracted much attention as a fluorescence probe for biological imaging due to their bright emission in near infrared (NIR) biological transparency window (700-1400 nm) where the light penetrates a living body deeply because of the low absorption of water and various biological tissues [1]. However, currently-used HiPco SWCNTs contain various chiral species, each of which has chirality dependent excitation (E_{22}) wavelength. If we use a monochromatic light source for the E_{22} excitation as in the previous work, the excitation efficiency should be very low. Therefore a single-chirality SWCNT was desired for high efficiency imaging. For this purpose, we have developed a novel gel chromatography method for chirality separation of SWCNTs and successfully separated high-purity single-chirality (9,4) SWCNTs in large scale. Since both the E_{11} emission and E_{22} excitation of (9,4) SWCNTs are in the biological transparency window, they could be an ideal fluorescence probe for the biological imaging. In this work, we demonstrate highly efficient biological imaging of mouse vasculature using biocompatible single-chirality (9,4) SWCNTs.

To make the (9,4) SWCNTs biocompatible, surfactants used in the separation were replaced with a biocompatible surfactant (DSPE-PEG). After the SWCNT solution was injected intravenously through a tail of mouse, NIR images of the mouse were recorded using an InGaAs 2D array camera under an illumination of a LED (~730 nm) light. The (9,4) SWCNT exhibited much brighter vascular images than unseparated HiPco. The high brightness of (9,4) enables the imaging using even two orders of magnitude lower dose per mouse than reported values. The use of biocompatible (9,4) SWCNTs as fluorescence probe will reduce any possible risk to the subject.

This work was supported by KAKENHI No. 25220602.

[1] G. Hong et al, Nature Medicine 18 (2012) 1841.

Growth Modes and Chiral Selectivity of SWNTs

Christophe Bichara
CINaM, Aix-Marseille University and CNRS
bichara@cinam.univ-mrs.fr

A detailed understanding of the catalyst/nanotube interface, ***under actual growth conditions***, is probably a key for a selective synthesis of single wall carbon nanotube (SWNT) by catalytic chemical vapor deposition (CCVD). I will show here how dedicated computer simulations, mostly based on a tight binding model for carbon and nickel [1], a typical catalyst, can provide a useful insight.

It starts with the complex stability pattern of atomic carbon dissolved in subsurface layers of crystalline Ni, that depends on the presence of a graphene layer on top of it [2]. For catalyst nanoparticles below 3 nm, relevant for the CCVD growth, the presence of carbon dissolved in the surface layers induces a gradual melting at temperatures well below the melting temperature of pure nanoparticles of the same size. Calculated size dependent phase diagrams for Ni-C nanoparticles [3] indicate that facetted crystalline nanoparticles are unlikely to be observed in this size range under growth conditions.

This raises the question of the role of the carbon dissolved in the catalyst during the growth, that is shown to have a strong influence on the wetting properties of the metal-SWNT interface [4]. Through careful Transmission Electron Microscopy observations [5], so called tangential and perpendicular growth modes were identified. Computer simulations were used to analyze these growth modes at the atomic scale, demonstrating that the tangential mode corresponds to a weak carbon supply and slow growth, while the perpendicular one is observed when the carbon fraction in the nanoparticle is larger [6]. Growth experiments designed to tune the carbon fraction in the nanoparticle by changing the carbon feedstock (CO and CH_4) confirm this analysis.

Finally we discuss the role of the different contributions to the stability and dynamics of the nanotube/nanoparticle interface on the chiral selectivity.

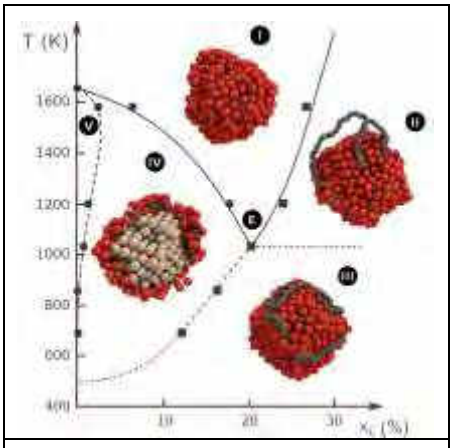

Phase diagram of a NP with 807 Ni atoms [3].

References
[1] Amara, H.; Ducastelle, F.; Roussel, J.-M.; Bichara, C.; Gaspard, J.-P. *Phys. Rev. B* **2009**, *79*, 014109.
[2] Weatherup, R. S.*et al. J. Am. Chem. Soc.* **2014**, *136*, 13698–13708.
[3] Magnin, Y.; Zappelli, A.; Amara, H.; Ducastelle, F.; Bichara, C. *Phys. Rev. Lett.* **2015**, *205502*, 1–5.
[4] Diarra, M.; Zappelli, A.; Amara, H.; Ducastelle, F.; Bichara, C. *Phys. Rev. Lett.* **2012**, *109*, 185501.
[5] Fiawoo, M.-F. C.; Bonnot, A.-M.; Amara, H.; Bichara, C.; Thibault-Pénisson, J.; Loiseau, A. *Phys. Rev. Lett.* **2012**, *108*, 195503.
[6] He, M.; Magnin Y.; Amara, H.; Jiang, H.; Fossard, L.; Castan, A.; Kauppinen, E. I.; Loiseau, A.; Bichara C. *submitted*.

True-Color Real-Time Imaging of Single-Walled Carbon Nanotubes via Enhanced Rayleigh Scattering

Wenyun Wu, Jingying Yue, Dongqi Li, Xiaoyang Lin, Xingcan Dai, Kaili Jiang
Department of Physics and Tsinghua-Foxconn Nanotechnology Research Center, Tsinghua University, Beijing 100084, P. R. China
JiangKL@tsinghua.edu.cn

Single-walled carbon nanotubes (SWCNTs) illuminated by white light should appear coloured due to resonance Rayleigh scattering. However, true colour imaging of SWCNTs on substrate has not been reported, because of the extremely low scattering intensity of SWCNTs and strong substrate scattering. Here we show that Rayleigh scattering can be greatly enhanced by interface dipole enhancement effect. Consequently, colourful SWCNTs on substrates can be directly imaged under an optical microscope by wide field supercontinuum laser illumination, which facilitates high throughput chirality assignment of individual SWCNTs [1].

For a better understanding of the enhanced Rayleigh scattering, the optical effect of a nanometer or sub-nanometer interfacial layer of condensed molecules surrounding individual nanomaterials such as single-walled carbon nanotubes (SWCNTs) has been studied theoretically and experimentally. This interfacial layer, when illuminated by light, will behave as an optical dipole lattice and contribute an instantaneous near field to enhance the local field on neighbouring atoms, molecules, or nanomaterials, which may lead to enhanced Raleigh scattering, Raman scattering, and Fluorescence. The theory of this interface dipole enhanced effect (IDEE) predicts that a smaller distance of nanomaterials to the plane of the interfacial layer, or a larger ratio of the dielectric constants of the interfacial layer to surrounding medium, will result in a larger field enhancement factor. This prediction is further experimentally verified by several implementations of enhanced Rayleigh scattering of SWCNTs as well as in-situ Rayleigh scattering of gradually charged SWCNTs. The interface dipole enhanced Rayleigh scattering not only enables true-colour real-time imaging of nanomaterials, but also provides an effective mean to peer into the subtle interfacial phenomena [2].

This approach, true-colour real-time imaging of single-walled carbon nanotubes via enhanced Rayleigh scattering, which is also termed “Rayleigh imaging microscopy”, is not restricted to SWCNTs, but widely applicable to a variety of nanomaterials, which enables people to explore the colourful nano-world under optical microscopes

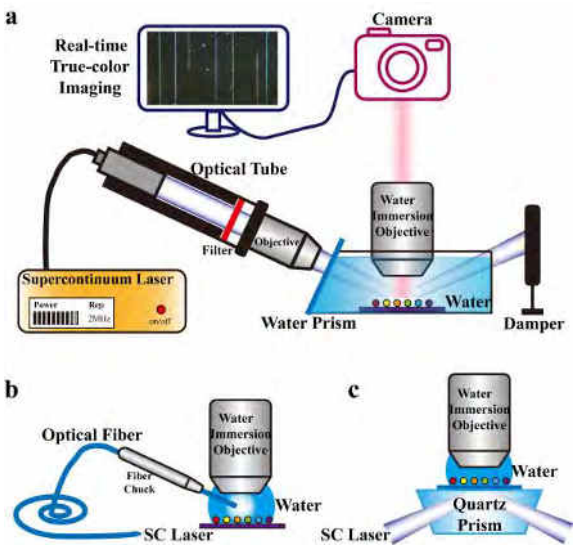

Fig. 1. Schematic illustration of Rayleigh imaging microscopy for true-color real-time imaging of SWCNTs, a, b, c, three different experimental setups.

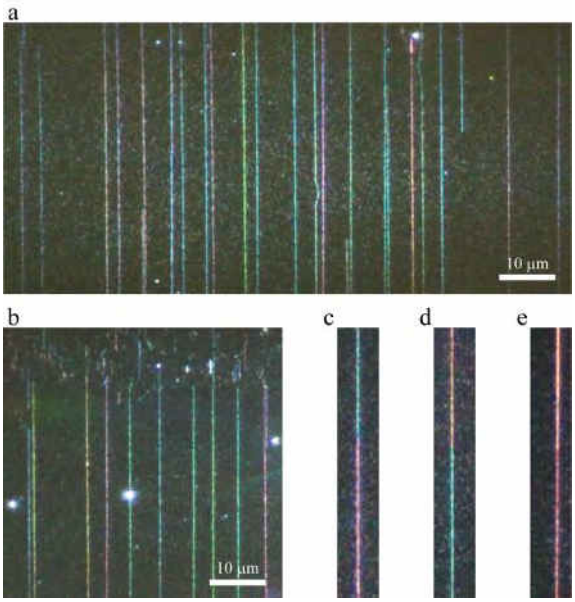

Fig. 2. True color imaging of SWCNTs. a, b,Typical true color image of horizontally aligned SWCNTs on Si wafer with 100 nm SiO2. c-e, Typical true color images of three individual SWCNTs with intramolecular junctions.

References

[1] W. Y. Wu, J. Y. Yue, X. Y. Lin, D. Q. Li, F. Q. Zhu, X. Yin, J. Zhu, J. T. Wang, Y. Chen, X. H. Wang, T. Y. Li, Y. J. He, X. C. Dai*, P. Liu, Y. Wei, J. P. Wang, W. Zhang, Y. D. Huang, L. Fan, L. N. Zhang, Q. Q. Li, S. S. Fan, and K. L. Jiang*, Nano Research, **8,** 2721 (2015).

W. Y. Wu, J. Y. Yue, D. Q. Li, X. Y. Lin, F. Q. Zhu, X. Yin, J. Zhu, X. C. Dai*, P. Liu, Y. Wei, J. P. Wang, H. T. Yang, L. N . Zhang, Q. Q. Li, S. S. Fan, and K. L. Jiang*, Nano Research, **8**, 303 (2015).

Optical Spectroscopy of Individual Nano-materials with Defined Atomic Structure

Kaihui Liu
School of Physics, Peking University, Beijing 100871, China
Email: khliu@pku.edu.cn

When the characteristic length of a material shrinks to 1 nm scale, many distinct physical phenomena, such as quantum confinement, enhanced many-body interactions and strong van der Waals inter-material couplings, will appear. To investigate these related fascinating low-dimensional physics, we need a tool to quantitatively link the atomic structures to the physical properties of very small nano-materials. In this talk, I will introduce our recently developed in-situ TEM + nanooptics technique [1,2], which combines capability of structural characterization in TEM and property characterization in nanooptics on the same individual nano-materials. Several examples of using this technique to study the physics in 1D carbon nanotube system [3-6] and 2D atomic layered materials [7-8] will be demonstrated.

[1] Kaihui Liu, Feng Wang* et al., “High-throughput Optical Imaging and Spectroscopy of Individual Carbon Nanotubes in Devices”, Nature Nanotechnology 2013, 8, 917-922
[2] Kaihui Liu, Feng Wang* et al, “Systematic Determination of Absolute Absorption Cross-section of Individual Carbon Nanotubes”, PNAS 2014, 111, 7564-7569
[3] Kaihui Liu, Steven G. Louie, Enge Wang*, Feng Wang* et al. “An atlas of carbon nanotube optical transitions”, Nature Nanotechnology 2012, 7, 325-329
[4] Kaihui Liu, Enge Wang and Feng Wang* et al., “Quantum coupled radial breathing oscillations in double-walled carbon nanotubes”, Nature Communications 2013, 4, 1375
[5] Kaihui Liu, Enge Wang, Feng Wang* et al., “Van der Waals-Coupled Electronic States in Incommensurate Double-walled Carbon Nanotubes”, Nature Physics 2014, 10, 737-742
[6] Shibin Deng, Kaihui Liu*, and Jin Zhang* et al., "High-Throughput Determination of Statistical Structure Information for Horizontal Carbon Nanotube Arrays by Optical Imaging", Advanced Materials 2016, 28, 2018-2023
[7] Kaihui Liu, Feng Wang* et al., “Evolution of interlayer coupling in twisted molybdenum disulfide bilayers”, Nature Communications 2014, 5, 4966.
[8] Xu Zhou, Shiwei Wu*, Hailin Peng*, Kaihui Liu* et al., “Strong Second-Harmonic Generation in Atomic Layered GaSe”, JACS 2015, 137, 7994-7997

Accessing kinetics of structural rearrangements in graphene via direct atomic imaging

A.Chuvilin
CIC nanoGUNE Consolider, Tolosa Hiribidea 76, 20018 Donostia-San Sebastian, Spain
IKERBASQUE Basque Foundation for Science, Maria Diaz de Haro 3, E-48013 Bilbao, Spain
a.chuvilin@nanogune.eu

The raise of nanoscience and nanotechnology and necessity to characterize the structure of individual objects consisting of a countable number of atoms determined the shift of structure characterization paradigm from bulk methods like X-ray diffractometry to local high resolution methods like electron microscopy. The similar shift in paradigm is urging now in chemistry – chemical processes defining structure and properties of nanoscale and low dimensional objects often constitute a negligible part of the total volume of the material, and thus their assessment by experimental bulk chemical methods if often impossible. The new concept is provided by the time resolved electron microscopy allowing for direct observation of atomic rearrangements.

We are developing the methodology to apply the formalism and approaches of the classical chemical kinetics for the quantitative description of atomistic processes observable in the microscope. We show that a proper statistical treatment of the data obtained in a range of experimental conditions allows determining the threshold energies for radiation induced reactions. But not only that: we show that true activation energies for thermally activated reaction pathways for individual defects can be estimated as well.

We apply this methodology for reactions of point defects in graphene. The cross-sections and threshold energies of irreversible (atom emission) and reversible (bond rotation, see Fig.1) processes are measured. Observation of statistically significant number of events at variable experimental conditions allows decoupling

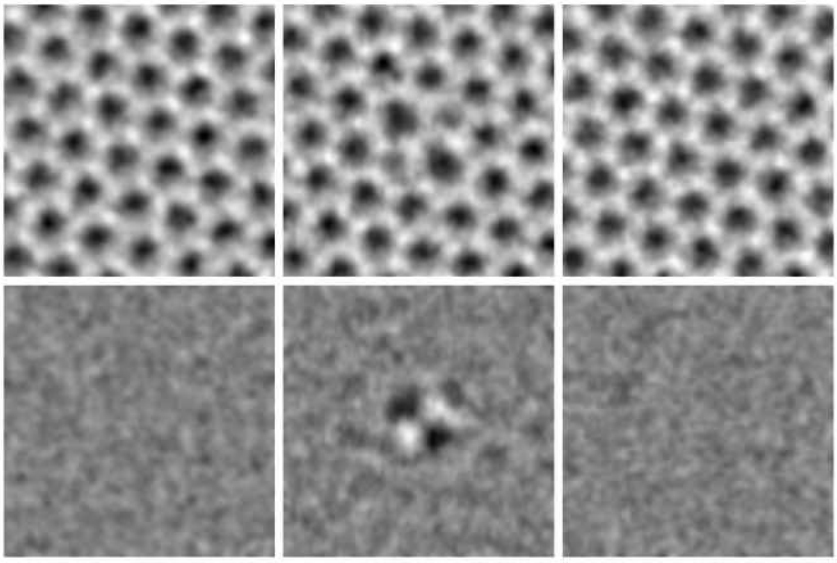

Fig. 1. Sequence of electron microscopy images showing the bond rotation reaction in graphene. The upper row – unprocessed images of the graphene lattice separated by time slices of 1s. The lower row – the same images filtered in order to remove the pattern of the lattice.

of radiation induced and thermal reaction pathways and obtaining independent estimations of cross-sections and activation energies for direct and backwards rotations. The cross-sections of direct rotation were found to be in a decent agreement with theoretical estimations. Interestingly the backwards rotation is characterized by very high cross-section exceeding theoretical values by 3-4 orders of magnitude. The values obtained rule out electron-nucleus collision as the main mechanism of energy transfer from electron beam to the sample. We speculate that the energy is transferred through electron-electron interactions via strong coupling of excited electron states with the phonon modes localized around the defect.

Acknowledgements.

The contribution of my co-workers from Nottingham University, KAUST, Novosibirsk Institute of Inorganic Chemistry and Graphenea Company is greatly appreciated. The work was partially supported by collaboration project with FEI Company and by FP7-PEOPLE-2011-IRSES N295180 (MagNonMag) project.

In situ Cyclic Telescoping of Multi-Walled Carbon Nanotubes in a Transmission Electron Microscope

Katherine Elizabeth Moore, Ovidiu Cretu, Masanori Mitome and Dmitri Golberg*
International Center for Materials Nanoarchitectonics (MANA), National Institute for Materials Science (NIMS), Namiki 1-1, Tsukuba, Ibaraki 3050044, Japan
**golberg.dmitri@nims.go.jp*

1. Objective and Summary

The past decade has seen a strong increase in research efforts dedicated to flexible electronics. These devices are ultimately expected to scale down to nanometer-size in order to fit current trends regarding size and portability. Carbon nanotubes have been considered as potential candidates for nanoscale devices since their discovery, due to their low-dimensionality and unique physical properties. As a result, a large number of interesting results have been reported concerning the fabrication and performance of single-nanotube electronic and nanoelectromechanical system (NEMS) [1,2] devices.

In this work, we study the cyclic telescoping of multi-walled carbon nanotubes (MWCNTs) inside a high-resolution transmission electron microscope (HRTEM) equipped with a sharp tungsten micromanipulator [3]. The nanotubes are observed in real time, while simultaneously measuring their electrical properties. Experiments are conducted by first 'sharpening' a MWCNT by approaching it with a piezo-controlled tungsten tip and applying a single voltage pulse. This results in controlled and localized peeling of the outer walls, giving rise to a telescope structure. The exposed core is then contacted with the tungsten tip and reproducibly pulled out then re-inserted, while measuring conductance behaviour at each movement step. Results demonstrate that an electrical current can be maintained for multiple in-and-out cycles, and for telescoping distances of up to 650 nm. The systems display complex conductance behaviour, with of most MWCNT telescopes demonstrating diminishing conduction (and current) as a function of the number of cycles, while for some these properties improve. Control experiments have been carried out to investigate the effect of current annealing and beam damage on whole MWCNTs. One potential application for these structures is use as flexible electrical contacts, which allow for relative motion of the two electrodes, while maintaining electrical conduction.

2. Results and Discussion

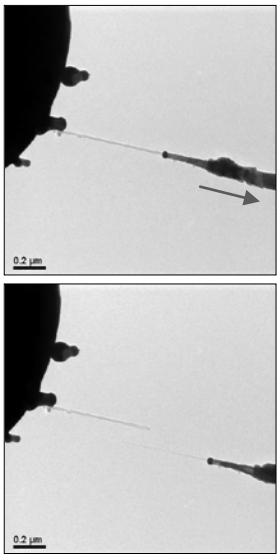

Fig. 1. An *in situ* telescoping run in HRTEM. The MWCNT inner core is entirely pulled out of the outer tubular shield.

Figure 1 shows representative telescoping of a MWCNT up to complete retraction of the inner core. An interesting observation is that the telescoped nanotubes can successfully recover from events that cause the complete de-coupling of the two segments. The core, which has been completely pulled out, can be repeatedly reinserted into the mother tube under delicate manipulations with a piezo-driven W tip. The conductance of the system returns to its previous value (for a similar telescoping distance), while the current through the system improves with respect to previous values. We conclude that the telescoped nanotubes are constantly in a state of equilibrium which is determined by the interplay of several environmental factors. In the absence of the electron beam of the microscope, the characteristics of the structures are influenced by mechanical deformations and structural reconfigurations due to Joule-heating induced temperature. Up to a certain dose rate, when present, the electron beam can lead to the improvement of the tube characteristics by creating links between adjacent walls, which comes in contrast to the degradation effects observed in standard experiments. Performance-wise, the structures display conductivity values which are better than the ones reported previously, which are maintained as the structure is de-coupled and re-attached, and which hold even for cases where the number of pulled walls is low (even for single-walled carbon nanotube retractions), making them attractive for future applications in flexible nanoelectronics.

3. References

[1] L.-M. Peng, Z. Zhang, S. Wang, Materials Today **17**, 433 (2014).
[2] A. Barreiro, R. Rurali, E.R. Hernandes, J. Mozer, T. Pichler, L. Forro, A. Bachtold, Science **320**, 775 (2008).
[3] D. Golberg *et al.* Advanced Materials **24**, 177 (2012).

Light Matter Quantum Interface Based on Single Colour Centres in Diamond

Fedor Jelezko
Institute of quantum optics, Ulm University, Germany
fedor.jelezko@uni-ulm.de

Efficient interfaces between photons and atoms are crucial for quantum networks and enable nonlinear optical devices operating at the single-photon level. In this talk I will highlight properties of single colour centres at low temperatures and show that single SiV and GeV colour centres in diamond are promising candidates for creating such interfaces. I will also show experiments aiming to create technologies allowing realization of fully integrated, scalable nanophotonic quantum devices.

Propagation of a Switching Front in 1D Memristive Network

V. A. Slipko[1], and Y. V. Pershin[2,3]

[1]*Department of Physics and Technology, V. N. Karazin Kharkov National University, Kharkov 61022, Ukraine*
[2]*Department of Physics and Astronomy and Smart State Center for Experimental Nanoscale Physics, University of South Carolina, Columbia, South Carolina 29208, USA*
[3]*Nikolaev Institute of Inorganic Chemistry SB RAS, Novosibirsk 630090, Russia*
pershin@physics.sc.edu

Graphene- and carbone nanotubes-based materials (see, e.g., Refs. [1,2]) offer an alternative pathway to fabricate functional devices with memory at nanoscale. We call such *dynamic* devices as memristors, memcapacitors and meminductors [3]. One of the most important of their functionalities is the ability to store and process information on the same physical platform. Importantly, the networks of memory devices process the information in the massively-parallel way [4], which is essentially different from the approach used in modern computers. This new emerging computing paradigm has been dubbed as *memcomputing* [5].

In this contribution, we discuss the application of memristors in a slightly different domain, namely, in the area of information transfer. Specifically, we demonstrate the possibility of a pulse front transfer in one-dimensional memristive network shown in Fig. 1(a). This network consists of only resistive components (resistors and memristors) and employs so-called bipolar voltage-controlled memristive device with threshold. Our calculations show that the voltage pulse applied to the first cell of network (see Fig. 1(a)) may initiate a serial switching of memristors in the circuit (the switching of M_1 from low to high resistance state initiates a similar switching of M_2 and so on).

In order to demonstrate the pulse front transfer, let's consider the Kirchhoff's circuit equations, complemented by the equations describing the memristor's dynamics. One can show that the stationary moving front can be described by the following two equations

$$V(t)\left(\frac{2}{r}+\frac{1}{R}+\frac{1}{M(t)}\right)-\frac{1}{r}\big(V(t-\tau)+V(t+\tau)\big)=\frac{V_p}{R}, \quad (1)$$

$$\frac{\mathrm{d}M}{\mathrm{d}t}=f(V,M), \quad (2)$$

where $V(t)$ is the voltage across the memristor, $f(V,M)$ is the function describing the change of memristor state, and all other coefficients can be deduced from Fig. 1(a). An interesting feature of Eq. (1) is the non-locality in time. Unfortunately, the above equations cannot be solved analytically in the general case.

Fig. 1(b) presents an example of numerical simulations of Fig. 1(a) circuit. This graph shows that indeed the excitation applied to the first memristor is transferred along the network. One can observe the serial change of memristor states that transfers the information about the applied pulse from left to right. Importantly, in the suggested circuit the information transfer occurs by means of purely resistive (dissipative) devices unlike the case of previously considered transmission lines with [6] or without memory. We anticipate a possibility of applications of the observed phenomenon in the future information processing electronics.

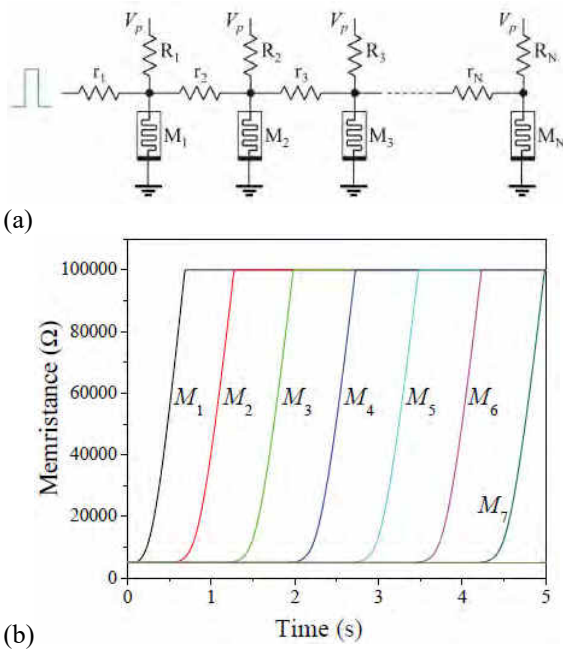

Fig. 1. (a) 1D memristive network explored in this work. (b) A selected simulation result.

VAS acknowledges the support by the Erasmus Mundus Action 2 ACTIVE programme (Agreement No. 2013-2523/001-001 EMA2). This work was partially supported by the Russian Scientific Foundation grant No. 15-13-20021.

[1] H. Y. Jeong, J. Y. Kim, J. W. Kim, J. O. Hwang, J.-E. Kim, J. Y. Lee, T. H. Yoon, B. J. Cho, S. O. Kim, R. S. Ruoff, and S.-Y. Choi, Nano Letters, **10**, 4381 (2010).
[2] S. K. Hwang, J. M. Lee, S. Kim, J. S. Park, H. I. Park, C. W. Ahn, K. J. Lee, T. Lee, and S. O. Kim, Nano Letters, **12**, 2217 (2012).
[3] M. Di Ventra, Y. V. Pershin and L. Chua, Proceedings of the IEEE, **97**, 1717 (2009).
[4] Y. V. Pershin and M. Di Ventra, Physical Review E, **84**, 046703 (2011).
[5] M. Di Ventra and Y. V. Pershin, Nature Physics, **9**, 200 (2013).
[6] Y. V. Pershin, V. A. Slipko, and M. Di Ventra, Applied Physics Letters, **107**, 253101 (2015).

Simultaneous Structural and Chemical Analysis of Carbon Nanotubes by Tip Enhanced Raman Imaging

Chi Chen[1,2]*, Norihiko Hayazawa[2], Satoshi Kawata[2,3]

[1] *Research Center for Applied Sciences, Academia Sinica, Taipei, 115, Taiwan.*

[2] *The Institute of Physical and Chemical Research (RIKEN), Wako, Saitama, 351-0198, Japan*

[3] *Department of Applied Physics, Osaka University, Suita, Osaka, 565-0871, Japan*

**E-mail: chenchi@gate.sinica.edu.tw*

TERS (tip enhanced Raman spectroscopy) opens a new horizon for nanoscale characterization [1, 2]. Atomic force microscopy (AFM) combined with TERS is generally used for hybrid morphology imaging and chemical analysis. However, for better spatial resolution, we constructed a scanning tunneling microscope (STM) based TERS system targeting at nanoscale Raman mapping of nano carbon materials.

In this abstract, STM-TERS imaging of the individual Raman modes of carbon nanotubes (CNT) is demonstrated with 1.7 nm lateral resolution based on the enhancement and positioning of a STM tip [1]. We obtained spectrally resolved TERS images simultaneously with STM scanning. Different Raman modes show characteristic distributions in the length scale of a few nanometers. With superior resolution, we observe beautiful underlying physical chemistry of CNTs, including diameter effect, local defect, and bundling effect in real space and further distinguish one of the CNTs as a multiwall CNT. In addition, micron-sized graphene grown by the chemical vapor deposition (CVD) is analyzed by TERS as well. It does not require ultrahigh vacuum and cryogenic environment to reach nanometers scale chemical analysis. High Raman sensitivity and high spatial resolution in real space make STM-TERS a powerful analytical tool for nano carbon materials.

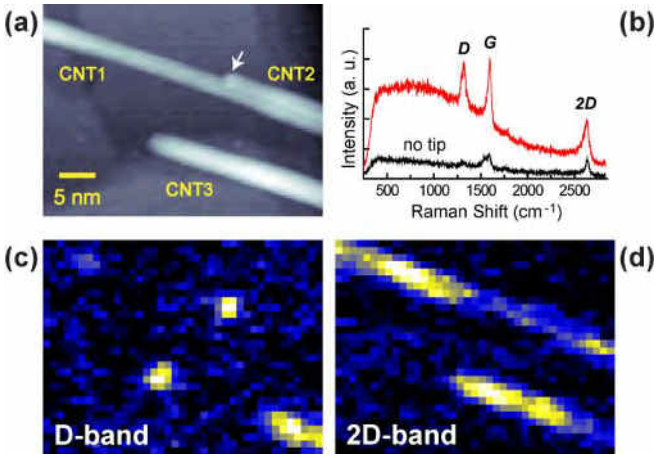

Fig. 1: **(a)** High-resolution STM topography (39×30 nm^2) of three CNTs. **(b)** Comparison of far-field Raman spectrum (no tip) and TERS spectrum taken at the arrow-indicated location on CNT-2. **(c)-(d)** Spectrally-resolved TERS images of D-band **(c)** and 2D-band **(d)**.

[1] Y. Inouye and S. Kawata, Opt. Lett. 19, 159, 1994
[2] A. Hartschuh, E. J. Sanchez, X. S. Xie, L. Novotny, Phys. Rev. Lett. 90, 95503 (2003).
[3]C. Chen, N. Hayazawa, and S. Kawata, *Nature Comm.* **5**, 3312 (2014)

Atom Probe Tomography analysis of single-crystal diamond micro needle

J. Houard[1*], M. Spies[1], I. Blum[1], A. Vella[1], V. I. Kleshch[2], A. N. Obraztsov[2,3]

[1] *Groupe de Physique des Matériaux, Université et INSA de Rouen - UMR CNRS 6634 - Normandie Université*
[2] Department of Physics, Lomonosov Moscow State University, Moscow 119991, Russia
[3] *Department of Physics and Mathematics, University of Eastern Finland, Joensuu 80101, Finland*
**Corresponding author jonathan.houard@univ-rouen.fr*

New carbon structures such as graphene, carbon nanotubes, and diamonds are promising for new applications in optoelectronic and photonic. In these applications, small concentrations of impurity can produce significant effects on the behavior of the device and hence, require high quality control on fabrication processes and advanced tools to characterize produced materials.

Atom Probe Tomography (APT) can be one of these analysis tools. APT enables the 3D reconstruction of a small volume of material with chemical identification of each atom of a sample (metallic, semiconducting and even in some cases, insulator) with a sub-nanometric spatial resolution [1]. Atoms are *field evaporated* from the surface of a needle shaped sample (end apex radius <50nm) by the combination of a high standing field (>10^9 volts per meter) and an ultrashort laser pulse (<10^{-12} second) that briefly heats tip of the sample. This triggers the departure of surface atoms, and their ionization. They then follow the field lines and are accelerated toward a spatially resolved detector. Chemical identification is done by time of flight mass spectrometry.

Previous works show that this analytical tool can be used on carbon nanostructures such as meteoritic nanodiamonds [2] or $^{12}C/^{13}C$ homojunctions [3]. However those works were only done on small crystallites embedded in a matrix, or on thin layers deposited on a substrate. Moreover the shaping of the sample as a very thin tip (as needed to perform APT) usually requires the use of Focused Ion Beam (FIB), which is time consuming and can affect the materials properties.

In this work, we present results of APT analysis of single-crystal diamond micro-needles obtained by Plasma Enhanced Chemical Vapor Deposition (PECVD) followed by a thermal oxidation [4]. The size of the micro-needle termination (10-50 nm) allows direct APT analysis. We will show, that even if bulk diamond is supposed to be transparent to the wavelengths that are used in this work (λ=343nm, 515nm or 1030nm), in the case of the micro-needles, the APT laser does heat the sample enough to field evaporate it.

A dedicated micro-photoluminescence setup was used on APT samples revealing intermediate energy levels in the band gap. We will show that these intermediate levels in the band structure enable the success of APT analysis on diamond micro-needles.

We gratefully acknowledge the financial support from the French Agence Nationale de la Recherche (ANR) through the program "Investissements d'Avenir" (ANR-10-LABX-09-01), LabEx EMC^3, projet ASAP.

V. I. Kleshch and A. N. Obraztsov are grateful for support from Russian Science Foundation (grant # 14-12-00511).

[1] B. Gault, F. Vurpillot, A. Vella, M. Gilbert, A. Menand, D. Blavette, B. Deconihout, Design of a femtosecond laser assisted tomographic atom probe, Review of Scientific Instruments, **77**, 043705 (2006)

[2] Philipp R. Heck, *et al*, Atom-probe analyses of nanodiamonds from Allende, Meteoritics & Planetary Science, **49** (3),453-467 ISSN 1945-5100 (2016)

[3] S. Mukherjee, H. Watanabe, D. Isheim, D. N. Seidman, and O. Moutanabbir Laser-Assisted Field Evaporation and Three-Dimensional Atom-by-Atom Mapping of Diamond Isotopic Homojunctions, Nano Letters **16** (2), 1335-1344 (2016)

[4] A. A. Zolotukhin, M. A. Dolganov, A. M. Alekseev, A. N. Obraztsov, Single-crystal diamond microneedles shaped at growth stage, Diamond and Related Materials, **42**, Pages 15-20, ISSN 0925-9635 (2016)

Structure-Controlled Synthesis of Single-Walled Carbon Nanotubes Using Intermetallic Compound Catalysts

Yan Li, Feng Yang, Xiao Wang, Juan Yang
College of Chemistry and Molecular Engineering, Peking University, Beijing 100871
yanli@pku.edu.cn

Single-walled carbon nanotubes (SWNTs) present structure-determined outstanding properties and SWNTs with a single (n, m) type are needed in many advanced applications. However, the chirality-specific growth of SWNTs is always a great challenge. Carbon nanotubes and their caps or catalysts can all act as the structural templates to guide the formation of SWNTs with a specified chirality (Fig. 1)[1]. SWNT growth via a catalyzed chemical vapour deposition CVD process is normally more efficient and therefore of great interest. We developed a new family of catalyst, tungsten-based intermetallic nanocrystals, to grow SWNTs with specified chiral structures. Such intermetallic nanocrystals present unique structure and atomic arrangements, which are distinctly different from the normal alloy nanoparticles or simple metal nanocrystals, therefore can act as the template to grow SWNTs with designed (n, m) structures. Using W_6Co_7 catalysts, we realized the selective growth of (12, 6)[2], (16, 0)[3], (14, 4) and other chiralities. By the cooperation of thermodynamic and kinetic factors, SWNTs with high chirality purity can be obtained (Fig. 2)[1].

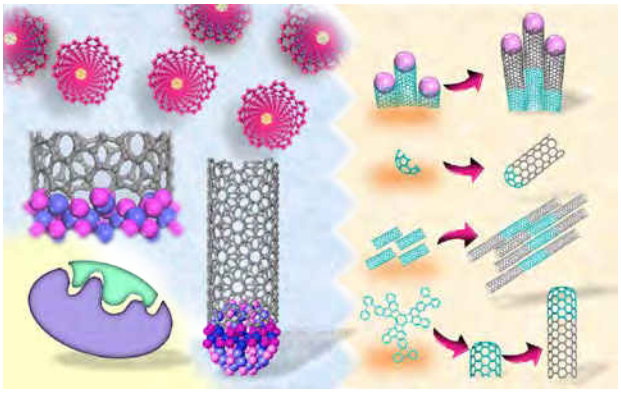

Fig. 1. Summary of the strategies for chirality-specific growth of SWNTs

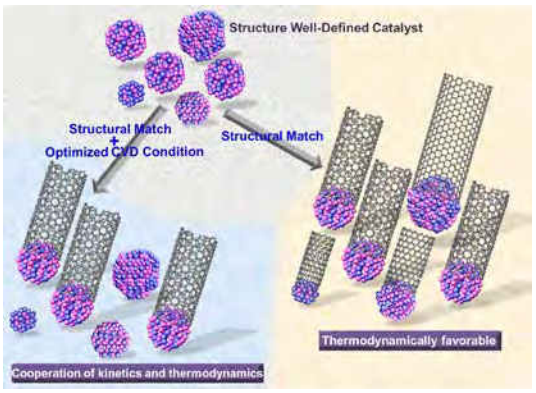

Fig. 2. Schematic illustration of the cooperative functions of thermodynamics and growth kinetics in Chirality-specific growth of SWNTs

Acknowledgement.

This research is financially supported by the NSFC (Projects 21125103, 91333105, and 21321001)

References

[1] F. Yang, X. Wang, M. Li, X. Liu, D. Zhang, J. Yang, Y. Li, Acc. Chem. Res., 2016, DOI: 10.1021/acs.accounts.5b00485.
[2] F. Yang, X. Wang, D. Zhang, J. Yang, D. Luo, Z. Xu, J. Wei, J.-Q. Wang, Z. Xu, F. Peng, X. Li, R. Li, Y. Li, M. Li, X. Bai, F. Ding, Y. Li, Nature, 510, 522 (2014).
[3] F. Yang, X. Wang, D. Zhang, K. Qi, J. Yang, Z. Xu, M. Li, X. Zhao, X. Bai, Y. Li, Journal of the American Chemical Society, 137, 8688-8691 (2015).
.

Catalytic Growth of Single-Wall Carbon Nanotubes: A Study using Environmental Transmission Electron Microscopy

Lili Zhang[1], Jens Kling[1], Thomas W. Hansen[1], Maoshuai He[2], Hua Jiang[3], Esko I. Kauppinen[3], Annick Loiseau[2], Jakob B. Wagner[1]

[1]*Technical University of Denmark, Center for Electron Nanoscopy, Fysikvej 307, 2800 Kgs. Lyngby, Denmark*

[2]*Laboratoire d'Étude des Microstructures, ONERA-CNRS, BP 72, 92322 Châtillon CEDEX, France*

[3]*Department of Applied Physics, Aalto University School of Science, P.O. Box 15100, FI-00076 Aalto, Finland*

Corresponding author e-mail address: lilizha@dtu.dk

The final chiral structure of single-wall carbon nanotubes (SWCNTs) can be determined by their initial cap nucleation from a catalyst particle. A mixture of as-synthesized SWCNTs of different structures is now the major challenge for their applications in nanoelectronics. In order to control the assemble processes of the carbon hexagonal network forming homogeneous nanotubes, which strongly relate to catalyst-tube interfacial properties and the diffusion dynamics of carbon atoms around the catalyst nanoparticle, we use environmental transmission electron microscopy (ETEM) to investigate the catalytic growth mechanism of SWCNTs [1] at a low pressure of 0.0001~10 mbar under 450~750 ^{0}C. The growth dynamics were monitored in real time, revealing that the choice of catalysts and carbon sources as well as local stress is key to their nucleation and growth termination [2] (Fig. 1). Furthermore, atomic structure and composition of catalysts were characterized *in situ* by means of ETEM with high spatial and temporal resolution. Combined with the analysis on the linking of catalyst features to the structure of SWCNTs, we realized a rearrangement of catalyst particles and multiple growth runs of SWCNTs [3] (Fig. 2).

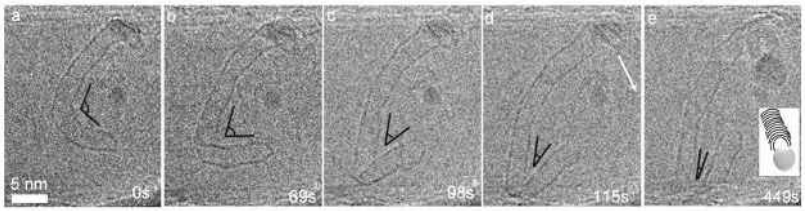

Fig. 1. Growth termination of a SWCNT. One end of the SWCNT was blocked during its growth, which forced the particle attached to the other end to nucleate several caps based on tip growth mode.

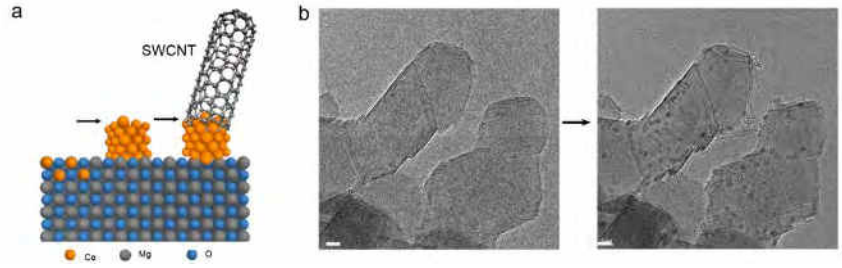

Fig. 2. Schematic (a) and TEM images (b-c) showing the *in situ* formation of catalyst particles and the growth of SWCNTs in the second cycle. Scale bars, 5 nm.

References

[1] He, M., et al., *Chiral-Selective Growth of Single-Walled Carbon Nanotubes on Lattice-Mismatched Epitaxial Cobalt Nanoparticles.* Sci. Rep., 2013. **3**.

[2] Zhang, L., et al., *Direct Evidence for Growth Termination and Multiple Nucleation of Single-Wall Carbon Nanotubes. In preparation.*

[3] Zhang, L., et al., *Renewable Catalysts for Repeated Growth of Single-Wall Carbon Nanotubes. In preparation.*

Theory and modelling of physical and bio- nanosensor systems

Yu Shunin[1, 6], D Fink[2], A Kiv[3], L Alfonta[3], A Mansharipova[4], R Muhamediyev[4], Yu Zhukovskii[1], T Lobanova-Shunina[5], N Burlutskaya[6], V Gopeyenko[6], S Bellucci[7]

[1]Institute of Solid State Physics, University of Latvia, Kengaraga Str. 8, LV-1063 Riga, Latvia
[2]Departamento de Fisica, Universidad Autónoma Metropolitana-Iztapalapa, PO Box 55-534, 09340 México, D.F., México
[3]Ben-Gurion University, PO Box 653, Beer-Sheva 84105, Israel
[4]Almaty University, Kazakhstan
[5]Riga Technical University, Faculty of Mechanical Engineering, Transport and Aeronautics, Latvia
[6]ISMA University, 1 Lomonosova Str., Bld 6, LV-1019, Riga, Latvia
[7]INFN-Laboratori Nazionali di Frascati, Via Enrico Fermi 40, I-00044, Frascati-Rome, Italy
Corresponding author e-mail address: yu_shunin@inbox.lv, shunin@isma.lv

The main objective of the current study is to demonstrate the implementation of advanced simulation models providing a proper description of electric responses in nanosensoring systems [1]. Initially, we consider physical nanosensors (pressure and temperature) based on functionalized CNTs and GNRs nanostructures. The model of nanocomposite materials based on carbon nanocluster suspension (CNTs and GNRs) in dielectric polymer environments (e.g., epoxy resins) is regarded as a disordered system of fragments of nanocarbon inclusions with different morphologies (chirality and geometry) in relation to a high electrical conductivity in a continuous dielectric environment. The electrical conductivity of a nanocomposite material depends on the concentration of nanocarbon inclusions (in fact, carbon macromolecules). Various nanocomposite morphologies are considered and computer simulation results are discussed [2].

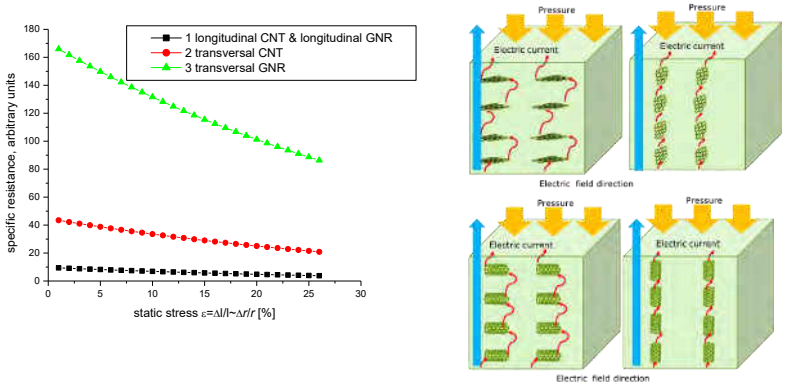

Fig.1. Specific resistance of CNTs- and GNRs- based nanocomposite (epoxy resin) via static stress. Below – variants of morphological orientations of nanocarbon inclusions.

Secondly, we pay attention to the development of bionanosensors based on polymer nanoporous structures (nanotracks) with various enzymes, which provide corresponding biocatalytic reactions and give reliably controlled ion currents [3,4]. In particular, we describe a concept for a glucose biosensor based on the enzyme glucose oxidase covalently linked to nanopores of etched nuclear track membranes. This device can be used to detect physiologically relevant glucose concentrations. The sensitive catalytic sensor can be made re-usable due to the production of diffusible products from the oxidative biomolecular recognition event.

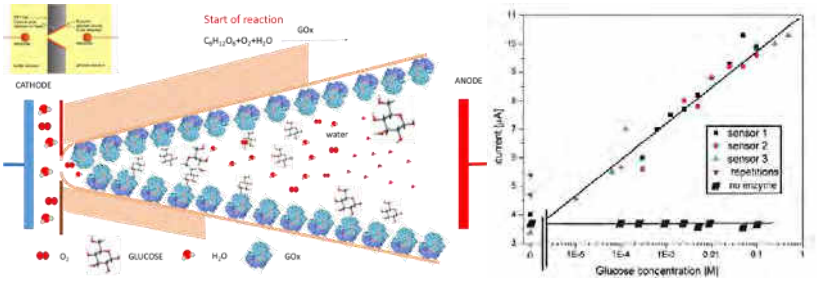

Fig.2. General scheme describing the detection process and modified polymer. Principle arrangement of experimental setup to study voltage-current dependencies in ion track-containing foils embedded in electrolytes. Performance comparison of three identically produced track-based glucose detectors against a calibration curve *I* (+5 V) vs. glucose concentration.

[1] Yu.N. Shunin, Yu.F. Zhukovskii, V.I. Gopejenko, N.Yu. Burlutskaya, S. Bellucci In: *Nanodevices and Nanomaterials for Ecological Security* Series: NATO Science for Peace Series B - Physics and Biophysics Eds Yu Shunin and A Kiv (Springer Verlag, Heidelberg, 2012) 237-262

[2] Y. Shunin, S. Bellucci, Y. Zhukovskii, T. Lobanova-Shunina, N. Burlutskaya, V. Gopeyenko *Computer Modelling & New Technologies* **19**(5) 14-20 (2015)

[3] D. Fink, I. Klinkovich, O. Bukelman, R. S. Marks, A. Kiv, D. Fuks, W.R. Fahrner, L. Alfonta *Biosensors and Bioelectronics* **24** 2702–2706 (2009)

[4] D. Fink, A. Kiv, Y. Shunin, N. Mykytenko, T. Lobanova-Shunina, A. Mansharipova, T. Koycheva, R. Muhamediev, V. Gopeyenko, N. Burlutskaya, Y. Zhukovskii, S. Bellucci *Computer Modelling & New Technologies* **19**(6) 7-13 (2015)

Optical study of multi-walled carbon nanotubes defectiveness synthesized by chemical vapor deposition with variable composition of Fe-Mo and Co-Mo catalysts

S.N. Bokova-Sirosh [a,b], V. L. Kuznetsov [c,d,e], M. A. Kazakova [c,d], D. V. Krasnikov [c,d] and E.D. Obraztsova [a,b]

[a] *A.M. Prokhorov General Physics Institute RAS, 38 Vavilov str., 119991, Moscow, Russia*
[b] *National Research Nuclear University «MEPhI», Kashirskoe shosse,31, Moscow, Russia*
[c] *Boreskov Institute of Catalysis SB RAS, Lavrentieva ave. 5, Novosibirsk, 630090, Russia*
[d] *Novosibirsk State University, Pirogova ave. 2, Novosibirsk, 630090, Novosibirsk, Russia*
[e] *National Tomsk State University, 36, Lenina Avenue, Tomsk, 634050, Russia*

Multi-walled carbon nanotubes (MWCNTs) are demanded today in a great number of applications [1-4]. Raman scattering is widely used for characterization of various types of carbon nanostructures [5]. This method is also sensitive to changing the structure and properties of MWCNTs.

In this work we have performed study of chemical vapor deposited (CVD) MWCNTs with Fe-Mo and Co-Mo catalysts containing a variable ratio of active metals. The purpose was to study of effect of the active component and ratio of the active catalyst metal component (Fe: Mo and Co: Mo) synthesis for their activity. The data were analyzed on the base of correlation of I2D/ID ratio and the average size of graphene fragments [6]. The fragments are considered as building blocks of MWCNTs. The addition of Mo in the catalyst (Fe-Mo/Al_2O_3 and Co-Mo/Al_2O_3) influences the structure of MWCNTs and allows to receive MWCNTs with different parameters (MWCNTs defectiveness rate and the average size of the inner tube) has been shown.

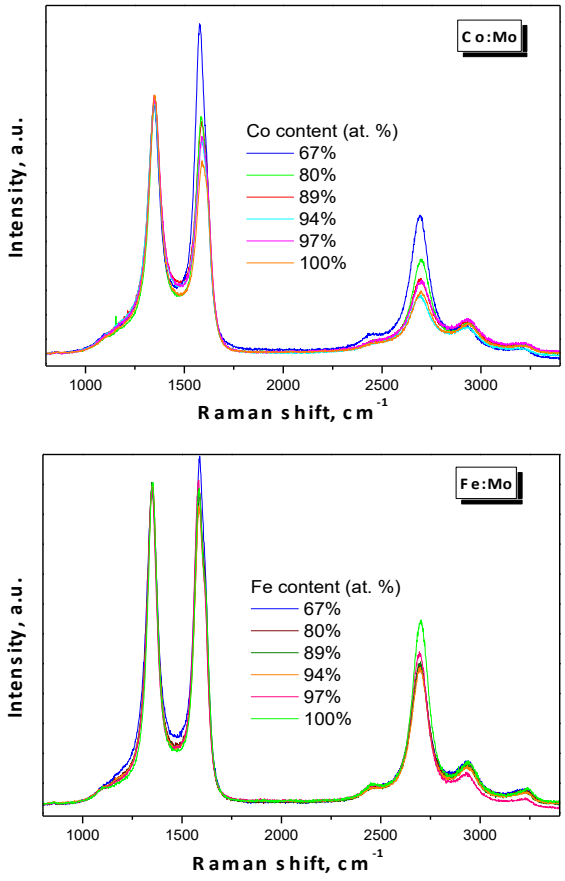

Fig. 1 The Raman spectra of MWNT synthesized on basis of Fe-Mo and Co-Mo catalysts.

Acknowledgements: This research was partially supported by the RAS research programs and RFBR 15-32-70013 mol_a_mos and 16-32-60046 mol_a_dk.

References:

1. M. S. Dresselhaus, G. Dresselhaus, J. C. Charlier, and E. Hernandez, Philos. Trans. R. Soc. Math. Phys. Eng. Sci. 362, 2065 (2004)
2. M. S. Dresselhaus, A. Jorio, and R. Saito, Annu. Rev. Condens. Matter Phys. 1, 89 (2010)
3. S. Yamashita, Y. Saito, and J. H. Choi (eds.), Carbon Nanotubes and Graphene for Photonic Applications (Woodhead Publishing Limited, Oxford, Cambridge, Philadelphia, New Delhi, 2013
4. M. F. L. De Volder, S. H. Tawfick, R. H. Baughman, A. J. Hart, Carbon Nanotubes: Present and Future Commercial Applications, Science 339, 535-539 (2013)
5. V.L. Kuznetsov, S.N. Bokova-Sirosh, S.I. Moseenkov, A.V. Ishchenko, D.V. Krasnikov, M.A. Kazakova, .A.I. Romanenko, E.N. Tkachev,and E.D. Obraztsova, Phys. Status Solidi B, 251, No. 12, 244-250 (2014)
6. S. N. Bokova-Sirosh ; V. L. Kuznetsov ; A. I. Romanenko ;M. A. Kazakova ; D. V. Krasnikov ; E. N. Tkachev ; Y. I. Yuzyuk ; E. D. Obraztsova "Investigation of defectiveness of multiwalled carbon nanotubes produced with Fe–Co catalysts of different composition" // *J. Nanophoton*. 10(1), 012526 (Mar 07, 2016). doi:10.1117/1.JNP.10.012526